GEOLOGICAL SURVEY OF CANADA

DEPARTMENT OF ENERGY,
MINES AND RESOURCES

PAPER 71-1
Part B

REPORT OF ACTIVITIES,

Part B: November 1970 to March 1971

rice, $2.00

1971

Technical editing and compilation
R. G. Blackadar
Layout
Leona R. Mahoney

GEOLOGICAL SURVEY

OF CANADA

PAPER 71-1
Part B

REPORT OF ACTIVITIES,
Part B: November 1970 to March 1971

DEPARTMENT OF ENERGY, MINES AND RESOURCES

Available by mail from *Information Canada*, Ottawa

from the Geological Survey of Canada
601 Booth St., Ottawa

and

Information Canada bookshops in

HALIFAX - 1735 Barrington Street
MONTREAL - 1182 St. Catherine Street West
OTTAWA - 171 Slater Street
TORONTO - 221 Yonge Street
WINNIPEG - 499 Portage Avenue
VANCOUVER - 657 Granville Street

or through your bookseller

Price: $2.00 Catalogue No. M44-71-1B

Price subject to change without notice

Information Canada
Ottawa
1971

CONTENTS

CONTENTS (cont'd)

CONTENTS (cont'd)

CONTENTS (cont'd)

REPORT OF ACTIVITIES, NOVEMBER 1970 TO MARCH 1971

INTRODUCTION

The forty-two reports that make up this publication describe briefly some of the work carried out by members of the Geological Survey of Canada between November 1970 and March 1971. Many of these contributions report the results of one aspect of a scientific project and are thus in the nature of "Progress Reports", some are designed to keep other earth scientists aware of the Survey's current approach to certain research problems and others are complete albeit brief reports on some aspect of geological research. The figures used to illustrate this publication are reproduced without change from material supplied by the authors. Manuscripts were accepted for inclusion in this report until April 30, 1971.

The Report of Activities (parts A and B), the reports on isotopic and radiocarbon dating, the annual index of publications and the volume of abstracts of papers published by Survey personnel in non-Survey publications provide an annual accounting of most of the published scientific output of the Branch. Requests for announcement cards, geological reports, maps or information on specific areas or topics should be addressed to: Geological Survey of Canada, Department of Energy, Mines and Resources, 601 Booth Street, Ottawa K1A OE8, Canada.

ANALYTICAL CHEMISTRY

1. ATOMIC ABSORPTION (AND FLAME EMISSION) SPECTROSCOPY

Project 690090

Sydney Abbey

New components installed in our atomic absorption system included a solid-state read-out module, including built-in scale expansion, damping, base-line drift compensation and linear absorbance signal; a new burner mount; hollow cathode lamps for the three rarer alkali metals; a mechanical beam-chopper and a wavelength scanner, permitting emission measurements with background correction; and a near-infrared-sensitive photomultiplier tube.

Thus far, the new components have not alleviated the problems in Si determination, but further work is contemplated. The components have helped to confirm the superior sensitivity of flame emission over atomic absorption in determining Rb, Li and Cs down to less than 1 ppm in rocks. A great improvement was also observed in potassium determination.

Additional hollow cathode lamps were also acquired and considerable work done in the determination of precious metals. Details are given in a separate report by J.G. Sen Gupta.

2. NOVEL APPLICATIONS OF AN "AUTOMATIC SULPHUR TITRATOR"

Project 690090

J.L. Bouvier, J.G. Sen Gupta and Sydney Abbey

In an effort to simplify and increase the production rate of the induction furnace method for sulphur determination, an automatic sulphur titrator was acquired, similar to that in use at the Geological Survey's Institute of Sedimentary and Petroleum Geology, Calgary. The instrument absorbs sulphur dioxide, resulting in a diminution in the colour of the starch-iodine complex, which is detected by a photocell, in turn actuating a relay which draws more iodate titrant into the absorption vessel. On the completion of absorption, the volume of titrant used is read on a burette. By eliminating the need for special absorption vessels containing excess iodate-iodide solution, which would require back-titration after absorption was completed, this device resulted in at least a three-fold increase in output and a marked diminution in the analytical skill required for the analysis.

Taking advantage of the fact that the non-aqueous titration of carbon dioxide involves a colour change as well, attempts were made to use the same automatic titrator for carbon determination. Results have been encouraging but not yet conclusive. There is reason to believe that this device will prove satisfactory for determining the carbon dioxide evolved either by combustion or acid-evolution. Such a scheme would represent a modest improvement in speed, a significant decrease in manipulative operations, and probably increased accuracy at the low end of the working range.

A third possible application of the same automatic titrator is in the determination of ferrous iron. The method under study is based on that used for chromite, where the sample is digested in a mixture of phosphoric and sulphuric acids, sulphur dioxide being evolved by reaction between ferrous iron and sulphuric acid. The automatic titrator has been applied to the measurement of the sulphur dioxide, which is proportional to the ferrous content of the sample. The method has worked well on both silicate and oxide samples, but certain contradictions between the proposed method and the classical Pratt procedure have been further complicated by unsatisfactory results from the latter method. Should the new method prove satisfactory, it would represent a small time-saving and great reduction in required skill, when compared to the classical procedure, and a more effective decomposition with no loss in speed when compared with the current "rapid" method.

3. APPLICATION OF SPECTROCHEMICAL METHODS TO TRACE ELEMENT DETERMINATIONS IN GEOLOGICAL MATERIALS

Project 690090

W.H. Champ

Analytical difficulties which had forced the discontinuance of our procedure for trace volatile elements in silicates were resolved and a much improved method established, enabling these analyses to be carried on with better precision and accuracy than before. This method employs factional distillation of the volatile elements from the sample in a globule-type DC arc. A buffer mixture of alumina and alkali salts gives better arc stability and precision than earlier methods, and matrix effects are small enough that most of the common silicate rocks and minerals can be analyzed, excluding the ultrabasic rocks. On a minimum 25 milligrams of sample we can determine 15 elements, as follows:

Zn Pb Ga Sn B Ge As mo Tl Sb Bi Cd Ag In Te.

Results are reported to two significant figures, $\pm$ 30%, within the concentration range of 0.1 to 1000 ppm. (The elements Hg, Au and Cu may be detected also, but quantitative determinations for them cannot be made.)

4. ATOMIC ABSORPTION SPECTROSCOPIC METHODS FOR DETERMINING THE NOBLE AND THE BASE METALS IN OSMIRIDIUM, NATIVE PLATINUM AND SPERRYLITE

Project 690090

J.G. Sen Gupta

Atomic absorption spectroscopic methods for determining the noble and the base metals in osmiridium, native platinum and sperrylite have been developed with synthetic solutions; the methods then applied to the analyses of some naturally occurring samples.

A comparative study of the three spectroscopic buffers (0.5% Cu - 0.5% Cd, 1% La, 1% Sr) revealed that 0.5% Cu - 0.5% Cd buffer is superior for atomic absorption determination of micro and macro amounts of all the noble metals in the said materials. For determining platinum and rhodium, the solutions should be diluted to a suitable volume to avoid interferences of the overwhelming amounts of the other noble metals. The base metals can be determined from either 1% La or 1% Sr buffer medium.

The decomposition of osmiridium was effected by dry chlorination at 700 - 750°C, and those of native platinum and sperrylite by a combination of aqua regia treatment and dry chlorination, or dry chlorination alone at elevated temperatures. Osmium and ruthenium were distilled from the chlorinated product by perchloric acid and collected in hydrobromic acid. After removing the excess acid, the determination of these two elements in the mixture (containing 0.5% Cu - 0.5% Cd as spectroscopic buffer) was completed by atomic absorption spectroscopy. After evaporation and conversion to chloride the remaining noble metals and the base metals were determined from various aliquots by atomic absorption spectroscopy in the presence of a suitable spectroscopic buffer as stated above.

CORDILLERAN GEOLOGY

92 C E F

5. CHEMISTRY AND PETROLOGY OF SOME MESOZOIC VOLCANIC ROCKS OF VANCOUVER ISLAND, BRITISH COLUMBIA

Project 680038

J.E. Muller

Introduction

The early-Mesozoic volcanic cycle of Vancouver Island is composed of a lower part of Triassic basaltic flows, pillow-lavas and breccias (Karmutsen Volcanics) and an upper part of Lower Jurassic andesitic to rhyodacitic flows, breccias and tuffs (Bonanza Volcanics) separated by Upper Triassic and Lower Jurassic sediments. Commonly these two volcanic sequences are different in appearance or can be separated readily on the basis of structure. But in many small outcrops a definite formation-assignment, essential for structural interpretation, cannot be made on megascopic or even microscopic characteristics. To aid classification and distinction of these two major rock-groups 6 samples of Karmutsen Volcanics, from a ± 6,000-foot section exposed on Mount Flanigan, west of Upper Campbell Lake and 19 samples of Bonanza Volcanics from a section, about 8,000 feet thick, exposed along the Pacific Ocean north of Cape Parkins, were selected for chemical analysis.

Chemical Analyses

The analyses were done by S. Courville of the Geological Survey using X-ray fluorescence, supplemented by rapid chemical analysis for FeO, Na_2O, P_2O_5, CO_2 and total H_2O. Table 1 shows the analyses (arranged in stratigraphic succession of the sections) and Figure 1 shows a Larsen plot of the data, together with some average compositions of classes of volcanic rocks according to Nockolds[1].

The plot shows excellent separation of Karmutsen and Bonanza Volcanics. The cluster of Karmutsen lavas, between -11.2 and -15.3 on the abscissa, contains on the silicic side Nockolds' "normal tholeiitic basalt". Values for three analyses of Karmutsen Volcanics from Queen Charlotte Islands[2] could not be plotted separately: two coincide with values on opposite ends of the Karmutsen-cluster and one coincides with the basic end of the Bonanza andesite group. Plotted on Kuno's[3] alkali-silica diagram the Karmutsen rocks are partly in the tholeiite field and partly in the high-alumina-basalt field.

The largest group of Bonanza Volcanics plots between -0.5 and -6.7 on the abscissa of the Larsen diagram. This cluster coincides, on its silicic side, with Nockolds' "average andesite"; the average of 5 Aleutian basaltic andesites[4] agrees with the basic side of this cluster. One basalt, similar in chemistry to Karmutsen Volcanics, is also present. Plotted on

Kuno's alkali-silica diagram Bonanza Volcanics are scattered across the three (tholeiite, high alumina and alkali) fields, but most of them are within the alkali field. As the petrographic character of these rocks, so far as can be ascertained in spite of fine grain-size and alteration is calc-alkaline, but albitized, it is suggested that the high alkali values are due to secondary enrichment in sodium.

Two analyses plot close to the "average dacite" of Nockolds[1] and five analyses cluster between the points for "average rhyodacite" and "average dellenite" (= quartz-latite). An analysis of "andesite" from the Yakoun Formation of Queen Charlotte Islands[2] would plot slightly to the left of the Bonanza dacites.

Fused-rock refractive indices

Refraction indices of fused rock were determined according to Mathews'[5] method by courtesy of B.N. Church of the British Columbia Department of Mines and Petroleum Resources (beads by L.E. Sheppard; refraction indices by E.F. Karpick). The results, shown on Table 1 and Figure 1, correlate very well with the analyses. Karmutsen basalts range between R.I. 1.596 and 1.622, Bonanza andesites between R.I. 1.558 and 1.583, and the one sample of basalt has an index of 1.594. Bonanza dacites (only two samples) range from R.I. 1.525 to 1.583 and rhyodacites from 1.491 to 1.504. Clearly this method can be used as a fairly reliable tool to determine the general composition of these volcanic rocks. Bearing in mind that apparently there are a few basaltic andesites in Karmutsen Volcanics and a few basalts in Bonanza Volcanics the method can be used with discretion to distinguish the two rock-groups. This has already been put into practice by K. Northcote (pers. comm.).

Petrography

Karmutsen basalts, either in flows or in pillows and breccias, are quite uniform in composition and chemistry. They are fine grained, dark greenish to brownish grey, brown weathering rocks and commonly show small feldspar phenocrysts and amygdules filled with secondary minerals. Thin sections show equigranular ophitic or porphyritic assemblages of labradorite and augite in about equal amounts, together with fine opaque matter and palagonite. Vesicles are filled with chlorite, quartz, epidote, and also commonly pumpellyite and in many rocks the feldspars are saussuritized.

Bonanza andesites are dark reddish to greenish grey rocks, less massive and more coarsely vesicular than Karmutsen basalts. They are generally fine grained to aphanitic, but there are distinctive coarse porphyries containing densely packed plagioclase phenocrysts to 1 cm long. The larger vesicles commonly contain calcite and rosettes of zeolite. Thin sections show saussuritic plagioclase, commonly in two generations and, where determinable, with composition of andesine or labradorite and intersertal grains of clinopyroxene. Hypersthene, definitely identified in some samples as a second pyroxene, may also be represented by rectangular pseudomorphs of talc and serpentine in other thin sections. The mesostasis consists mainly of chlorite, serpentine and opaque matter. Clouthier[6] detected by X-ray diffraction the minerals ripidolite (a chlorite) and laumontite in some of the writer's samples.

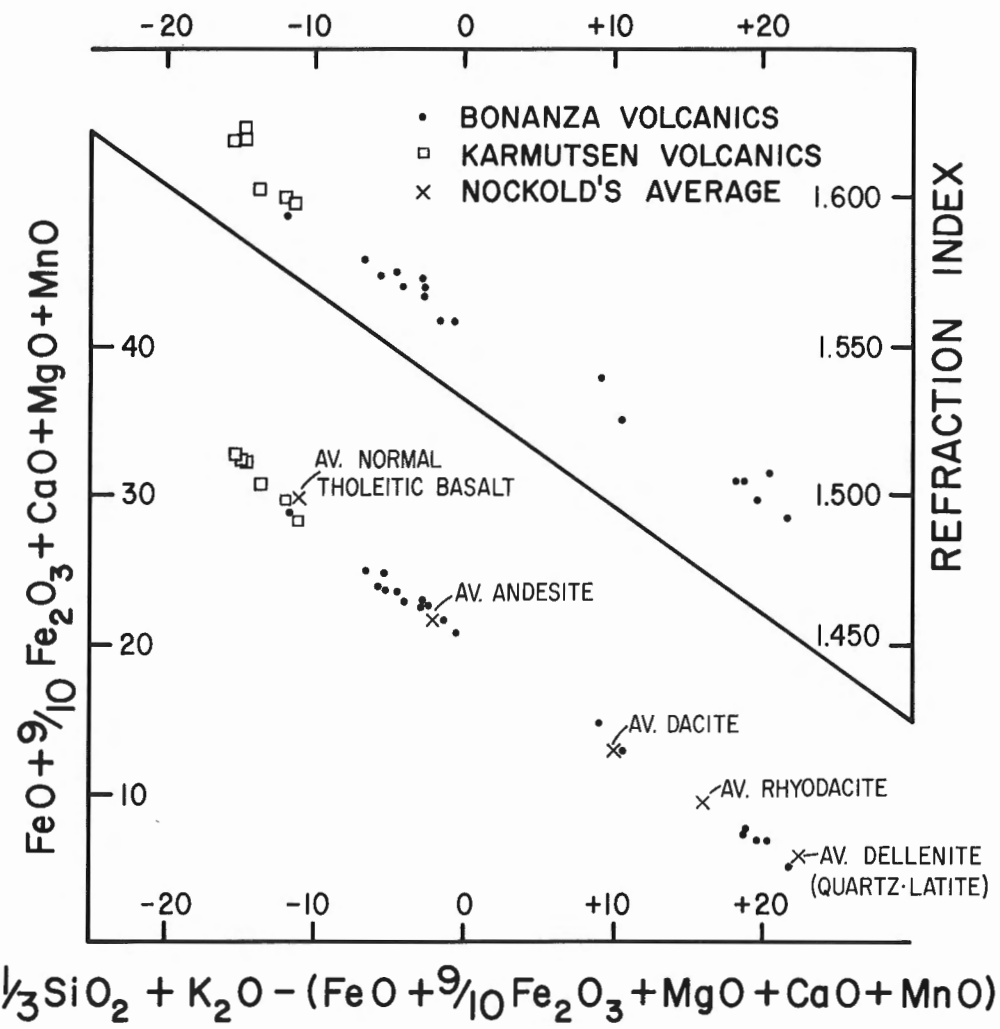

Figure 1. Fused-rock refraction indices and Larsen plot of compositions of some Mesozoic volcanics of Vancouver Island together with Nockolds' averages for some volcanic rocks.

Bonanza dacites are reddish to greenish grey rocks of lighter hues than the andesites, commonly containing conspicuous white or pinkish plagioclase phenocrysts 1 to 2 mm long and small specks of hematite. Thin sections show phenocrysts of largely altered oligoclase-andesine and minor pyroxene, also mostly altered, in a diffuse matrix of feldspar and interstitial quartz. Bonanza rhyodacites are reddish, greenish and pinkish grey aphanitic or vitrophyric rocks with white or pink feldspar phenocrysts, a few mm long. Thin sections show the albitic phenocrysts in a matrix of fine feldspar and quartz, chlorite and hematite. Staining of some sections of these rocks failed to reveal any potash feldspars.

TABLE 1

Bonanza Volcanics, north of Cape Parkins

	SiO_2	TiO_2	Al_2O_3	Fe_2O_3	FeO	MnO	MgO	CaO	Na_2O	K_2O	P_2O_5	CO_2	H_2O	Total	R.I.
1	68.6	0.55	15.2	2.4	2.0	0.08	1.7	1.2	5.0	3.1	0.12	0.7	1.1	101.8	1.504
2	67.8	0.55	15.0	2.3	1.8	0.08	1.5	1.4	5.2	2.6	0.12	1.6	0.9	100.9	1.504
3	48.6	1.02	19.6	2.8	5.6	0.16	4.5	9.3	3.7	0.8	0.05	0.5	2.2	98.8	1.574
4	48.7	1.53	17.2	3.7	6.4	0.26	8.0	5.6	4.4	1.0	0.42	0.1	3.9	101.2	1.578
5	50.0	2.03	15.8	3.8	7.4	0.24	6.2	4.8	5.2	1.1	0.52	0.2	3.3	100.6	1.574
6	53.5	1.96	14.8	3.6	7.4	0.19	5.2	5.8	4.2	1.5	0.61	0.1	2.5	101.4	1.567
7	51.1	1.40	15.4	4.4	5.4	0.14	5.1	6.8	4.8	1.7	0.42	1.6	2.5	100.8	1.570
8	52.1	1.70	15.3	4.3	5.7	0.18	4.7	6.4	3.8	1.5	0.37	0.1	2.4	98.6	1.569
9	47.9	1.28	19.2	3.9	5.3	0.14	3.7	9.4	3.3	0.7	0.28	2.5	3.0	100.6	1.580
10	43.7	1.59	16.9	7.1	4.7	0.16	9.3	5.8	3.8	1.0	0.09	0.8	4.6	99.5	1.594
11	50.1	0.86	17.4	2.9	4.9	0.14	6.7	5.4	4.5	2.2	0.17	1.0	3.6	99.9	1.559
12	55.7	0.69	16.5	1.9	5.2	0.17	4.7	9.0	3.4	1.0	0.18	0.2	2.7	101.3	1.558
13	49.4	0.82	17.5	1.9	4.5	0.15	4.2	10.9	4.4	1.2	0.22	2.8	1.4	99.4	1.570
14	69.6	0.27	13.5	0.9	1.8	0.06	1.4	2.2	2.3	2.1	0.03	2.9	2.0	99.1	1.506
15	72.4	0.30	13.0	0.5	2.9	0.11	1.9	1.3	4.4	2.2	0.03	0.3	1.1	100.4	1.498
16	51.4	2.21	14.2	2.4	7.9	0.26	5.1	7.4	3.9	0.8	0.63	1.4	2.6	100.2	1.583
17	74.4	0.29	12.8	0.3	2.2	0.09	1.6	0.7	5.0	1.5	0.03	0.1	0.7	99.7	1.491
18	60.4	1.11	15.3	2.1	5.0	0.16	3.1	4.1	4.2	2.8	0.26	1.0	1.9	101.4	1.538
19	61.2	1.13	14.9	2.7	4.0	0.14	3.3	2.4	5.4	1.9	0.29	0.2	1.7	99.3	1.525

3, 4, 5, 6, 7, 8, 11, 12, 13: aphanitic and fine-grained andesite flows

9: coarsely porphyritic andesite flow

18, 19: fine-grained and aphanitic porphyritic dacite

1, 2, 14, 15, 17: fine-grained and aphanitic porphyritic rhyodacite

Karmutsen Volcanics, Mt. Flanigan

	SiO_2	TiO_2	Al_2O_3	Fe_2O_3	FeO	MnO	MgO	CaO	Na_2O	K_2O	P_2O_5	CO_2	H_2O	Total	R.I.
1	49.2	1.56	15.0	4.4	7.3	0.18	6.9	10.0	3.4	0.4	0.12	tr	1.1	99.1	1.598
2	47.3	2.38	13.0	5.2	8.8	0.23	7.0	9.3	2.7	0.5	0.21	tr	2.9	99.5	1.622
3	47.4	1.25	13.9	4.1	6.5	0.17	7.7	10.5	3.5	tr	0.10	0.1	3.8	99.0	1.601
4	47.7	2.24	13.9	4.6	9.0	0.20	6.3	10.4	1.7	0.2	0.18	tr	2.8	99.2	1.618
5	48.8	2.31	12.9	4.3	9.1	0.19	6.4	11.2	1.9	0.1	0.21	tr	1.7	99.1	1.618
6	49.5	1.23	17.1	1.5	7.5	0.14	5.4	13.1	2.3	0.1	0.12	tr	1.1	99.1	1.596

1 - 4 : basalt flows, finely amygdaloidal;

5 : pillow lava

6 : porphyritic basalt flow

Mesozoic volcanic history

The Mesozoic volcanic history of Vancouver Island is characterized by the initial outpouring of as much as 20,000 feet of tholeiitic flood-basalts including pillows, breccias or flows forming a north-south elongated volcanic shield. Upper Triassic and locally Lower Jurassic volcaniclastic and carbonate sedimentation followed and was in turn succeeded by Lower Jurassic and ? later outpouring of andesitic to rhyodacitic flows and their associated tuffs, breccias and minor greywackes. Present distribution and thickness (8,000 feet in one measured section) suggests the younger rocks are part of submarine cones, located mainly on the west-side of the basaltic shield. Emplacement of granitic rocks of the Island Intrusions into the volcanic shield occurred in Midde Jurassic time, after and perhaps also in conjunction with the extrusion of andesitic and more silicic volcanics.

There appears to be an analogy between the Triassic-Jurassic volcanic history of Vancouver Island and the Cenozoic history of western Washington and Oregon[7]. There too an early Eocene tholeiitic shield more than 15,000 feet thick and parallelling the present coastline for about 400 miles is overlain by volcaniclastic sediments followed by Late Eocene to Oligocene andesitic volcanics that were erupted from cones that formed along the eastern edge of the basaltic shield. This volcanic pile has been inferred to have been built directly on oceanic crust[8].

Another possible analogy is the mechanism of development of the Aleutian Island Arc, as diagrammatically shown by Coats[9]. Three figures show development of the "subduction zone" below the island arc (before "subduction" and "plate tectonics" had become fashionable geotectonic terms) and magmas being generated above that zone in the mantle. The first stage shows "shield volcanoes" built on oceanic crust; as movement along the "thrust fault" proceeds eruption of the shield volcanoes moves oceanward. In the third stage "andesitic strato volcanoes" appear on the side of the shield-volcanoes. It is inferred that part of this island arc rests on older eugeosynclinal sequences, and part of its rests on oceanic crust.

The Vancouver Island Mesozoic volcanic complex is known to overlie a partly metamorphosed pre-Pennsylvanian volcanic complex (Sicker Group and Westcoast Gneiss Complex) and one may reasonably infer that this complex rests on or merges into oceanic crust. The Mesozoic sequence has therefore the chemical-petrographic characteristics and the structural setting compatible with that of an early-Mesozoic island arc off the North American paleocontinent.

Conclusions

The analyses and petrographic examination reveal a good distinction between Karmutsen and Bonanza volcanics. The uniformity of many thousands of feet of pillow lavas or basaltic flows of the Karmutsen Formation as seen in the field is reflected in rather uniform petrographic and chemical composition as well as fused-rock refraction index. In contrast the Bonanza Volcanics, highly variable in lithology in exposed sections containing lavas, tuffs, breccias and minor sediments also exhibit a much larger range of chemical and petrographic composition and of refraction index.

The chemistry, petrology and tectonic setting of the early Mesozoic volcanic sequence of Vancouver Island seems to be consistent with the idea that they represent the remains of a Triassic-Jurassic island arc.

---

[1]Nockolds, S.R.: Average chemical compositions of some igneous rocks; Geol. Soc. Am., vol. 65, pp. 1007-1032 (1954).

[2]Sutherland Brown, A.: Geology of the Queen Charlotte Islands, British Columbia; B.C. Dept. Mines Petrol. Resources, Bull. 54 (1968).

[3]Kuno, H.: Differentiation of basaltic magmas; Basalts, The Poldervaart Treatise on rocks of basaltic composition, vol. 2, pp. 623-688 (1968).

[4]Coats, R.R.: Basaltic andesites; Basalts, The Poldervaart Treatise on rocks of basaltic composition, vol. 2, pp. 689-736 (1968).

[5]Mathews, W.H.: A useful method for determining approximate composition of fine grained igneous rocks; Am. Mineralogist, vol. 36, pp. 92-101 (1951).

[6]Clouthier, G.A.: An examination of the Lower Bonanza, Cape Parkins, Vancouver Island; unpubl. bachelor thesis, Univ. B.C. (1970).

[7]Snavely, P.D. and Wagner, H.C.: Tertiary geologic history of western Oregon and Washington; State of Wash., Div. Mines Geol., Report of Investigations 22 (1963).

[8]Hamilton, W. and Myers, W.B.: Cenozoic tectonics of the western United States; Rev. Geophys., vol. 4, pp. 509-549 (1966).

[9]Coats, R.R.: Magma type and crustal structure in the Aleutian arc; Am. Geophys. Union, Geophys. Monogr. 6, pp. 92-109 (1962).

General

ECONOMIC GEOLOGY

6. NIOBIUM (COLUMBIUM) AND TANTALUM DEPOSITS

Project 700069

K.R. Dawson

An exhaustive search of the journals for papers dealing with these elements has been made that resulted in the identification of approximately 240 Canadian and 52 foreign deposits and occurrences. The search was organized to assemble standard sets of descriptive parameters including the geographical location, mineral species, host rocks, country rock, structures, state of development, grade and reserves. The data sets for Canadian deposits and occurrences were extended to include brief geological descriptions, corporate history, physiographic province, and bibliography. They are found in three geological environments in Canada, placers, granitic pegmatites and alkaline-carbonatite complexes. The minerals pyrochlore and columbite have proven to be the most widespread in these deposits.

Canadian production of Nb comes from an alkaline syenite-carbonatite complex and Ta production comes from a zoned granitic pegmatite. Several potential producers of Nb have been identified that have not proven economic under present day market conditions. These include the Nova Beaucage, near North Bay; Nemegosenda Lake near Chapleau; the Alpha-B orebody south of Moosonee and possibly the St Honoré near Chicoutimi. All of these are related to alkaline syenite-carbonatite complexes. Nb reserves in placer deposits are known in British Columbia but their full extent has not been tested. Tantalum on the other hand occurs widely as an accessory in pegmatite dykes but Canada's known reserves of the element are small.

Research is being done in connection with the classification of the deposits of the two elements and one scheme will be chosen that suites the Canadian geological situation.

---

[1]Heinrich, E. Wm.: The geology of carbonatites; Rand McNally and Company, Chicago (1966).

[2]Parker, R.L. and Fleischer, M.: Geochemistry of niobium and tantalum; U.S. Geol. Surv., Prof. Paper No. 612 (1968).

[3]Pecora, W.T.: Carbonatites, A review bulletin; Bull. Geol. Soc. Am., vol. 67, No. 11 (1956).

[4]Tuttle, O.F. and Gittins, J.: Carbonatites; Interscience Publishers, N.Y. (1966).

---

7. GEOLOGY OF LEAD AND ZINC DEPOSITS IN CANADA

Project 650056

D.F. Sangster

I - Follow-up studies

Various aspects of follow-up work relating to last summer's field activities (Geol. Surv. Can. Paper 71-1; Pt. A, pp. 91-94) can be reported at this time.

1. Samples of argillite, from the vicinity of the Tom Group, Yukon (NTS 105 O/1) lead-zinc-barite deposits, were submitted for paleontological examination in an effort to determine the age of host rock of this important strata-bound and stratiform sulphide body. Following is an excerpt from Paleontology Report F1-11-1970-DCM by D.C. McGregor: "Markings on the surface of some of the samples are probably the remains of fragments of wood. They are much too poorly preserved to be identified. The presence of fossil wood would date the sediments as Devonian or younger". Chert-pebble conglomerate in the host rocks at Tom Group can now be correlated with a similar conglomerate in Devono-Mississippian strata to the southwest.

Recognition of these host rocks as Devono-Mississippian is significant because it identifies an attractive and alternate time-stratigraphic unit for lead-zinc exploration in addition to that of the well-known Upper Proterozoic-Lower Cambrian in the Canadian Cordillera. Extensive lead-zinc mineralization is known to occur in the Devono-Mississippian of the Interior Plains of North America (e.g. Pine Point is in Middle Devonian and Tri-State in Mississippian strata) and it would now appear that this important metallogenic unit continues into the Cordillera.

2. Selected samples of host rock at the Bathurst-Norsemines deposit, N.W.T. (NTS 76 F/16) were examined in thin section and the essentially quartzite nature of the rock in hand specimen was confirmed. The rock consists of over 85 per cent quartz with subordinate amounts of muscovite and, locally, sillimanite. The presence of the latter mineral implies high-grade metamorphism which is also evident in the quartzite, now completely recrystallized. The possibility that the rock represents a metamorphosed rhyolite tuff is considered to be remote because of the extremely high quartz content of the rock and the absence of feldspar in the matrix. Thin sections of limestone, also present in the immediate vicinity of the sulphide deposit, show that it has apparently undergone the same metamorphism as the quartzite and tends to confirm the largely sedimentary nature of the host rocks to this important Cu-Pb-Zn-Ag deposit. This is in contrast to the largely volcanic character of the host rocks enclosing similar massive Cu-Zn sulphide ores in the Superior Province. One might infer from this that, at least in the Slave Province where the proportion of volcanics to sediments is considerably less than in the Superior Province[1], exploration for massive sulphide deposits should extend beyond the classical "greenstone belts" and out into the surrounding sediments.

II. Pb-isotope studies

In an attempt to expand on some of the metallogenic concepts in the Precambrian as proposed by Roscoe[2], particularly in the light of recent theories relating to Archean protocontinents as suggested by Goodwin[3,4], the writer has been compiling published Pb-isotope data on Precambrian stratabound massive sulphide deposits.

Early in this compilation it became evident that massive sulphide ores of the Flin Flon–Snow Lake belt contain lead of distinctly different composition from that in similar deposits in the Archean of the Superior Province. Host rocks to the Flin Flon deposits, the Missi volcanics, have traditionally been considered of Archean depositional age[5].

As a check on the Pb-isotope compositions of the Flin Flon–Snow Lake orebodies, suitable material was collected from the Western Nuclear, Flin Flon, Schist Lake, Anderson Lake, Stall Lake, and Osborne Lake deposits and was submitted for isotopic analysis.

The deposits are typical of the so-called "volcanic exhalative" or "volcanogenic" stratabound type and, in common with such ores, appear to be coeval with the host volcanics. This type of deposit normally contains "ordinary" or "single stage" leads[6] and dating of the ore deposits by the Pb-Pb method should yield ages close to those of the enclosing host rocks.

Final results are pending more precise determinations but preliminary analyses show a small, but probably real, spread of isotopic ratios with an average close to that of the main Flin Flon orebody itself.

The Flin Flon isotopic data give a preliminary model lead age of 1850 ± 44 m.y., thereby suggesting that the Amisk volcanics are of Aphebian, and not Archean, age. The data agree well with a recent, very precise, determination of Flin Flon lead by Stacey et al.[7] which yields a model lead age of 1840 ± 10 m.y. If this age is accepted, the Amisk volcanics, and their contained massive sulphide deposits, would have been deposited just prior to the Hudsonian orogeny which resulted in widespread recrystallization at about 1735 m.y. although deformation likely reached a peak about 100 million years earlier[5]

An Aphebian age for the Amisk volcanics was implied in 1965 by Byers et al.[8] who concluded that rocks of the Flin Flon area had undergone only one major orogeny and that it was Hudsonian. This conclusion has been supported by recent structural studies[9] in the Missi sediments overlying the Amisk volcanics. If these rocks were Archean, it is extremely unlikely that they would have escaped the widespread Kenoran orogeny; recognition of only one (Hudsonian) orogeny strongly suggests that these rocks are post-Kenoran in age. Structural studies on the orebodies themselves[10,11,12] show that the structures of the ores parallel those of the enclosing rocks and that both ores and host rocks have been metamorphosed together.

Thus, Pb-Pb ages of the Flin Flon–Snow Lake orebodies, combined with structural studies, offer compelling evidence of a Proterozoic age for this highly-mineralized volcanic belt. Thus, a periodicity in major Precambrian metallogenic epochs is suggested, one occurring around 2900 to 3000 m.y.[2] and another at about 1850 m.y. Furthermore, analysis of lead from the Brabant Lake deposit[13], occurring in the same volcanic belt as the Fox Lake and Ruttan Lake deposits north of Flin Flon, yields a model lead age similar to that of Flin Flon, suggesting yet another belt of Cu-Zn-bearing Proterozoic rocks in the Lynn Lake region.

A final manuscript, reporting on details of the Pb-isotope studies in the Flin Flon–Snow Lake ore-field, is in preparation.

---

[1]McGlynn, J.C. and Henderson, J.B.: Archean volcanism and sedimentation in the Slave Structural Province; pp. 31-44, in Symposium on Basins and Geosynclines of the Canadian Shield, ed. by A.J. Baer, Geol. Surv. Can., Paper 70-40 (1970).

[2]Roscoe, S.M.: Geochemical and isotopic studies, Noranda and Matagami areas; Trans. Can. Inst. Mining Met., vol. LXVIII, pp. 279-285 (1965).

[3]Goodwin, A.M.: Evolution of the Canadian Shield; Proc. Geol. Assoc. Can., vol. 19, pp. 1-14 (1968).

[4]Goodwin, A.M.: Archean protocontinental growth and early crustal history of the Canadian Shield; 18th Int. Geol. Congr., vol. I, pp. 69-89, (1968).

[5]Stockwell, C.H. et al.: Geology of the Canadian Shield; Ch. IV in Geology and Economic Minerals of Canada, Geol. Surv. Can., Ec. Geol. Rept. 1, 5th ed. (1970).

[6]Kanasewich, E.R.: The interpretation of lead isotopes and their geological significance; pp. 147-223, in Radiometric dating for geologists, Hamilton, E.I. and Farquhar, R.M. (ed.), (1968).

[7]Stacey, J.S., Delevaux, M.E. and Ulrych, T.J.: Some triple-filament lead isotope ratio measurements and on absolute growth curve for single-stage leads; Earth and Plan. Sci. Letters, vol. 6, pp. 15-25 (1969).

[8]Byers, A.R., Kirkland, S.J.T. and Pearson, W.J.: Geology and mineral deposits of the Flin Flon area, Saskatchewan; Sask. Dept. Min. Resources, Rept. 62 (1965).

[9]Stauffer, M.R. and Mukherjee, A.: Superimposed deformations in the Missi metasedimentary rocks near Flin Flon, Manitoba; Can. J. Earth Sci., vol. 8, No. 2, pp. 217-242 (1971).

[10]Martin, P.L.: Structural analysis of the Chisel Lake orebody; Trans. Can. Inst. Mining Met., vol. LXIX, pp. 208-214 (1966).

[11]Coats, C.J.A., Clark, L.A., Buchan, R. and Brummer, J.J.: Geology of the copper-zinc deposits of Stall Lake Mines Ltd., Snow Lake area, Manitoba; Econ. Geol., vol. 65, pp. 970-984 (1970).

[12]Howkins, J.B. and Martin, P.L.: A comparison between the Flin Flon and Snow Lake orebodies of Hudson Bay Mining and Smelting Co. Ltd.; Paper presented to the 72nd Ann. Gen. Mtg., Can. Inst. Mining Met. (1970).

[13]Sinha, A.K.: Model lead and radiometric ages from the Churchill Province, Canadian Shield; Geochim. et Cosmochim. Acta, vol. 34, pp. 1089-1106 (1970).

---

8. GEOLOGICAL STUDY OF SILVER DEPOSITS IN CANADA

Project 680060

R.I. Thorpe

Mineralogy

More than 200 polished sections have been prepared for mineralogical study of ores from silver-bearing deposits. Polished section study of ore from some of the veins of the Ainsworth camp, British Columbia, resulted in the identification of a small to minor amount of stannite in ore from a few of the deposits. A total of 26 polished sections were studied, and these were from 22 specimens collected from the area many years ago and kindly supplied to the writer by the British Columbia Department of Mines and Petroleum Resources. Stannite was most abundant in a specimen of ore from the Tariff property. A very few grains of stannite were noted in ore from the Little Donald, Silver Glance and Ida C properties. The recognition of stannite in these ores may be of little significance in itself, but could be a geochemical indication that intrusions of the Nelson batholith are favourable for tin prospecting.

The Tariff and Little Donald properties are located west of Mile Point near an intrusive lens of granite. The Silver Glance vein is just south of Lendrum Creek and about 1 1/4 miles northwest of Florence Townsite. The Ida C property is about 1/2 mile east of the Silver Glance vein. For further location information on all these properties see reference 1.

Electron microprobe determination of the silver, mercury and tin contents of a suite of tetrahedrite-tennantite specimens is being done. The object of this study is to test the usefulness of minerals of the tetrahedrite-tennantite series as geochemical indicators for these elements.

Lead isotopic results

Lead isotopic results have been obtained by the writer for eleven samples of galena from the silver veins of the Great Bear Lake area, Northwest Territories. These are interpreted (see Thorpe, separate contribution, this report) as indicating an age of about 1625 m.y. for the

mineralization. Two galena samples from silver veins in the Hope Bay area, east of Bathurst Inlet in the Slave Province, suggest an age of about 1490 to 1535 m.y., although this is based on preliminary data and may be subject to later revision. There is very little geochronological data for the area, but there is a distinct possibility that the diabase sills in the area are of approximately this age. A sample collected by H. H. Bostock from a porphyritic diabase body at Rockinghorse Lake gave a whole rock K-Ar age of 1570 ± 115 m.y.[2]. This location is about 200 miles from Hope Bay, but the date may be a valid one for the extensive diabase sills which are very continuous along and near the base of the Goulburn Group[3]. These sills extend east to Bathurst Inlet and could be cogenetic with those at Hope Bay. Fraser (pers. comm.) has recently obtained a whole rock K-Ar age of 1560 ± 118 m.y. for a sample from a diabase dyke just east of Bathurst Inlet (at 67°25'N, 107°34'W). This dyke belongs to a swarm with a north-northwest to north trend distinct from the northwest trend of the Mackenzie swarm that is widely represented in the western Canadian Shield. Even if the diabase sills at Hope Bay are found to be related to the younger (mean age 675 m.y.) diabase sills of the Coronation Gulf–Bathurst Inlet area[4], the dyke age obtained by Fraser still suggests an event in the area that could be related to the silver mineralization.

---

[1] Fyles, J.T.: Geology of the Ainsworth-Kaslo area, British Columbia; B.C. Dept. Mines Petroleum Resources, Bull. No. 53, 125 pp. (1967).

[2] Wanless, R.K., Stevens, R.D., Lachance, G.R. and Delabio, R.N.: Age determinations and geological studies, K-Ar isotopic ages, Report 9; Geol. Surv. Can., Paper 69-2A, p. 38 (1970).

[3] Fraser, J.A.: Geological notes on northeastern District of Mackenzie, Northwest Territories; Geol. Surv. Can., Paper 63-40, 20 pp. (1964).

[4] Fahrig, W.F., Irvine, T.N. and Jackson, G.D.: The paleomagnetism of the Franklin intrusions; Can. J. Earth Sci. (in press).

EXPLORATION GEOPHYSICS

9. ELF NATURAL ELECTROMAGNETIC FIELD INVESTIGATIONS

Project 680123

R.H. Ahrens and L.S. Collett

Since our experience with airborne AFMAG surveys as an aid to mapping tectonic geological features (refs. [1, 2, 3, 4]), there are certain improvements that can be made to the present state of the art. One major disadvantage in the method is the seasonal nature of useful field strengths. An investigation has been initiated to study the nature of the natural electromagnetic fields at extremely low frequencies (ELF), especially in the Schumann resonance band from 8 to 40 Hz. The EM fields in this audio and sub-audio frequency range will presumably allow for reconnaissance surveys to be conducted on a year-round basis.

A theoretical study has been done on an orthogonal 3-coil sensor system for determining the wave structure of the ELF EM fields. Equipment is being designed to measure the relative magnitude of the total magnetic field vector. Effort is being concentrated on the build-up time and current response from a plane EM wave induced voltage in a resonant circuit where the direction of the planar wave is in general not normal to the surface of incidence. The design idea of the receiving system is outlined in the block diagram shown in Figure 1. The magnetic component of the plane EM wave induces in the three orthogonally positioned coils L_1, L_2 and L_3. The periodically time varying voltages are preamplified, filtered and frequency up-converted (FUC) from 8 Hz to 9800 Hz. Sensitive Fluke Model 207-1 VLF receivers are used to detect the resultant frequency from the sensors. The induced voltages and their phase differences are monitored.

The equipment is divided into two units, console-1 as shown in Figure 1 and console-11. In console-1, the data are recorded in analogue form and the construction is now nearing completion. Consideration for the design of the second console-11 is for statistical studies of the data which will be recovered by the use of real time cross-correlation and Fourier analysis techniques.

The purpose of studying these ELF natural electromagnetic fields is to learn more about their behaviour so that equipment specifications can be determined for the next generation airborne system to be used for reconnaissance surveys.

---

[1] Collett, L.S.: AFMAG/ELF surveys, Uranium City area, Saskatchewan, upper Nelson River area, Manitoba; in Report of Activities, Part A, April to October, 1968; Geol. Surv. Can., Paper 69-1A, p. 79 (1969).

[2] Collett, L.S.: AFMAG survey, St. Mary's River area, Nova Scotia; in Report of Activities, Part A, April to October, 1969; Geol. Surv. Can., Paper 70-1A, pp. 70-71 (1970).

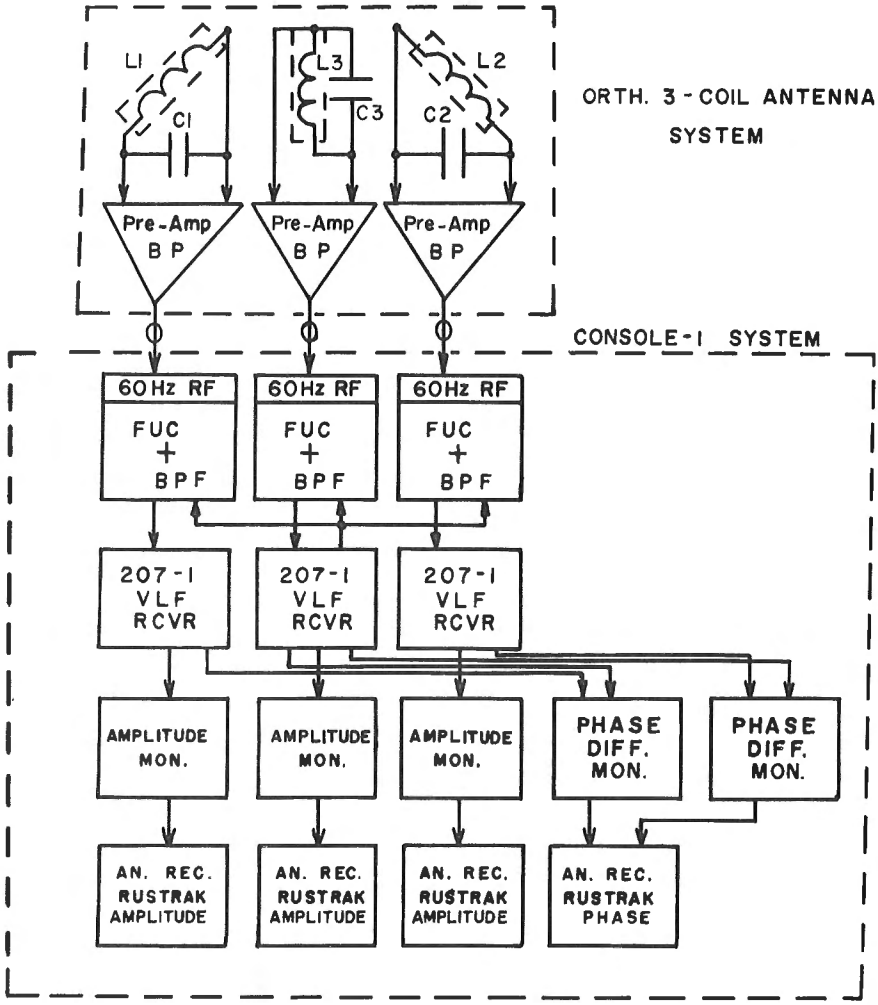

FIG-1 SCHEMATIC OF ANTENNA AND CONSOLE-I SYSTEM FOR GROUND AND AIRBORNE ELF RECEPTION

NOTE CONSOLE-II IS AN EXTENSION TO REALTIME CORRELATION, SIGNAL AVERAGING AND POWER SPECTRA DETERMINATION

[3]Collett, L.S.: AFMAG surveys; in Report of Activities, Part A, April to October, 1970; Geol. Surv. Can., Paper 71-1A, p. 47 (1971).

[4]Collett, L.S. and Bell, C.K.: AFMAG use in geological interpretation; Can. Mining Met. Bull., vol. 64, No. 706, pp. 39-47 (1971); Trans. Can. Inst. Mining Met., vol. LXXIV, pp. 33-41 (1971).

---

10. AIRBORNE RADIOMETRIC SURVEY MAPS AND PROFILES

General

Project 670050

A.G. Darnley and R.L. Grasty

Previous reference has been made[1, 2] to the fact that the Geological Survey of Canada conducted airborne gamma-ray spectrometer surveys with high sensitivity equipment in the Bancroft area of Ontario and Eldorado (Uranium City) areas of Saskatchewan in 1969, and in the Elliot Lake, Ontario, and Fort Smith/Great Slave Lake, NWT areas in 1970.

The main portion of the Bancroft survey is now available on OPEN FILE, and can be obtained by special order from Campbell Reproductions Ltd., 85 Sparks Street, Ottawa, Ontario, or inspected at Geological Survey of Canada libraries in Ottawa, Calgary and Vancouver.

It consists of data compiled for an area of approximately 400 square miles bounded by Latitudes 44°51' and 45°15' and Longitudes 77°48' and 78°05'W. The measurements were made using twelve 9 x 4 in. NaI (Tl) detectors (a total volume of approximately 3000 cu. in) with a 128 channel spectrum analyser, flown at a mean terrain clearance of 400 feet and a mean speed of 120 m.p.h. Details concerning the survey are published elsewhere[3].

The data are presented in both profile and contour map form. There are profiles along 61 flight lines (mean spacing 0.25 mile), plotted at a scale of 1:250,000 and seven maps on a scale of 1:50,000. All profiles and contours have been computer plotted, the contouring program used being that developed by Holroyd and Bhattacharyya[4]. The contour maps will be published in due course in the Geological Survey of Canada Geophysical Map Series. The profiles will only be available through the OPEN FILE release.

Each profile shows:

i) Integral counts per 0.5 s (0.4 → 2.80 Mev).

ii) Potassium counts per 2.5 s.

iii) Uranium counts per 2.5 s.

iv) Thorium counts per 2.5 s.

v) Ratio uranium:thorium counts.

vi) Ratio uranium:potassium counts.

vii) Ratio thorium:potassium counts.

viii) Terrain clearance, in feet.

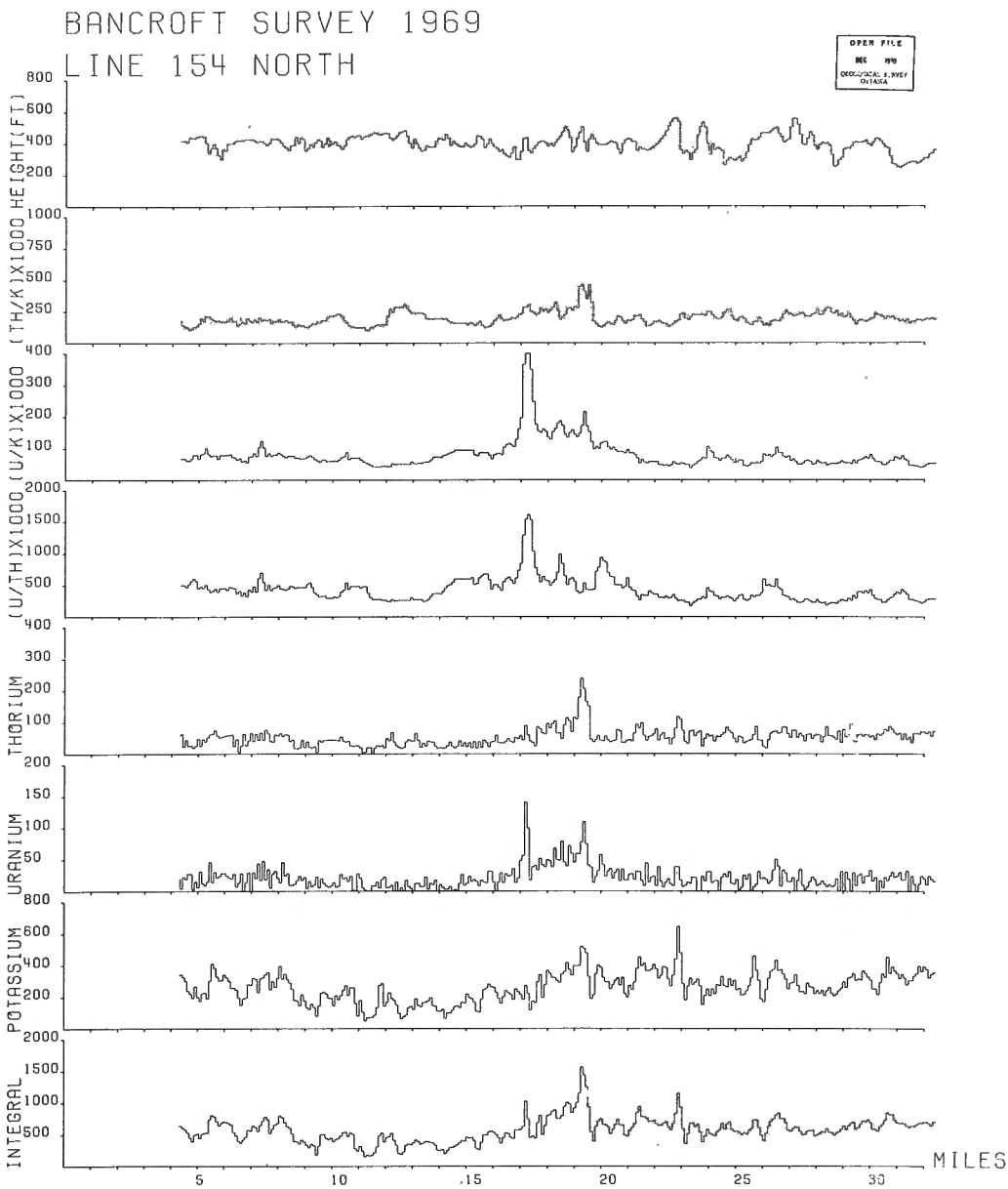

Figure 1. Example of a computer controlled plot of a fully correlated gamma-ray spectrometer profile. This line crosses the uraniferous belt about 0.3 mile east of the Greyhawk property.

Figure 2. (opposite) Example of a portion of the U:Th ratio map. Mean spacing between flight lines is 0.25 mile. Centres of principal anomalies are located over Bicroft (lower left) and Faraday (centre) dumps.

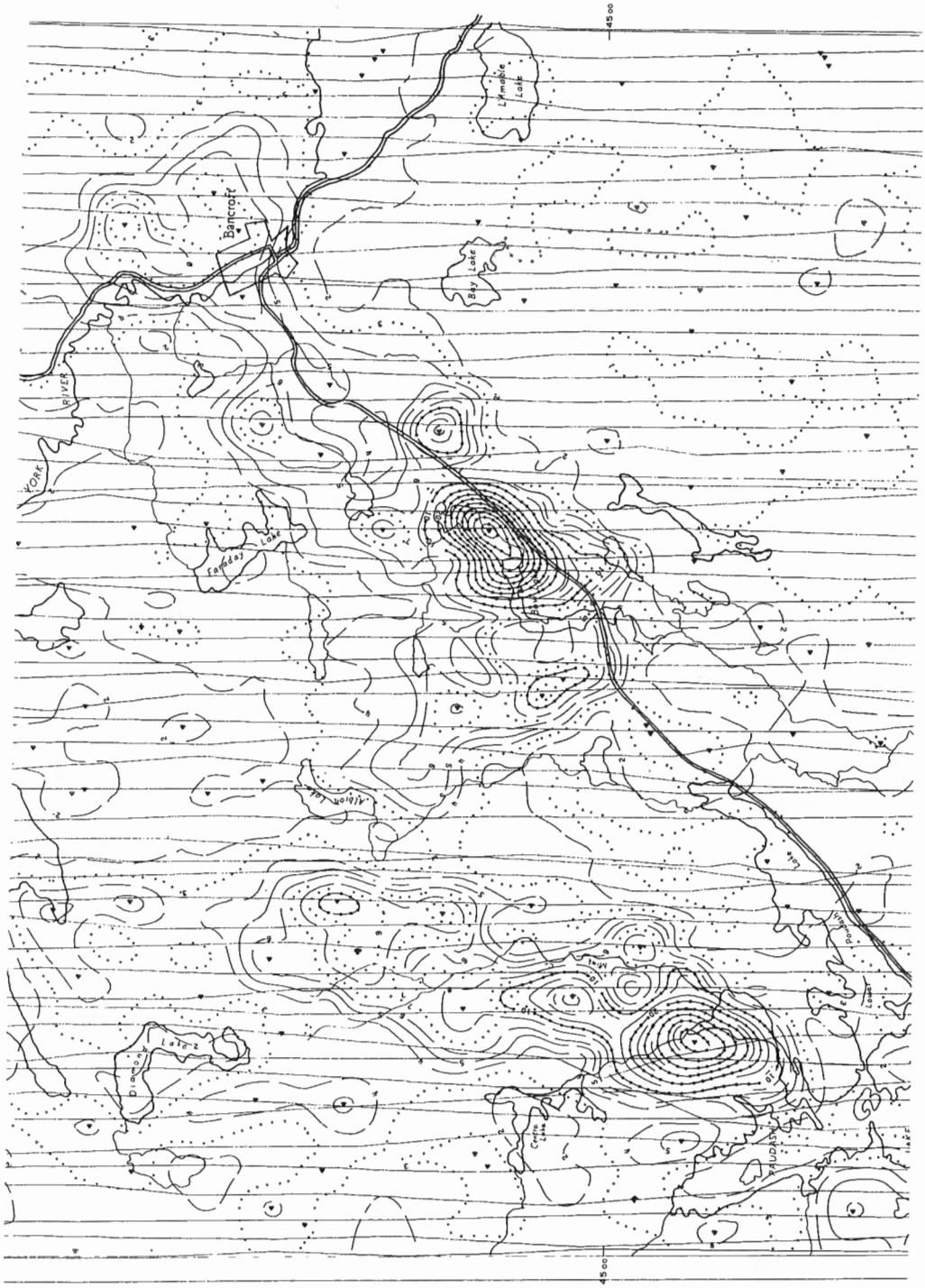
4500
Bancroft
Bay Lake
YORK RIVER
Talpiddy Lake
Albion Lake
Diamond Lake
4500

plotted against distance along each line. Items (i) to (v) inclusive, and the derived ratios (v) to (vii) inclusive, are corrected for atmospheric background radiation, and deviations from the nominal terrain clearance, following procedures already described[3, 5]. Potassium and uranium counts are corrected for Compton scattering following the procedure in[6].

Separate maps show items (i) to (vii) listed above, with contour intervals of 10 counts for (i) to (iv). These contour intervals are approximately equivalent to 0.06 per cent K, 0.4 ppm U, and 1 ppm Th. Each radiometric map is reproduced on a base showing individual flight lines and the principal geographic features in the area. The maps are intended to provide an overall picture of the radiometry of the area, whilst the profiles provide more detailed information along the lines of flight. Examples of a profile and of part of a map are shown in Figures 1 and 2.

The ratio displays accentuate any unusual relative concentration of the radioelements, and may be considered as emphasizing enrichment (or impoverishment). Thus the U:Th and U:K ratio displays are important with respect to possible economic occurrences. Whilst high values of these ratios are not certain indicators of mineralization, the probability is much increased where these ratios are high.

The surveys of the Eldorado (Uranium City) area of Saskatchewan is now in the final stage of preparation for OPEN FILE release and is expected to be available to the public when this report is published. Release of the other areas flown and publication of maps will follow in due course. The general format is expected to remain similar, although detailed improvements in data reduction procedures will be made from time to time.

---

[1]Darnley, A.G. and Grasty, R.L.: in Rept. of Activities, April to October, 1969; Geol. Surv. Can., Paper 70-1A, p. 72 (1970).

[2]Darnley, A.G.: in Rept. of Activities, April to October, 1970; Geol. Surv. Can., Paper 71-1A, pp. 48-49 (1971).

[3]Darnley, A.G. and Grasty, R.L.: Mapping from the air by gamma-ray spectrometry; in Proceedings Third International Geochemical Prospecting Symposium, Special Volume; Can. Inst. Mining Met., Montreal (1971).

[4]Holroyd, M.T. and Bhattacharyya, B.K.: Automatic contouring of geophysical data using bicubic spline interpolation; Geol. Surv. Can., Paper 70-55 (1970).

[5]Darnley, A.G., Brisbow, Q. and Donhoffer, D.K.: Airborne gamma-ray spectrometer experiments over the Canadian Shield; Symposium Nuclear Techniques and Mineral Resources, International Atomic Energy Agency, Vienna, pp. 163-186 (1968).

[6]Grasty, R.L. and Darnley, A.G.: Calibration of gamma-ray spectrometers for ground and airborne use; Geol. Surv. Can., Paper 71-17 (1971).

General

11. THEORETICAL STUDY ON MEMBRANE POLARIZATION AND COMPLEX MOBILITY IN MOIST ROCKS

Project 630049

G. Finzi-Contini*

In this short paper, a number of items related to the electrical behaviour of certain moist rocks that show membrane polarization effects, are dealt with theoretically. One of the important ideas in this work is the consideration of the complex mobility of mobile charges moving along pores in moist rocks that exhibit membrane polarization. The ideas in this work have been derived from Madden and Marshall[1], Fraser et al.[2] and Finzi-Contini[3,4].

The mobile charge, q, in the following equation is acted upon by a number of forces; namely, a linear lattice electrostatic force ($-Q^*x$), a viscous force ($-K\dot{x}$; $\dot{x}=dx/dt$) and finally the electric field force $qE_o e^{-i\omega t}$:

$$K\dot{x} + Q^*x = qE_o e^{-i\omega t} \tag{1}$$

Resolving (1) and neglecting the non-steady state term, the following solution can be derived

$$\frac{dx/dt}{E_o e^{-i\omega t}} = \left[\frac{K\omega^2}{K^2\omega^2 + Q^{*2}} - j\,\frac{Q^*\omega}{K^2\omega^2 + Q^{*2}}\right] q = \dot{U} \tag{2}$$

where $\dot{U}$ is the theoretical complex mobility. It should be noted that the real and imaginary parts of this mobility are non-linear functions of frequency, $f(\omega=2\pi f)$.

Rearranging (2) and considering the typical cubic lattice length $2a$[3,4] one can write:

$$j = \frac{d\ q(x/a)\ /dt}{4a^2} = \frac{q^2}{4a^3}\left[\frac{K\omega^2}{K^2\omega^2 + Q^{*2}} - j\,\frac{Q^*\omega}{K^2\omega^2 + Q^{*2}}\right] E_o e^{-i\omega t} \tag{3}$$

where j is a current density. The term in the square bracket can be assumed to be a specific admittance; it should be noted that the latter gives a leading current density with regard to the applied electric field, $\vec{E}$.

This specific admittance can be used to build up analog electric circuits having non-linear parameters with frequency. It is perhaps interesting to remember that different specific admittances can be considered with reference to both negative and positive charges[5]. Their behaviour could be described by introducing certain values for K.

One should also note that both these non-linear conductivities and non-linear capacitances with frequency can be inserted in other electrical networks in order to simulate membrane polarization.

---

*Canada Council Fellow, 1970-71 (Osservatorio Geofisico, University of Siena, Siena, Italy).

Acknowledgments

This work was supported by a Fellowship from the Canada Council of Arts to whom I am very grateful. I wish to express my thanks to L.S. Collett, Head, Electrical Methods Section, Exploration Geophysics Division for giving me the opportunity to work for a period of 4 months in his laboratory; also I wish to thank Dr. T.J. Katsube for the many helpful discussions on the improvement of the lattice theory.

[1]Madden, T.R. and Marshall, D.J.: Induced Polarization. A study of its causes and magnitudes in geologic materials. Final report RME-3160, Mass. Inst. Technol., June 1959.

[2]Fraser, D.C., Keevil, N.B., Jr. and Ward, S.H.: Conductivity spectra of rocks from the Craigmont ore environment; Geophys., vol. 29, No. 5, pp. 832-847 (1964).

[3]Finzi-Contini, G.: Un modello fisico-matematico simulante fenohem non-lineari di polarizzazione indotta. Atti Acad. Naz. Lincei, Rend. CL. Sc. Fis., Serie VIII, XLVI, FASC. N. 6, pp. 1-6 (1969).

[4]Finzi-Contini, G.: Sulla polarizzazione indotta simulata mediante un modello fisico-matematico. Ist. Di Fisica Terrestre, Geodesia E Geografia Fisica, Univ. Di Padova, Pubbl. N. 148, 1970.

[5]Finzi-Contini, G.: Theoretical study on membrane polarization in moist rocks at low frequency. Final report to Canada Council of Arts, 1971, Ottawa (in preparation).

12. SEISMIC SURVEY, SOUTHWESTERN CAPE BRETON ISLAND, NOVA SCOTIA

Project 680037

R.M. Gagne

A shallow seismic survey was conducted on southwestern Cape Breton Island between August 23 and September 2, 1970, in the project area of D.R. Grant, Quaternary Research and Geomorphology Division (Fig. 1). A portable seismograph, Huntec model FS-3, was used to test the feasibility of the shallow refraction seismic method to determine the distribution and thickness of surficial materials within the area. "Abundant glacial debris, disruptive topography and shifting ice flow were thought to favour the burial of preglacial valleys and their alluvium, providing groundwater aquifers for current community water supply programs"[1]. Seismic locations were selected in co-operation with the project geologist.

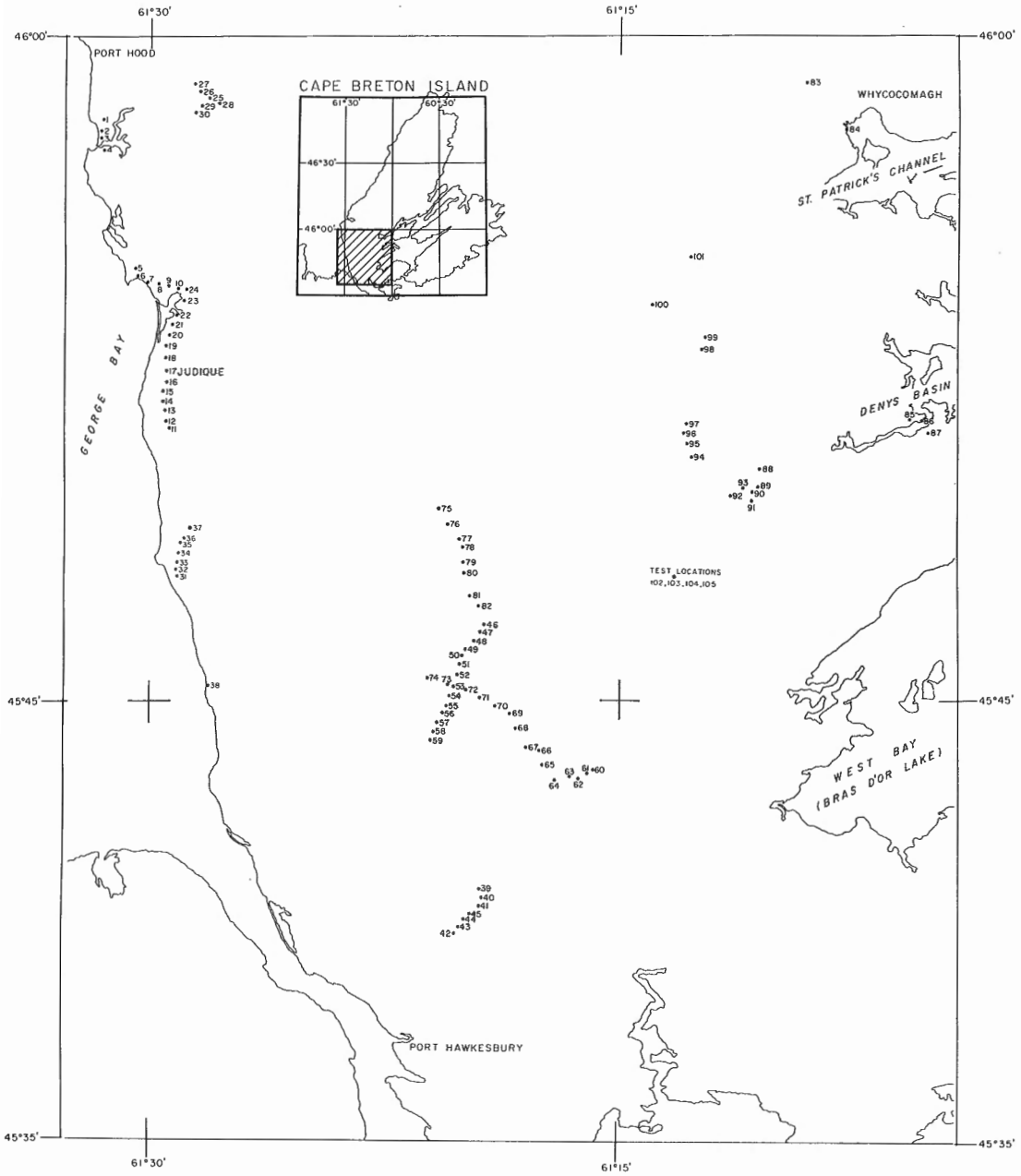

Figure 1. Location of seismic control, southwestern Cape Breton Island.

The topography of the area is incised by a network of steep-sided V-shaped valleys. The survey area is covered by a thin cover of glacial drift composed chiefly of till and stratified sand and gravel, with recent deposits of stream alluvium, beach sand and gravels.

Bedrock underlying the glacial drift varies in age from Carboniferous to Pre-Carboniferous[2]. The lithology of bedrock formations differs only slightly with sandstone being its major constituent.

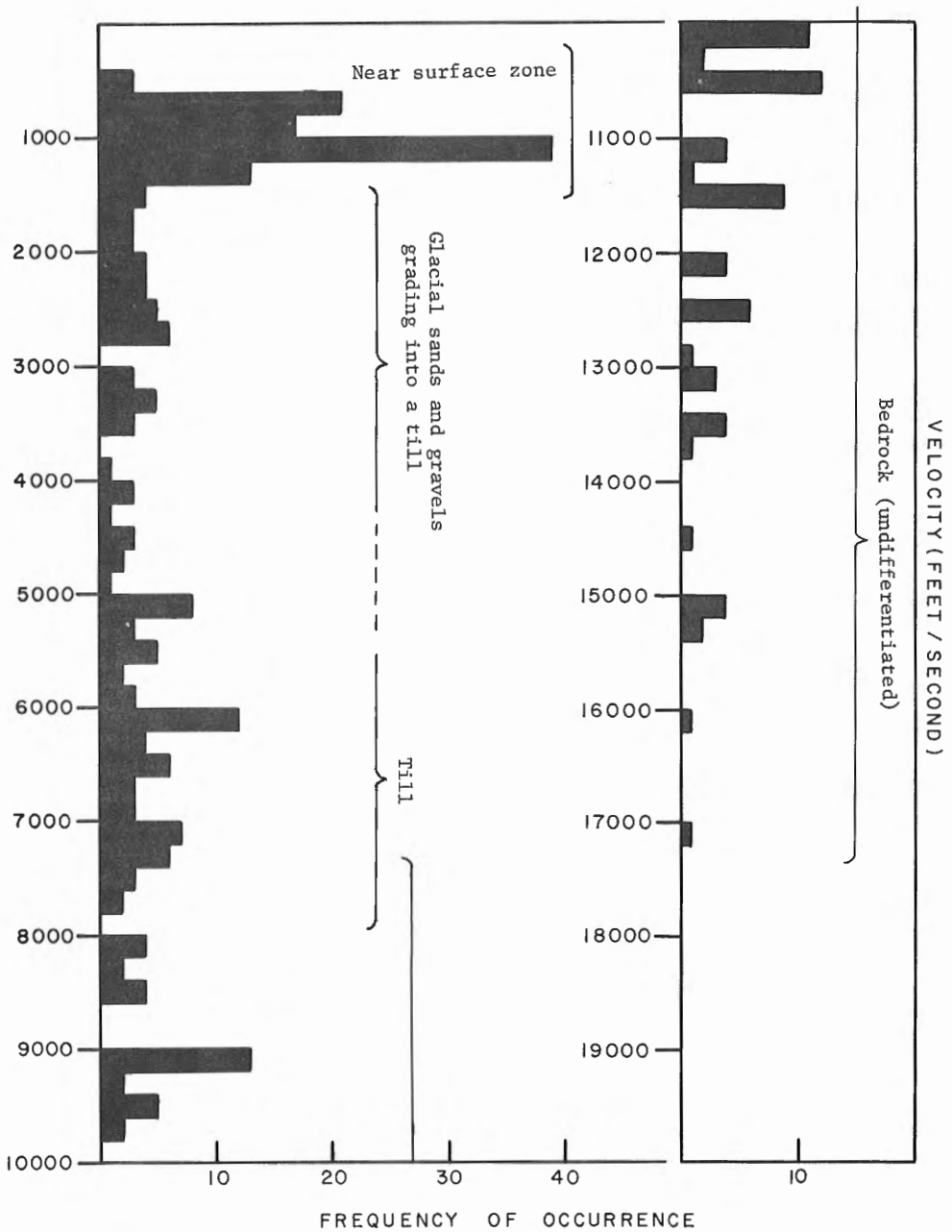

Figure 2. Histogram of observed velocities versus frequency of occurrence, southwestern Cape Breton Island.

The histogram of occurrence versus the apparent velocities from single-ended refraction profiles (Fig. 2) indicates the possibility of correlating seismic velocities with surficial materials over the project area. Profiles are shown as straight line sections with the refraction velocities obtained shown within the section (Figs. 3 to 7).

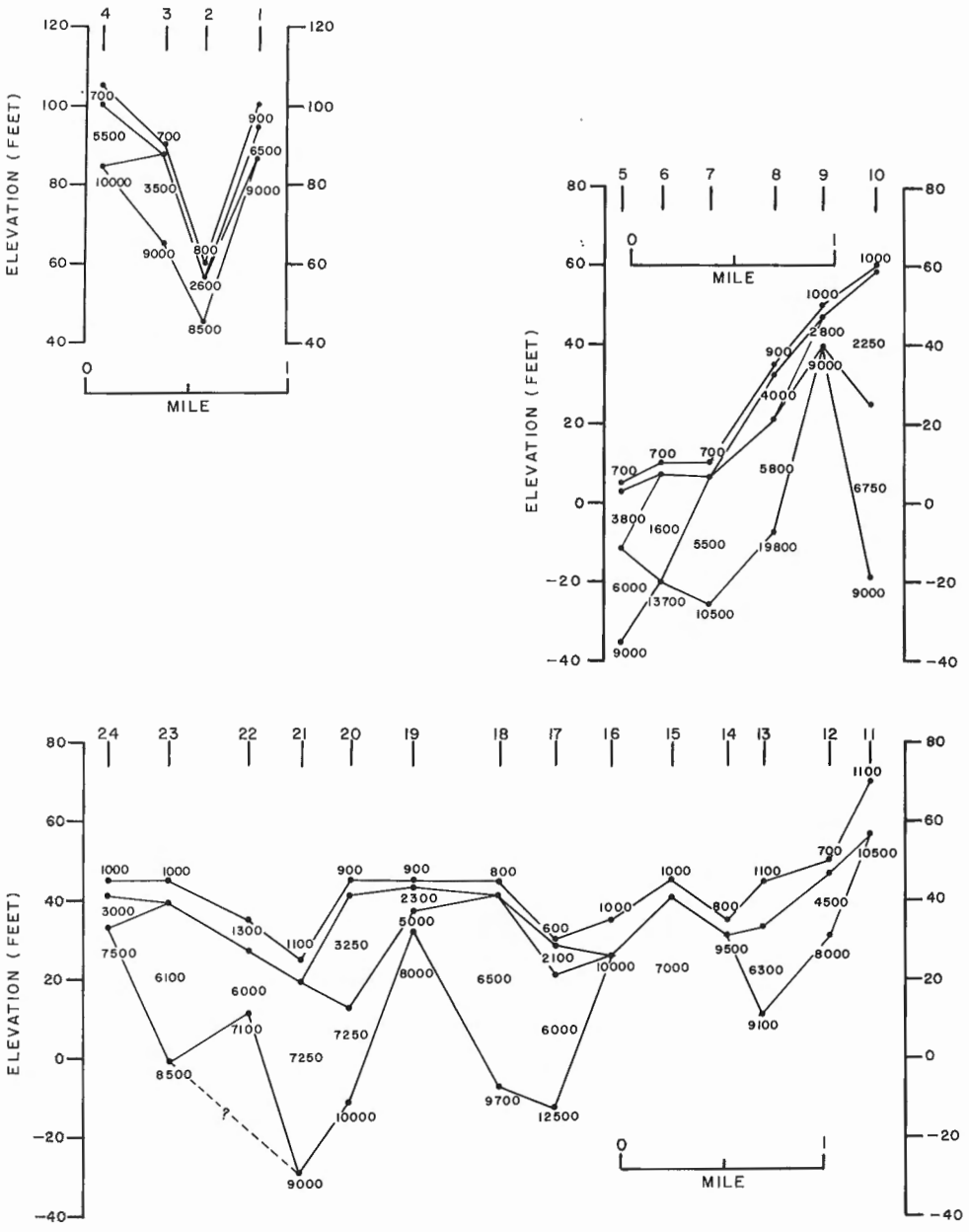

Figure 3. Seismic sections, southwestern Cape Breton Island.

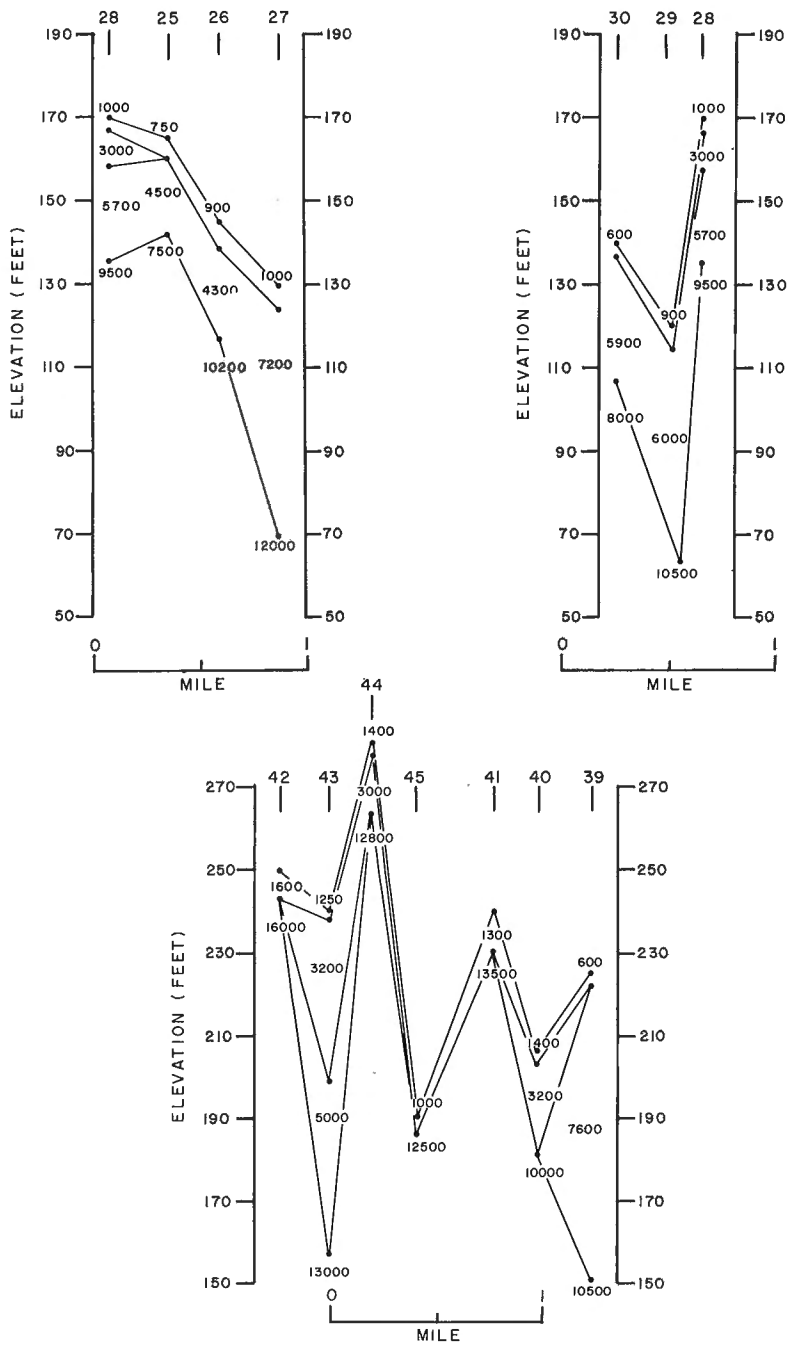

Figure 4. Seismic sections, southwestern Cape Breton Island.

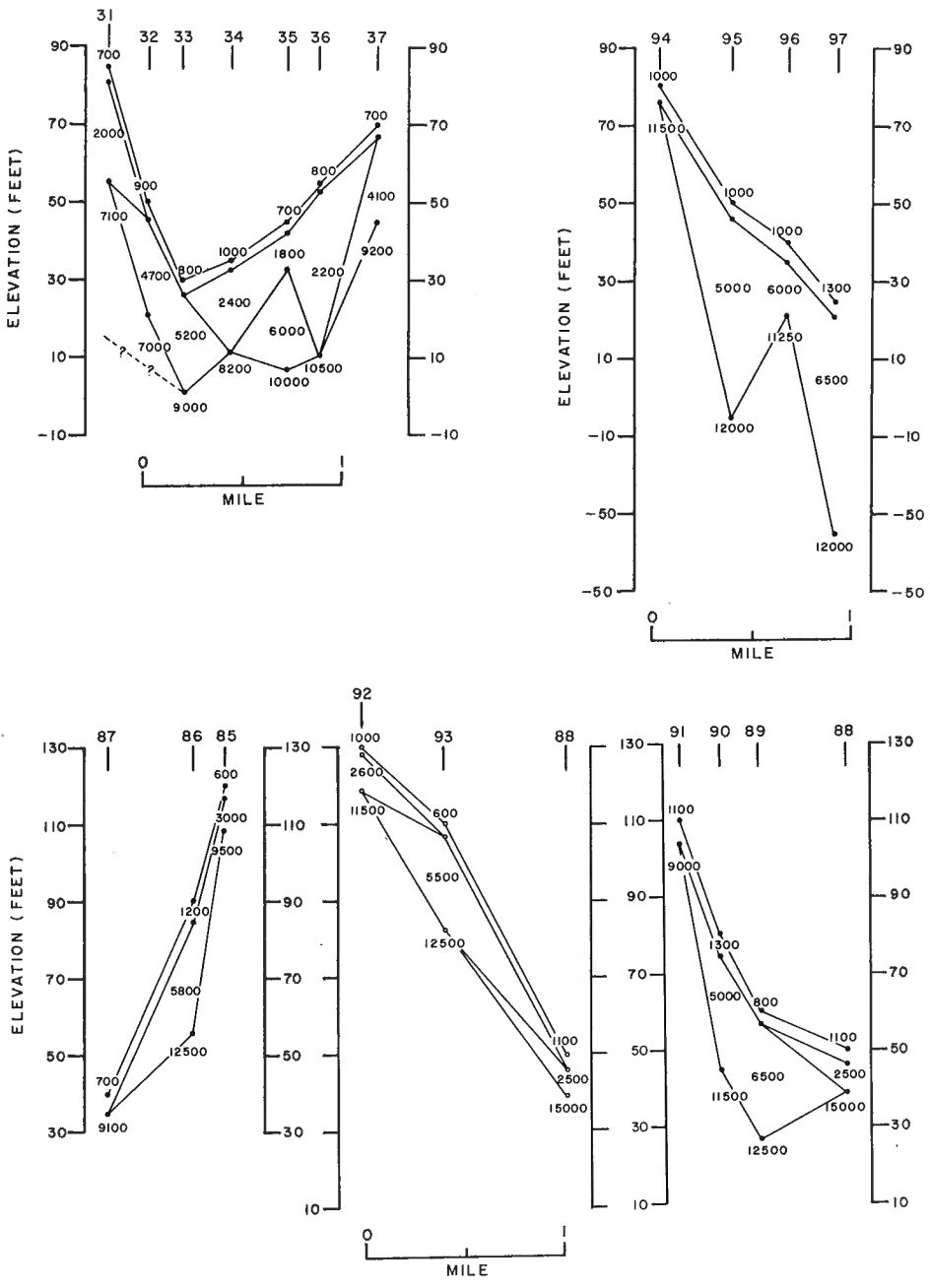

Figure 5. Seismic sections, southwestern Cape Breton Island.

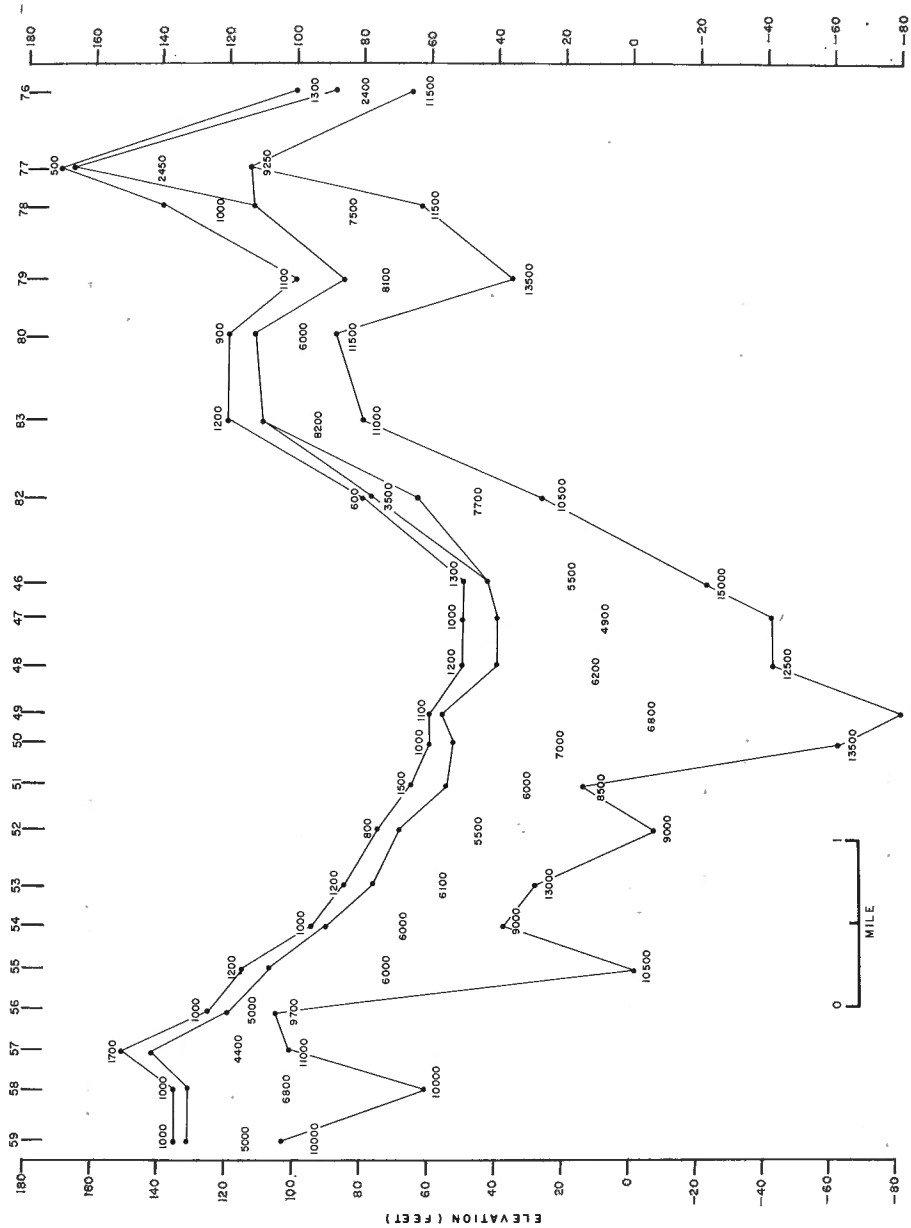

Figure 6. Seismic section, southwestern Cape Breton Island.

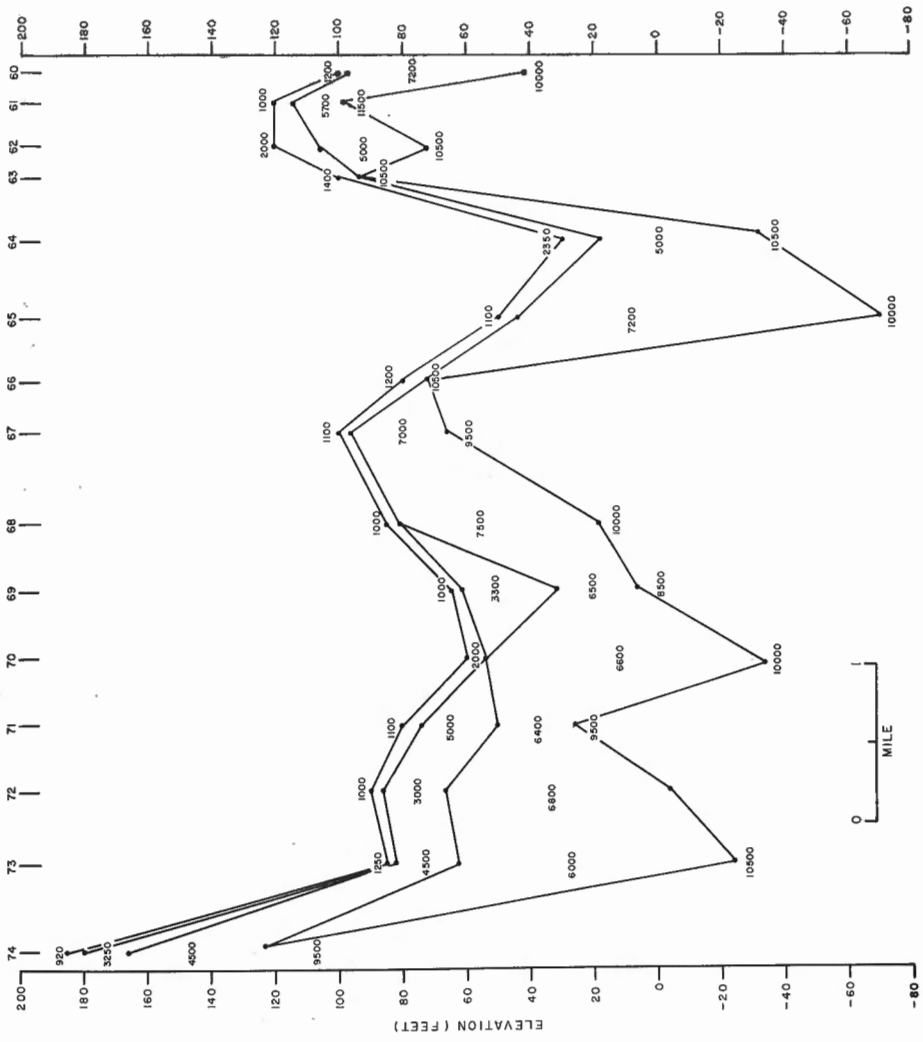

Figure 7. Seismic section, southwestern Cape Breton Island.

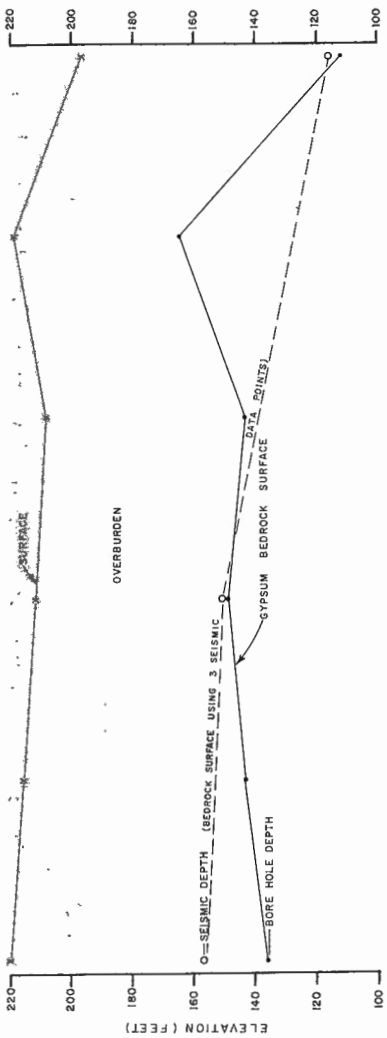

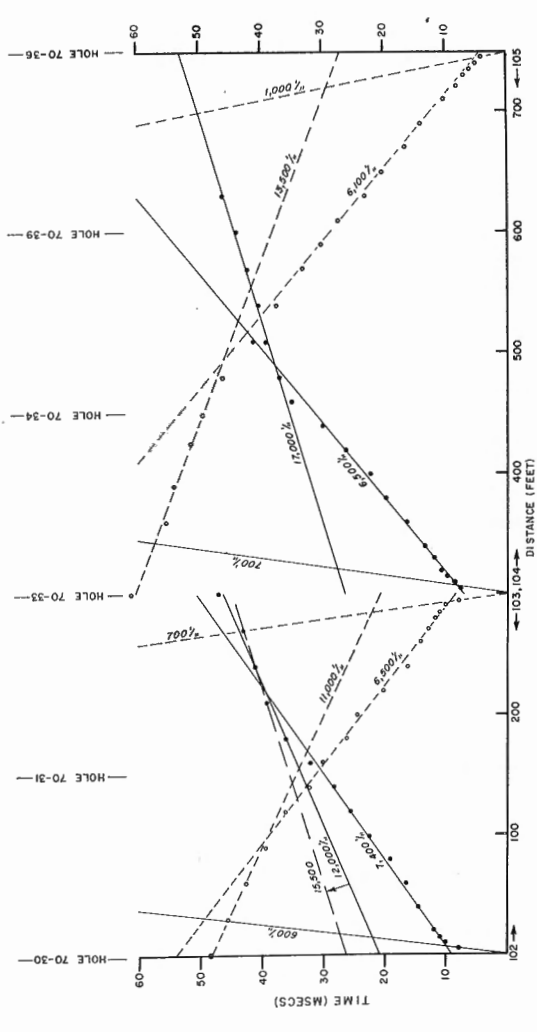

Figure 8. Time-distance plot and comparison section of test site, Georgia-Pacific Gypsum quarry, Cape Breton Island.

Seismic lines were run in the western part of the project area across present stream alignments, it being postulated that preglacial drainage from the east could have produced channels which were later filled in. Locations 1 to 4, Figure 3, are located at the mouth of the Little Judique Brook and exhibit a bedrock depression beneath the present stream course. A layer of recent sand (velocity range 2600 to 3500 feet per second) was deposited along the mouth of the stream with a till deposit along the steep valley sides.

Locations 5 to 24, Figure 3, and locations 31 to 37, Figure 5, were run along the east coast of George Bay in an attempt to delineate the preglacial drainage from the Craignish Hills. These profiles reveal a very irregular bedrock surface infilled with till and, in some areas, covered with recent sands and gravels (velocity range 4000 to 7800 feet per second). Based on limited control it can be deduced that the present drainage appears to occupy re-excavated bedrock channels. No other bedrock channels were detected along these lines.

Profiles run across the valley of the Little Judique Brook at locations 25 to 30 inclusive, Figure 4, indicate a narrow bedrock depression below the present course of the stream.

A line approximately 3 miles north of the town of Port Hawkesbury at locations 39 to 42, Figure 4, indicates that a narrow bedrock depression exists below the present course of North Little River and Northwest Arm Brook.

Profiles run on the floor of the Inhabitants Valley reveal meandering channels which are postulated to have been cut by a previous water course. These channels are filled with till which must date from a previous nonglacial period (Figs. 6 and 7).

Selected locations west of River Denys Basin reveal that the present day river occupies a bedrock channel which has been infilled with till, locations 88 to 97, Figure 5.

A test site on the property of Georgia-Pacific Gypsum Division quarry near River Denys yielded records of poorer quality than normally obtained in the area. Operational difficulties were encountered because of the surface conditions. The author would like to gratefully acknowledge the kind assistance of Mr. J. Graham, Geologist, Georgia-Pacific Gypsum for release of borehole data for correlation with seismic data. Comparison of borehole and seismic data revealed that overburden thicknesses on profiles which were computed from rather poor seismic data yielded reasonable correlation with borehole depths (Fig. 8). On reinterpretation of profile 102, which is a very poor record, a very low bedrock velocity was removed and a minimum depth calculation based on 15,500 feet per second (average of apparent bedrock velocities from profiles 105 and 104 yielded a depth of 71.5 feet, a 17 per cent error). The accuracy is directly dependent on the surface conditions for record quality and closeness of profile spacing for detail required.

Approximately 1 mile north of profile 38 near latitude 45°45' on George Bay, exposures indicate an overburden section of a gravel layer from 10 to 30 feet in thickness overlying 30 feet of till. Seismic velocities of 500, 2600, 6600, and 10,200 feet per second were recorded at this location with computed thicknesses of 3, 8 and 42 feet.

Conclusions

1. It is possible to depict the bedrock topography in the project area using the seismic method.

2. The quality of refraction seismic data is fair to good and the seismic velocities computed within the overburden are usually consistent. It is therefore possible to make general correlations of drift materials with seismic velocities within the area.

3. The observed velocities indicate that no relationship exists between unreversed refraction velocities and bedrock lithology within the project.

4. It is impossible to map the bedrock topography of any area of 500 square miles with 100 profiles; it would be necessary to run closely spaced profiles because of the complex, irregular bedrock topography.

---

[1]Grant, D.R.: Surficial geology, southwestern Cape Breton Island, Nova Scotia; Geol. Surv. Can., Paper 71-1, Part A, pp. 161-164 (1971).

[2]Kelley, Danford G.: Baddeck and Whycocomagh map-areas; Geol. Surv. Can., Mem. 351 (1967).

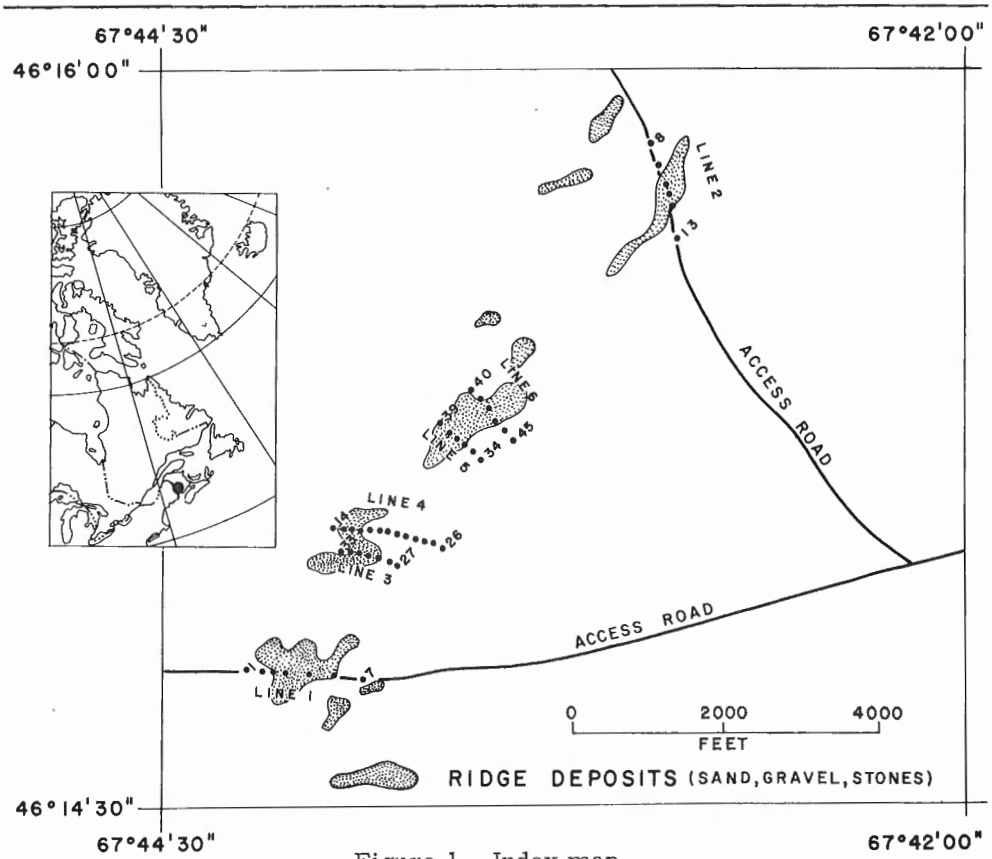

Figure 1. Index map.

#13 Gagne

13. A HAMMER SEISMIC SURVEY, WOODSTOCK AREA, NEW BRUNSWICK 21J/4, 5

Project 670075

R.M. Gagne

A seismic survey using a Huntec model FS-3 hammer seismograph was conducted over Pliestocene deposits, 12 miles northwest of Woodstock, New Brunswick (Fig. 1). The purpose of the survey was to determine the bedrock topography beneath the deposits in order to assist in the definition of the direction of ice movement at the time of deposition.

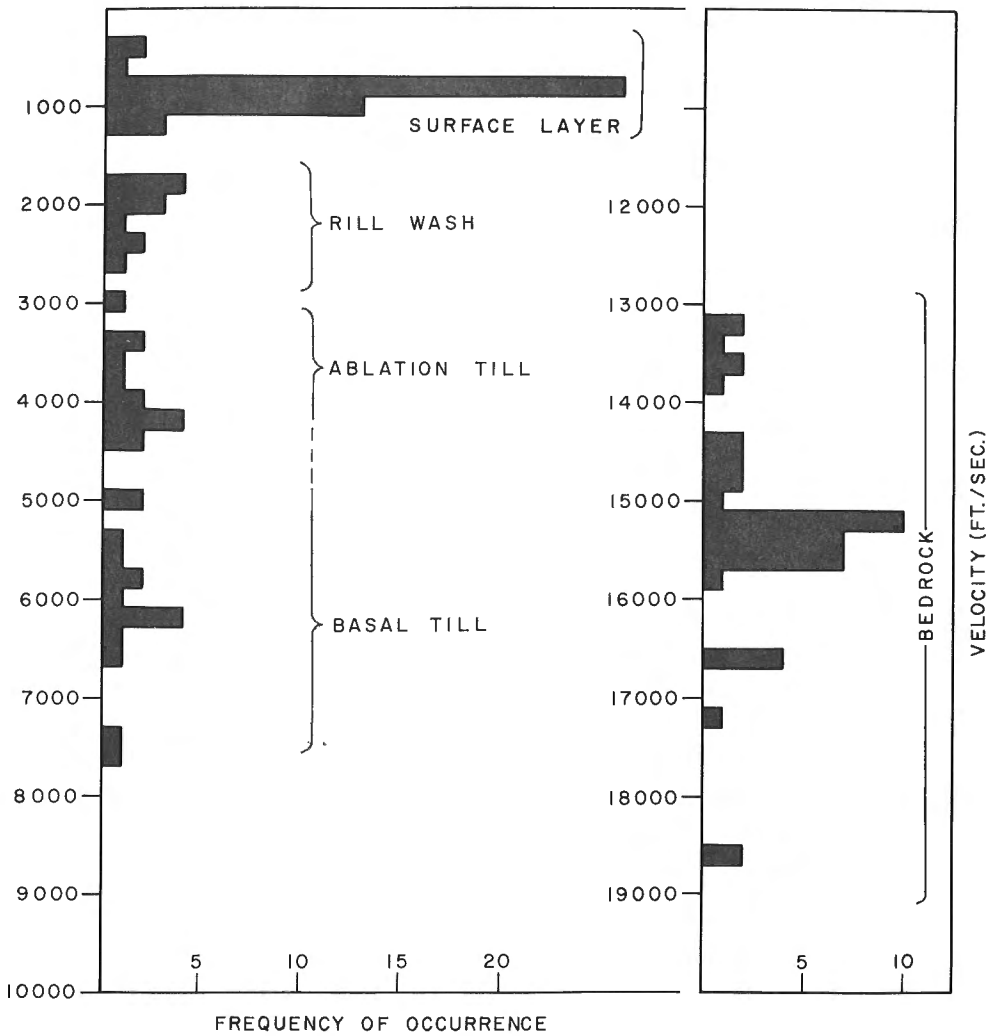

Figure 2. Histogram of velocity versus frequency of occurrence.

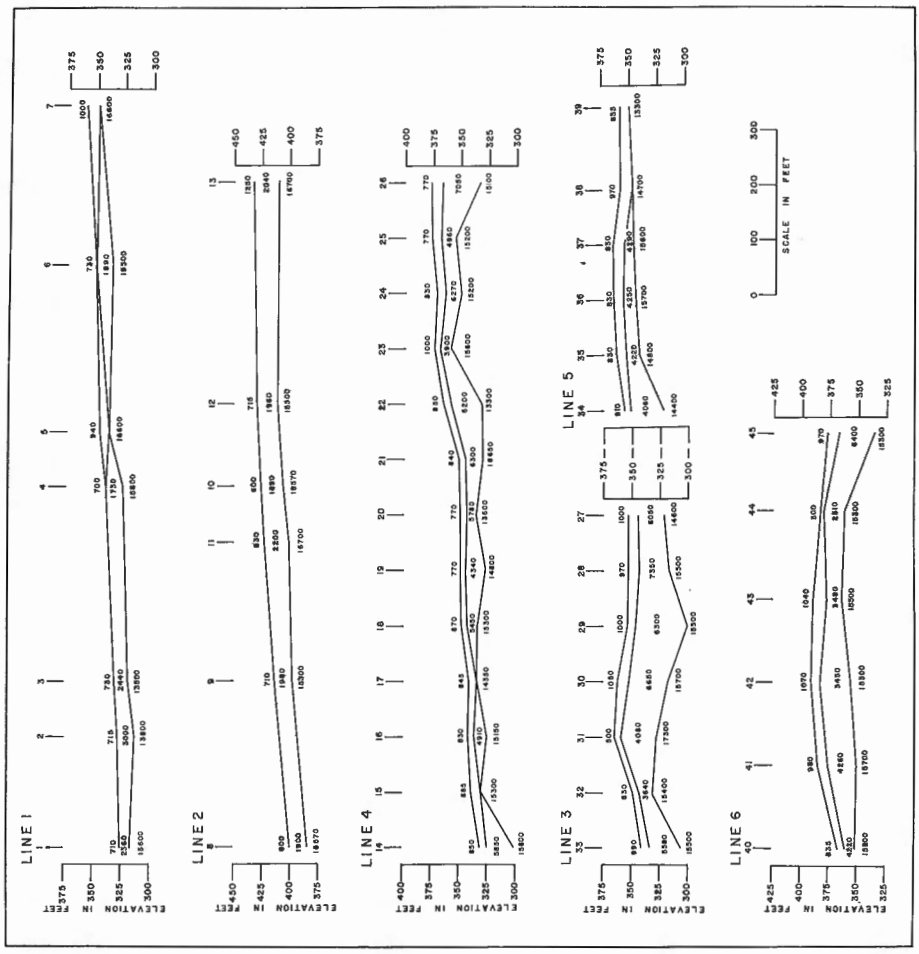

Figure 3. Sections showing results of seismic survey.

Forty-five seismic stations were surveyed. On lines 3, 4, 5 and 6 unreversed profiles were completed every 100 feet while on lines 1 and 2 reversed seismic profiles were completed.

Surface relief of the project area varies between 325 feet a.s.l. at seismic station 1 and 434 feet a.s.l. at station 13.

Surficial geology of the area has been mapped in detail by Lee[1]. The area is covered by a thin layer of rill wash overlying either the basal till or bedrock. A compacted till may underlie other units and in some localities is exposed. The third unit in the area is an abalation till which is loosely compacted and oxidized throughout. The bedrock is dark grey slate, with buff and green slate and greywacke of Silurian age.

A histogram of velocity versus frequency of occurrence (Fig. 2) indicates four possible ranges of apparent velocities. A surface layer is observed with a velocity range of 300 to 1,400 feet per second. A velocity grouping of 1,600 to 2,700 feet per second is observed extensively over the area and has been correlated with the rill wash. The range of 3,300 to 4,800 feet per second may represent the loosely compacted abalation till while the higher range of 5,000 to 7,300 feet per second may represent the basal till unit. Bedrock apparent velocity appears to be in excess of 13,000 feet per second.

The results of the seismic survey are graphically portrayed by the sections of Figure 3. The total thickness of overburden varies from 7 feet at station 39 on line 5 to 57 feet at station 29 on line 3. In general, the surface layer and layer of rill wash in total are less than 10 feet thick.

A portable hammer seismograph was found to be adequate to define the bedrock surface in the Woodstock area. The seismic results on these short lines are complementary to the geological study but do not detail the bedrock surface; additional control would be required to contour the bedrock surface. Present data indicate that the Pleistocene deposit essentially lies on a bedrock surface conformable to the present day surface, the former exhibiting slightly more relief.

---

[1] Lee, Hulbert A.: Surficial geology of Canterbury, Woodstock, Florenceville and Andover map-areas, York, Carleton and Victoria Counties, New Brunswick; Geol. Surv. Can., Paper 62-12.

---

14. LOW-LEVEL AEROMAGNETIC SURVEYS IN THE LABRADOR SEA

Project 650007

Peter Hood and Margaret E. Bower

Since 1962, the Geological Survey of Canada and the National Aeronautical Establishment have co-operated in a low-level aeromagnetic reconnaissance of the continental shelves and deep-ocean basins adjacent to eastern Canada. Aeromagnetic profiles at about 60-mile intervals have been obtained from the southern tip of Greenland to Kane Basin between Ellesmere

Island and northern Greenland. Figure 1 shows most of the total intensity profiles obtained in the Labrador Sea with the regional gradient removed. The correlation between the anomalies occurring on the flight lines is indicated by the dashed lines, and the inferred position of the axis of the dormant Labrador ridge, which coincides with a central U-shaped anomaly, by the thick black

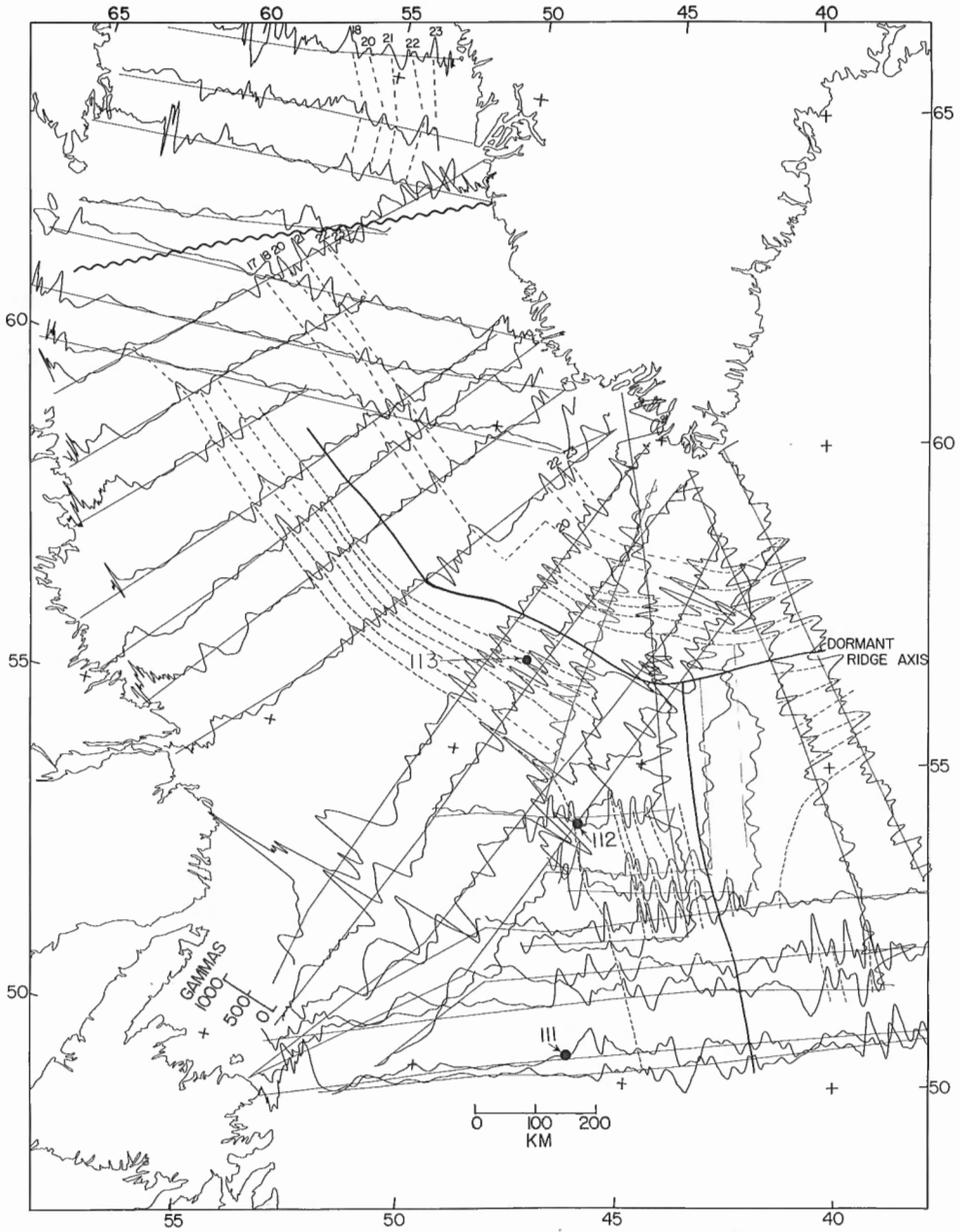

LABRADOR SEA PROFILES

line. There is a marked symmetry about this central U-shaped anomaly on a number of the profiles, and this is reasonably good evidence that sea-floor spreading has occurred in the Labrador Sea.

Consideration of the pattern formed by the dashed lines leads to the conclusion that a triple spreading junction has existed south of Cape Farewell at the southern tip of Greenland at approximately 56°N 44°W. Thus sea-floor spreading would have taken place in three directions about the triple junction which makes the magnetic anomaly pattern difficult to unravel in that area. The locus of the dormant Labrador Sea ridge can be traced around the southern tip of Greenland using other aeromagnetic profiles obtained in the North Atlantic Ocean and joins with the dormant ridge earlier postulated by Godby et al.[2], which formed part of the double-ridge system generated in the North Altantic during the late Mesozoic and early Tertiary period.

In order to ascertain the spreading sequence in the Labrador Sea, a comparison of the observed anomalies has been made with those generated by the computer using the Lamont geomagnetic polarity time scale and a spreading rate of 1 cm/year for a 2-km-thick layer. An examination of the time scale shows polarity periods corresponding to Anomalies 20, 21, 22 and 23 would have produced a well-resolved, distinctive band of anomalies in the Labrador Sea because each was generated over a relatively long period of time during which the field did not change polarity, and there is good separation between the polarity periods. It is not possible to be certain about the positive identification of these anomalies, but it is concluded that the distinctive ones seen on the flanks of the mid-Atlantic ridge (between 350-450 km from the crest) and in the Labrador Sea are in fact Anomalies 20-23. It is thus inferred that the spreading in the Labrador Sea ceased at a time when the earth's magnetic field was reversed just after Anomaly 13 was generated which would have been about 36 million years ago.

The positions of holes 111 (Orphan Knoll), 112, and 113 drilled on Leg 12 (June-July 1970) of the Joides Deep Sea Drilling Project are given on the figure. From the foregoing analysis Hole 113 falls close to Anomaly 16 and the basement material would therefore be expected to have an Eocene age of about 41.5 million years; the hole did not actually penetrate to the igneous basement[2]. The basement beneath hole 112 is also inferred to have an age of about 53 million years (Anomaly 21) which is at the Eocene-Paleocene boundary.

It is concluded that sea-floor spreading started in the Labrador Sea at the end of the Cretaceous Period (about 65 million years ago) although it is possible that a proto-Labrador Sea was already in existence at that time. Thus it can be expected that the sedimentary formations on the continental shelves bordering the Labrador Sea are mostly Mesozoic or younger in age, which makes the shelves attractive areas for the petroleum industry to prospect.

---

[1] Godby, E.A., Hood, P.J. and Bower, M.E.: Aeromagnetic profiles across the Reykjanes Ridge southwest of Iceland; J. Geophys. Res., vol. 73, No. 24, pp. 7637-7649 (1968).

[2] Anonymous: Deep sea drilling project, Leg 12; Geotimes, vol. 15, No. 9, pp. 10-14 (1970).

15. A COMPUTER METHOD TO OBTAIN THE VELOCITY-DEPTH FUNCTION FROM SEISMIC REFRACTION DATA

Project 680037

J.A.M. Hunter

The interpretation stage of refraction seismic surveying is often susceptible to various forms of "noise" or interpretive uncertainty. This can occur at the data receiving end, such as noise occurring on seismic records, or it can occur in the treatment of the data either in the "picking" stage or in the refractor interpretation. An operator can be easily trained to reduce record noise by introducing proper field procedures, and can easily acquire skill in the identification of first arrival onsets; however, the interpretation of refractor layering from these arrival times is an art which may take considerable time to perfect. The identification of refractors is subject to strong human bias which in turn affects the velocity-depth structure. To this end, this paper presents a method to minimize, by computer means, the human bias in refraction interpretation, and to delay the human interpretive influence until after the velocity-depth function has been obtained.

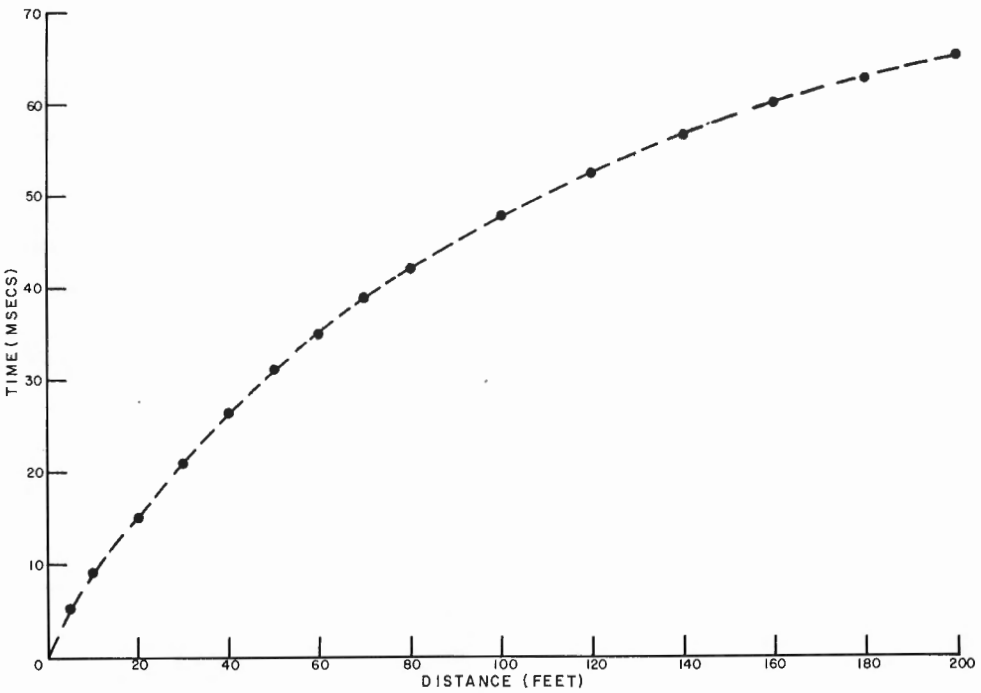

Figure 1. Refraction travel-time distance plot showing continuous velocity increase.

This method gives good results under the following assumptions for the earth model:

1) The velocity increases with depth and can be described by the first arrival times (no hidden layers).

2) Subsurface layering is horizontal, and all velocities are constant laterally, but may be constant or increase with depth within any one layer.

A typical example of a refraction travel-time distance plot showing a continuous velocity increase with depth is given in Figure 1. Any attempt to draw straight line segments of 3 or more points through the data would effect an interpretive bias. The best approach to the problem is to consider each point as an arrival from a distinct layer. Hence, for the k_{+1} data point the thickness of the k^{th} layer would be the familiar equation:

$$Z_k = \frac{V_{k-1} V_k}{2\sqrt{V_k^2 - V_{k-1}^2}} \left\{ C_k - \sum_{i=1}^{k-1} 2Z_i \cdot \frac{\sqrt{V_k^2 - V_{i-1}^2}}{V_k \cdot V_{i-1}} \right\} \quad \ldots\ldots\ldots\ldots\ldots\ldots (1)$$

where V_k = velocity as given by the k and k+1 points

C_k = the intercept time obtained from:

$$C_k = T_k - X_k/V_k \quad \ldots\ldots\ldots\ldots\ldots\ldots (2)$$

where T_k = the travel time

X_k = shot-geophone distance

Thus, if the velocity can be measured at each point on the time-distance plot, the velocity-depth function can be obtained.

Most travel-time distance plots for actual field cases do not follow a smooth curve exactly because of scatter of time from picking errors and local velocity and depth variations. Prior to obtaining a velocity-depth function the plot must be smoothed so that effects of these minor irregularities are reduced. However, the smoothing must not be such that sharp velocity transitions are lost.

The computer program to smooth and transform the time-distance plot has been written in Fortran II for a small 6K-word remote-terminal computer, but with minor changes it can be used with most computer systems. The program sequence is as follows:

a) A three-point least-squares velocity fit is made at each data point.

b) A search of the computed velocities is made to determine whether velocity reversals occur along the time-distance curve. If a velocity decrease occurs at a data point, marker array elements corresponding to data points on either side of this data point, as well as this anomalous point, are set to non-zero values.

c) The marker array is searched for non-zero values. If such occur, the travel times associated with these elements are again computed using the least-squares velocities and intercept times. The marker array is re-set to zero.

d) The three-point velocity determinations are re-computed for all data points and velocity reversals are noted again. When recursive smoothing has reduced velocity reversals to 10 feet per second the are finally eliminated by assuming the preceding velocity. At this point the velocity-depth function is computed using equation (1).

DISTANCE X	OBSERVED T	COMPUTED T'	DEPTH Z	VELOCITY (ft./ms.) V
5.	5.0	5.0	.0	1.00
10.	9.0	9.0	1.9	1.67
20.	15.0	15.0	1.9	1.67
30.	21.0	21.0	4.7	1.82
40.	26.5	26.5	9.3	2.22
50.	31.0	31.0	13.1	2.50
60.	35.0	35.0	13.1	2.50
70.	39.0	39.0	22.0	3.33
80.	42.0	42.0	26.7	3.64
100.	47.5	47.5	32.5	4.00
120.	52.5	52.5	43.8	5.00
140.	56.5	56.5	53.8	5.71
160.	60.0	60.0	72.5	8.00
180.	62.5	62.5	72.5	8.00

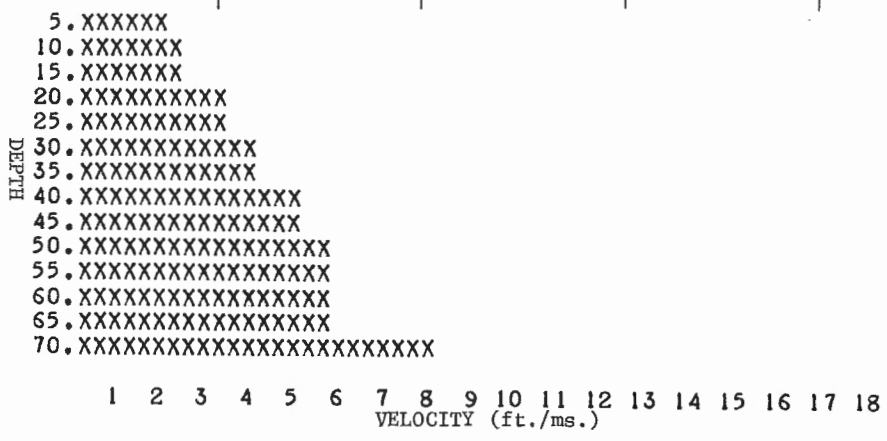

Figure 2. Typical printed output for time-distance data given in Figure 1.

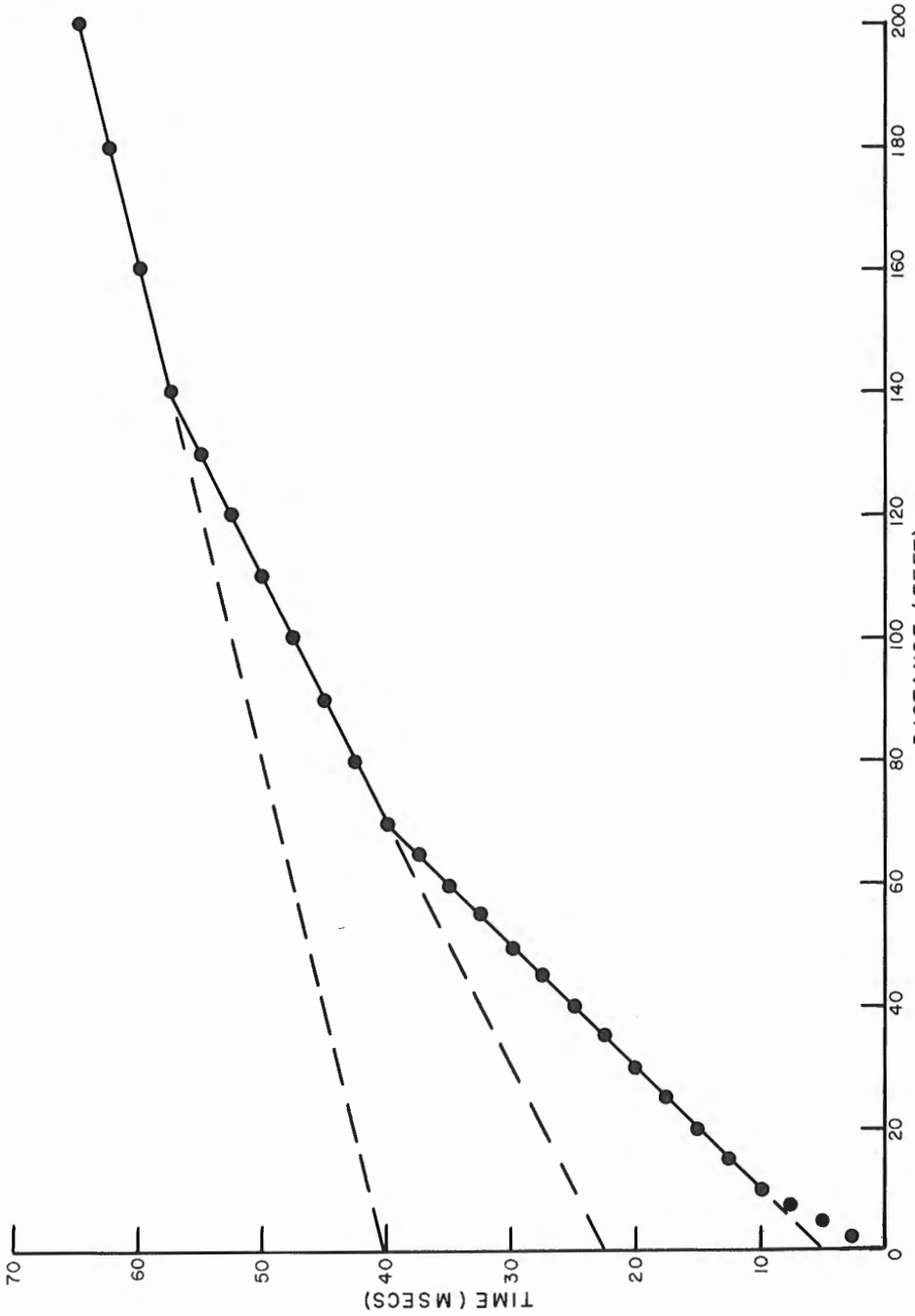

Figure 3. A four layer refraction case with time-distance plot.

Examples of the computer routine

A typical printed output is given in Figure 2 for the time-distance data given in Figure 1. The printer-plot output can be considered a good visual aid for interpreting the velocity-depth function.

As a check on the routine, a four layer refraction case with time-distance plot, Figure 3, was inputted. Table I is the printed output from the program showing the velocity-depth function and a perfect fit of observed and smoothed travel-times. This demonstrates that the smoothing routine preserves sharp velocity increases in the time-distance curve.

To test the smoothing routine, two types of travel-time anomalies were considered. Both types were tested using the four layer case of Figure 3 as a base. The first type is a late arrival anomaly of 5 milliseconds at a distance of 40 feet. This is a rather extreme deviation but could result from either a mis-pick of the first arrival or an actual velocity or depth anomaly in the region of the 40 feet spacing. The smoothed time-distance curve is shown as dashed line in Figure 4 an elargement of the first portions of the plot.

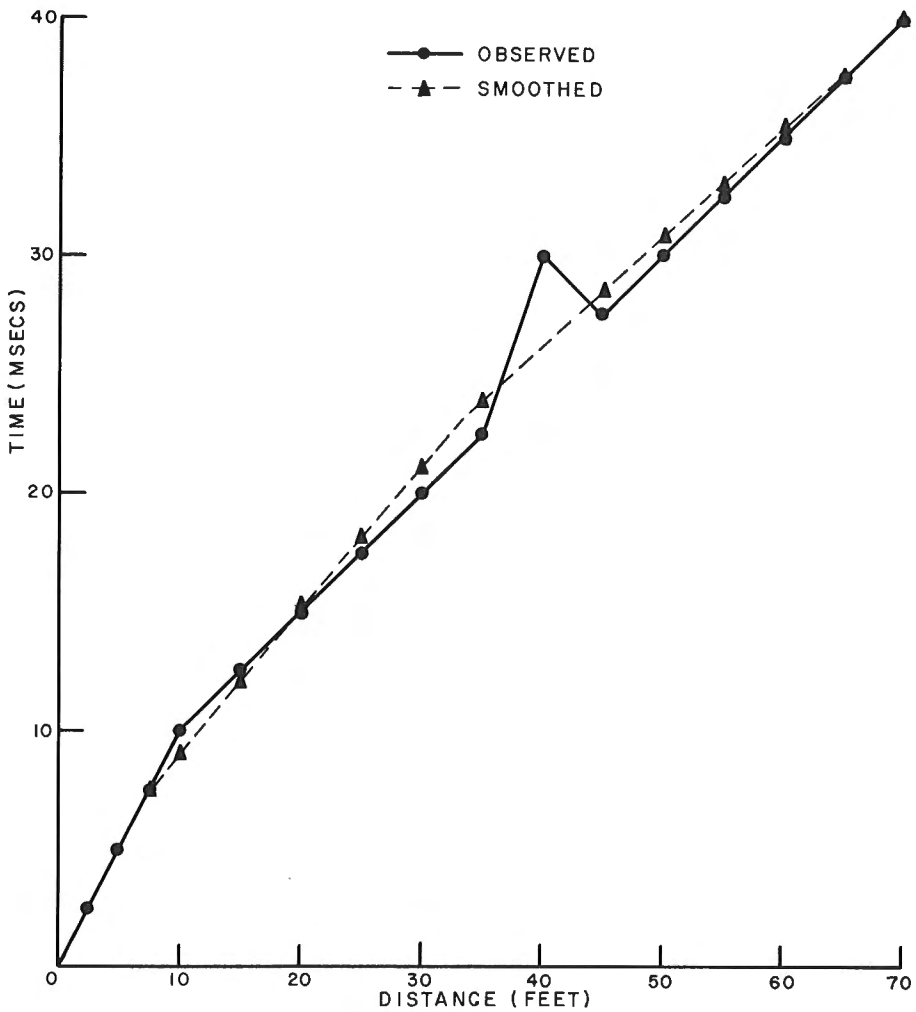

Figure 4. Enlargement of first portion of plot in Figure 3.

Depth computation based on the smoothed curve give values of 8 feet for the first horizon rather than the correct value of 2.2 feet. However, for successive layers, the computed depth values are respectively 10 per cent and 2 per cent too large. The decreasing effect on deeper horizon-depth calculations is particularly important since, for shallow refraction work, the target horizon is generally the deepest one.

The second type of travel time anomaly is the travel-time decrease shown as the solid line in Figure 5. This could also arise from extreme changes in depth to the refractor or local velocity changes in the overlying layer. The smoothing performed by the computer routine is shown as the dashed line in Figure 5, and is quite close to the original curve with the anomaly removed. The smoothing for this type of anomaly is much finer since the

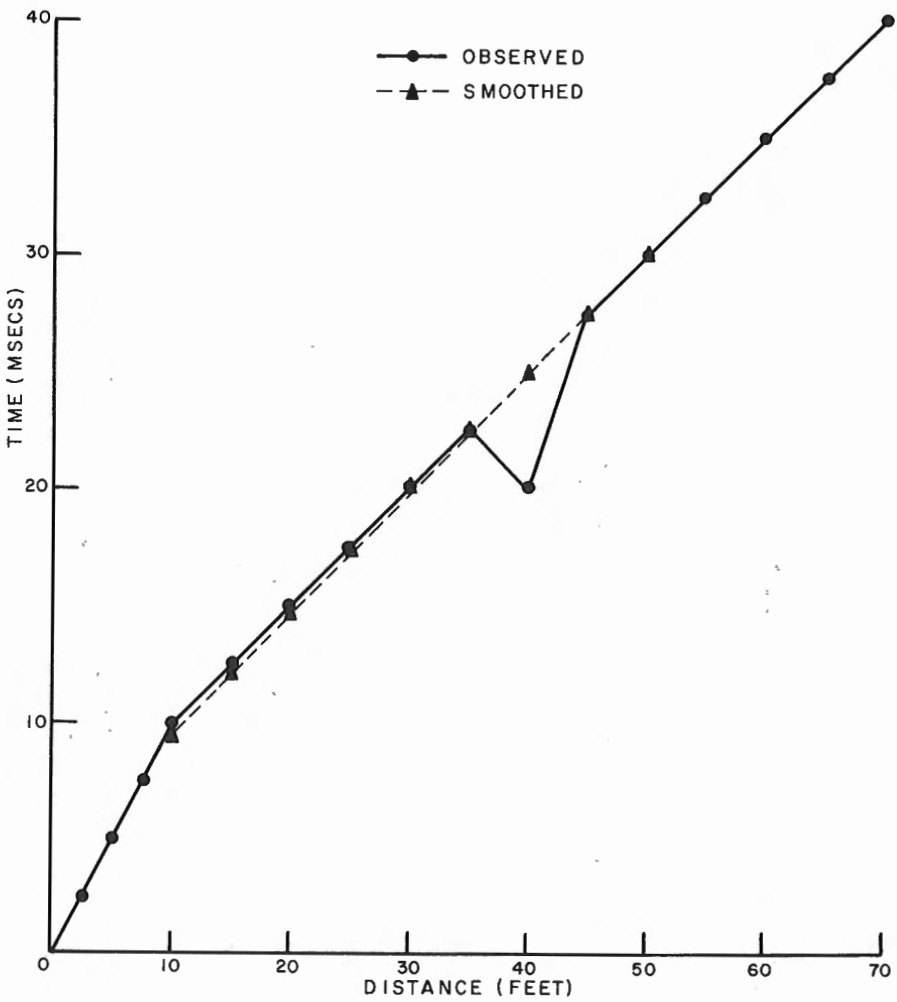

Figure 5. A second type of travel time anomaly, travel time decrease.

TABLE I

DISTANCE X	OBSERVED T	COMPUTED T'	DEPTH Z	VELOCITY (ft./ms.) V
2.	2.5	2.5	.0	1.00
5.	5.0	5.0	.0	1.00
7.	7.5	7.5	.0	1.00
10.	10.0	10.0	2.9	2.00
15.	12.5	12.5	2.9	2.00
20.	15.0	15.0	2.9	2.00
25.	17.5	17.5	2.9	2.00
30.	20.0	20.0	2.9	2.00
35.	22.5	22.5	2.9	2.00
40.	25.0	25.0	2.9	2.00
45.	27.5	27.5	2.9	2.00
50.	30.0	30.0	2.9	2.00
55.	32.5	32.5	2.9	2.00
60.	35.0	35.0	2.9	2.00
65.	37.5	37.5	2.9	2.00
70.	40.0	40.0	22.4	4.00
80.	42.5	42.5	22.4	4.00
90.	45.0	45.0	22.4	4.00
100.	47.5	47.5	22.4	4.00
110.	50.0	50.0	22.4	4.00
120.	52.5	52.5	22.4	4.00
130.	55.0	55.0	22.4	4.00
140.	57.5	57.5	57.9	8.00
160.	60.0	60.0	57.9	8.00
180.	62.5	62.5	57.9	8.00

TABLE II

DISTANCE X	OBSERVED T	COMPUTED T'	DEPTH Z	VELOCITY (ft./ms.) V
5.	5.0	5.0	.0	1.00
10.	13.0	13.0	4.7	2.18
15.	17.0	15.3	7.8	3.96
20.	18.0	16.6	9.4	4.43
30.	19.0	18.8	10.6	4.58
40.	20.5	21.0	10.6	4.57
60.	24.0	25.4	10.6	4.57
80.	29.0	29.7	10.6	4.57
100.	33.0	34.1	10.6	4.57
120.	37.0	38.5	10.6	4.57
140.	41.0	42.9	10.6	4.57
160.	46.0	47.2	10.6	4.57
180.	51.0	51.6	10.6	4.57
200.	56.0	56.0	23.6	4.77
230.	63.0	62.3	25.9	4.78
260.	68.5	68.6	25.9	4.78
290.	75.0	74.9	25.9	4.78
320.	81.0	81.1	25.9	4.78
350.	87.0	87.4	25.9	4.77
380.	93.0	93.7	25.9	4.77
410.	99.0	100.0	25.9	4.77
440.	107.0	106.3	44.9	4.91
470.	112.0	112.4	58.9	5.04
500.	120.0	118.3	61.3	5.05
530.	125.0	124.3	61.9	5.05
560.	129.0	130.2	61.9	5.05
590.	136.0	136.2	61.9	5.05
620.	141.0	142.1	61.9	5.04
650.	148.0	148.1	61.9	5.04
680.	154.0	154.0	176.2	7.50
710.	158.0	158.0	323.7	15.00
740.	160.0	160.0	323.7	15.00
770.	162.0	162.0	323.7	15.00
800.	164.0	164.0	323.7	15.00
830.	166.0	166.0	503.2	30.00

computer technique is based upon removing velocity reversals (velocity decreases with distance). The depth computed to this horizon is 5.8 feet in contrast to the correct value of 2.2 feet showing that the error is large for the effected horizon. However, the errors in computing the depths to the deeper horizons are 2.7 per cent and 0.9 per cent respectively for the model, suggesting again the decreasing effect of the smoothing error with depth.

As an example of the routine applied to a field case, Figure 6 shows the time-distance plot of a refraction profile in the Ottawa area. The printed velocity-depth function is given in Table II. The plot was interpreted in the field by conventional means as a three layer case with V_o = 855 feet per second, V_1 = 4,720 feet per second and V_2 = 19,200 feet per second giving a depth of d_1 = 5.5 feet and d_2 = 270.5 feet. The computer fit, however, gives a 7-layer case with velocities of V_o = 1,000 - 4,428, V_1 = 4,570, V_2 = 4,776, V_3 = 5,045, V_4 = 7,500, V_5 = 15,000 and V_6 = 30,000 feet per second, with depths of d_1 = 10.6, d_2 = 25.9, d_3 = 62, d_4 = 176, d_5 = 323 and d_6 = 503 feet.

At this point the interpreter should consider the velocities of 7,500 and 30,000 feet per second as questionable since they are based on one data point each. However, the velocity 7,500 feet per second may occur as a velocity increase within the 5,045 feet per second layer and in that respect may be real. The 30,000 feet per second velocity is given by the last data

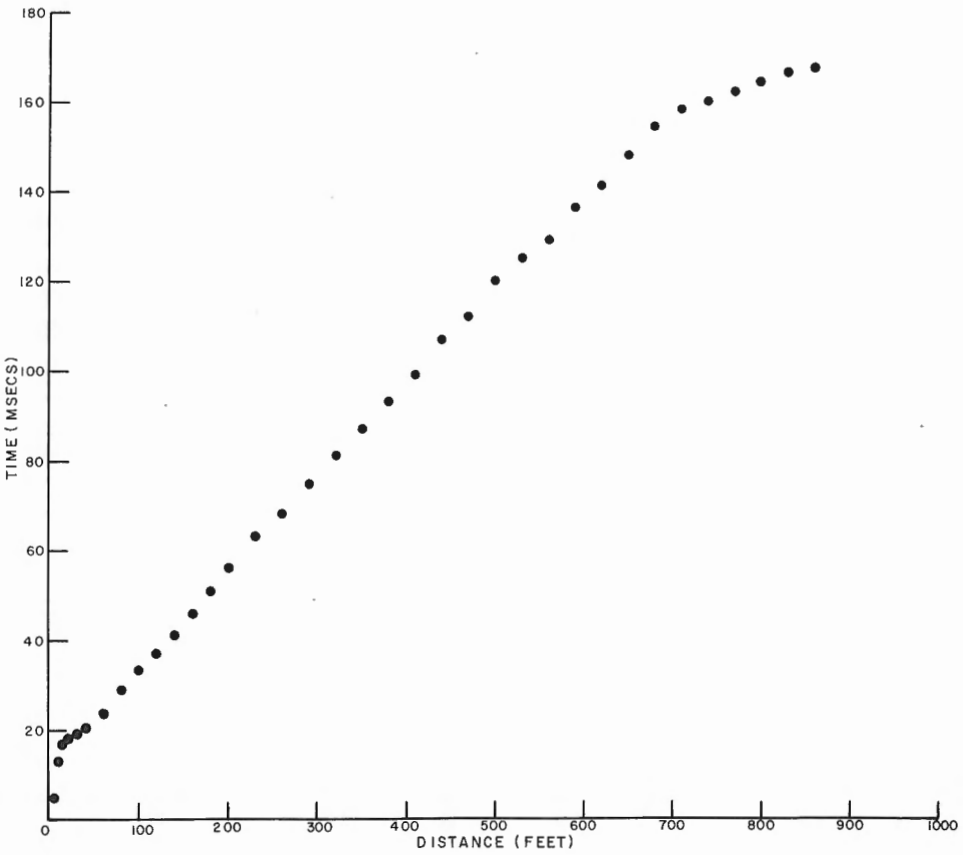

Figure 6. Time-distance plot of a refraction profile in the Ottawa area.

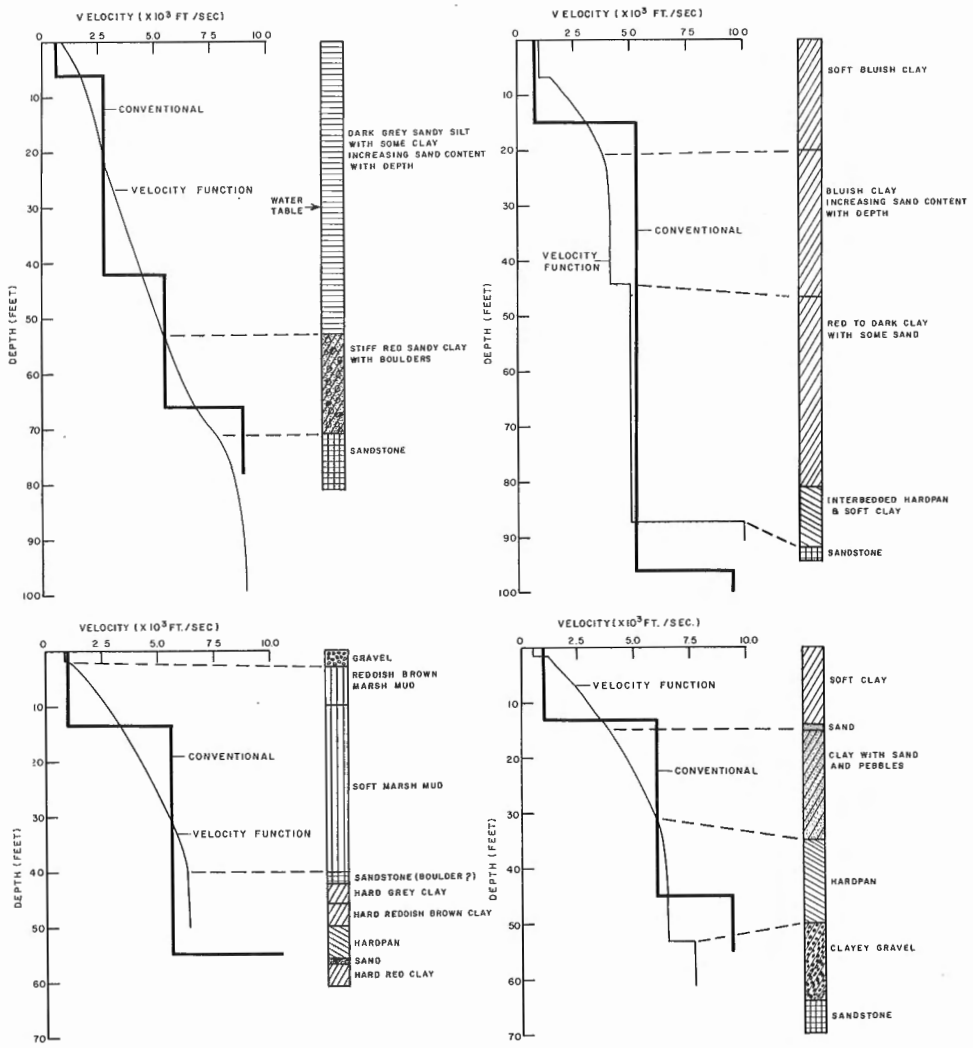

Figure 7. Examples of interpreted velocity-depth functions for hammer seismic profiles compared with conventional multilayered refraction interpretation.

point and because of this, may be rejected as an unsmoothed travel-time anomaly. This example demonstrates the ability of the computer fit to detect fine velocity changes as well as the need for operator interpretation of the velocity-depth function.

Figure 7 shows some examples of interpreted velocity-depth functions for hammer seismic profiles as compared to the conventional multilayered refraction interpretation and the driller's logs from adjacent drillholes. The conventional interpretive method introduces abrupt seismic interfaces which may not be realistic. The velocity-depth function interpretation suggests on the other hand that velocity gradients exist within lithologic units; velocity contrasts exist between units but may not necessarily be large or abrupt.

16. A HAMMER SEISMIC INVESTIGATION OF THE PERMAFROST LAYER, MACKENZIE DELTA

Project 680037

J.A.M. Hunter and R. Good

A seismic survey was undertaken during July-August 1970 at selected sites in the lower Mackenzie River Delta and along the coast of the Beaufort Sea in co-operation with Dr. J.R. MacKay (Project 680047). The seismic experiment was designed to measure the thickness of the permafrost layer by the reflection technique since velocity inversions commonly occurring at the base of the permafrost negate the use of conventional refraction

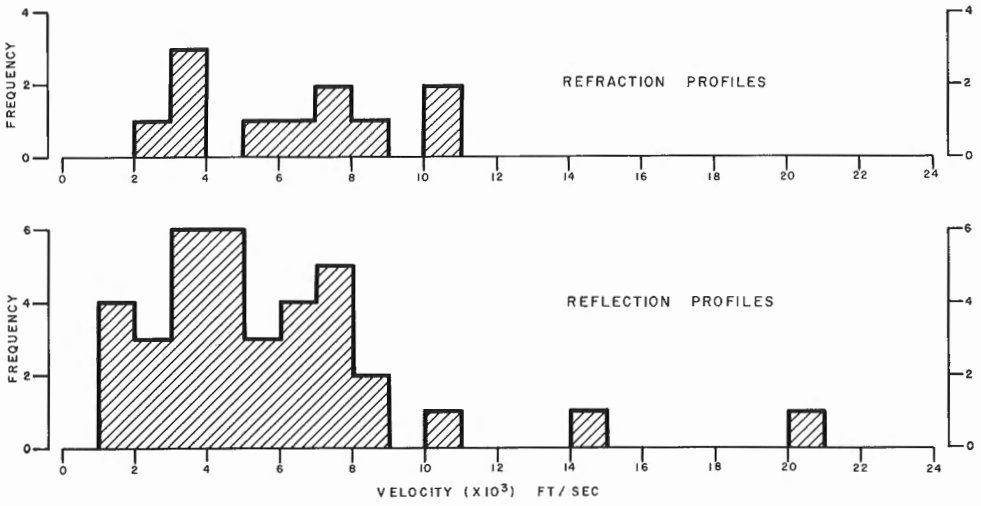

Figure 1. Histogram of observed velocities from hammer seismic profiles.

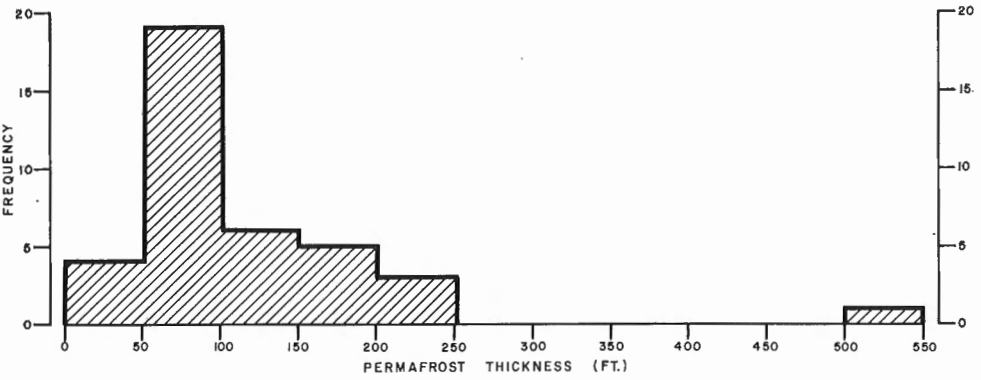

Figure 2. Histogram of permafrost thicknesses as determined from seismic profiles.

techniques. In total 47 locations were investigated, the majority being reflection profiles with a few refraction profiles to provide horizontal velocities. Interpretable data were obtained from 39 reflection and from five refraction profiles, the record quality varying from fair to poor even when explosives were used as a source of energy. This suggests that the active layer of the permafrost is a substantial absorber or attenuator of source energy.

Velocities observed on both the reflection and refraction profiles are displayed in histogram form in Figure 1. The reflection profile velocities most commonly recorded were 4,000 and 7,500 feet per second. These have been interpreted as representing the shear and compressional reflected waves respectively from the base of the permafrost layer. An investigation of later arrivals of energy on the refraction records, also presented in Figure 1, coincide with the velocities derived from the reflection records. The thickness of the permafrost varies from 4 feet in regions of discontinuous permafrost to values in excess of 500 feet. The thicknesses determined during this abbreviated survey are shown in histogram form in Figure 2.

The average Poisson's ratio computed for the permafrost zone is approximately 0.30, a value greater than that generally interpreted to rock but less than that measured in soils.

17. SEISMIC REFLECTION TEST, QUYON, QUEBEC

31 F

Project 680037

J.A.M. Hunter and R.M. Gagne

The area chosen for the reflection survey tests is near Quyon, Quebec, where a regional refraction seismic survey indicated that refracted arrivals from bedrock were sometimes weak and bedrock depths were taxing the limit of the hammer seismic refraction method. Refraction results indicated that bedrock depths increased away from the river to a maximum value adjacent to the escarpment in the Quyon area. The tests were performed along two roads, Figure 1, at right angles to the Gatineau Hills Escarpment.

The instrument used was the Huntec FS-3 hammer seismograph which has been described in detail by such as Hobson[1] and Paterson and Meidev[2]. The instrument was operated in the reflection mode following the two-geophone spatial filtering technique described by Meidev[3], a technique involving coincidence window matching of arrivals from geophones in line with the hammer source resulting in velocity rejection filtering of arrivals.

Two methods were tested on the survey lines. On line A a continuous series of single-ended reflection spreads were obtained, each of 300 feet total length with 50-foot spacing of hammer blows, for a total traverse length of 1.5 miles. Line B was surveyed with a series of split spreads positioned at the locations of the refraction profiles done in the regional survey. The total length of each split spread was 600 feet with 300 feet each side of the geophone pair and a 50-foot spacing between hammer blows.

For both survey lines the correlation gate width for coincidence recording of geophones was constantly adjusted between 2.5 and 3.0 milliseconds as reception conditions varied along the profiles. With a geophone

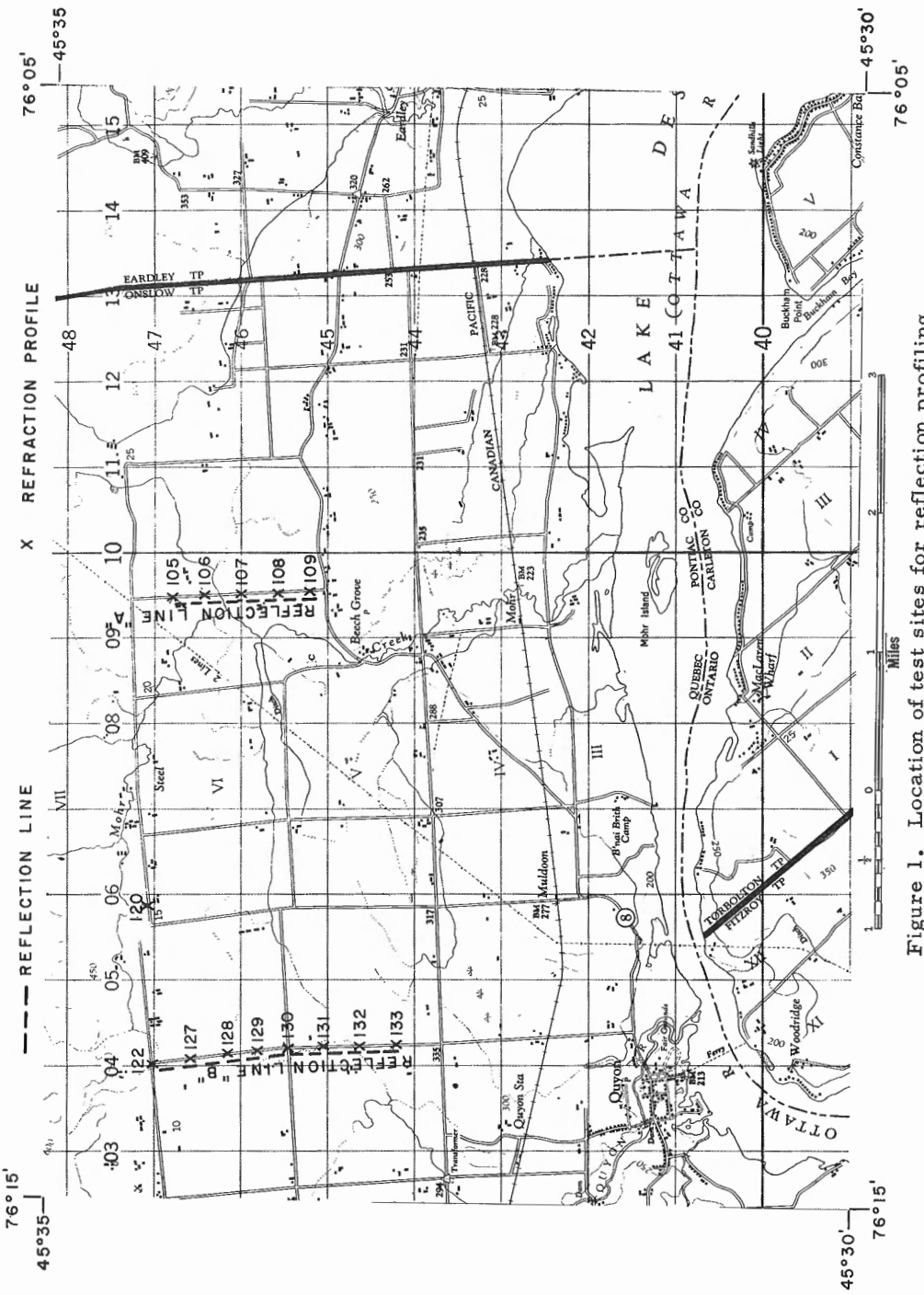

Figure 1. Location of test sites for reflection profiling.

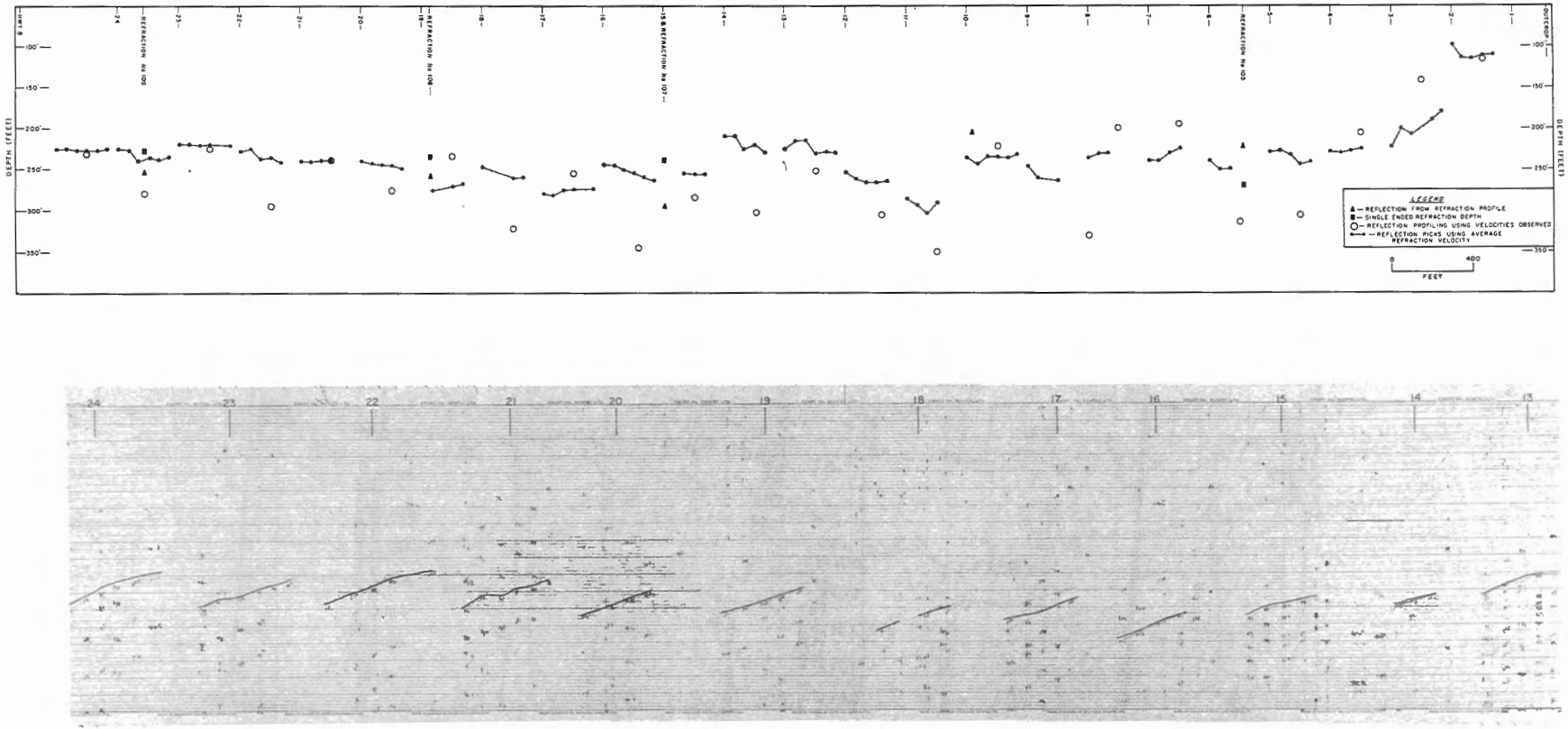

Figure 2. Line A - FS-3 field reflection records and interpreted section.

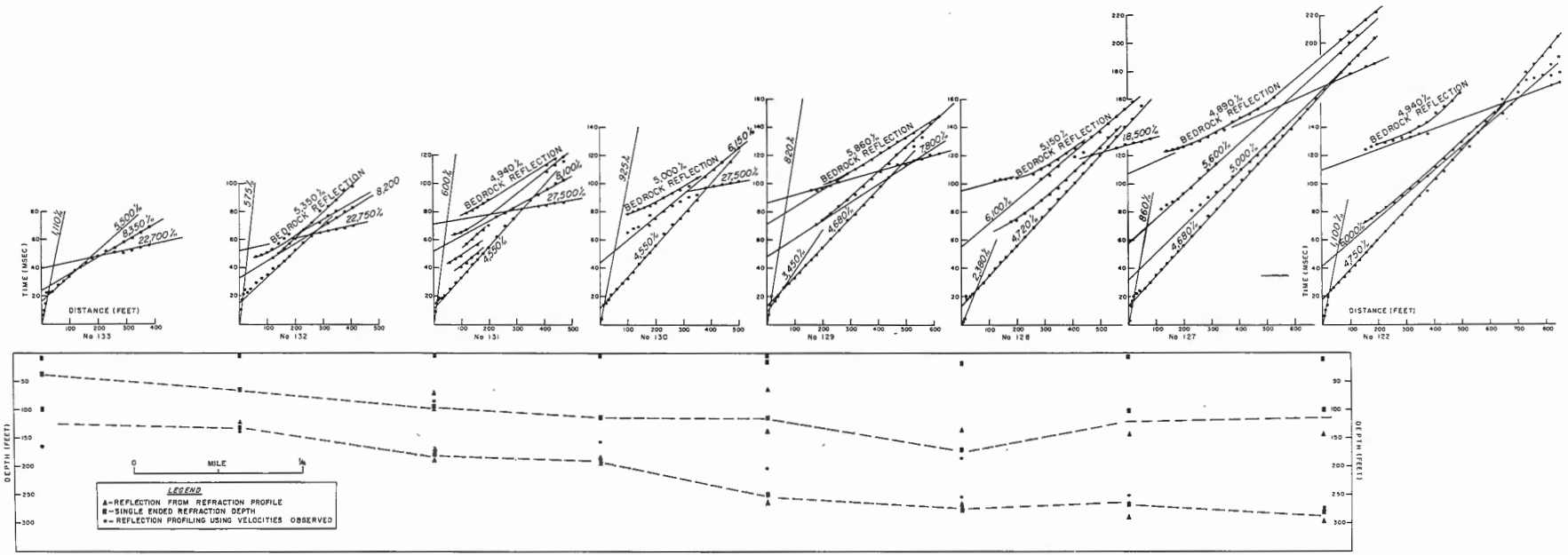

Figure 3. Line B - Reflection profiling results and interpreted reflections from refraction records.

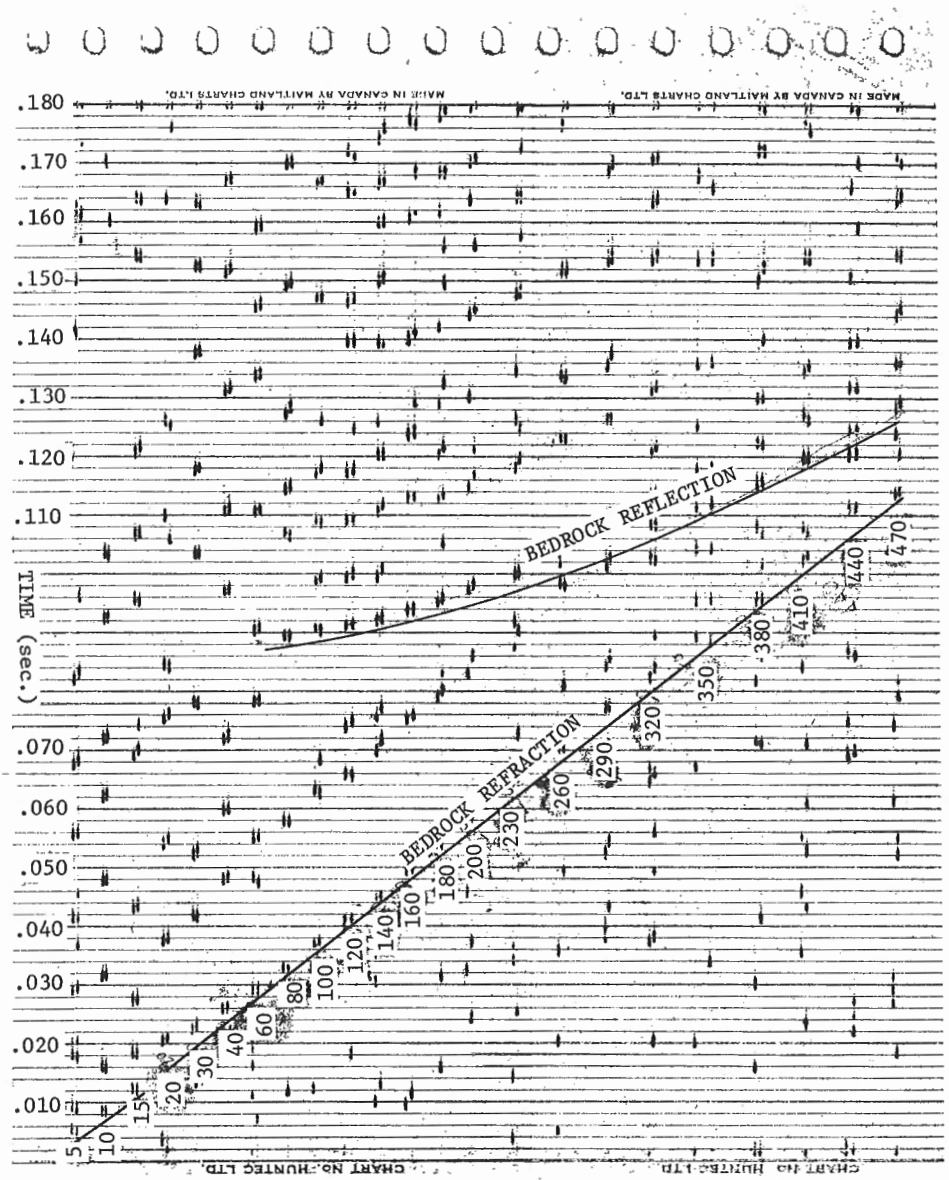

Figure 4(a). Refraction profile No. 120 - field record.

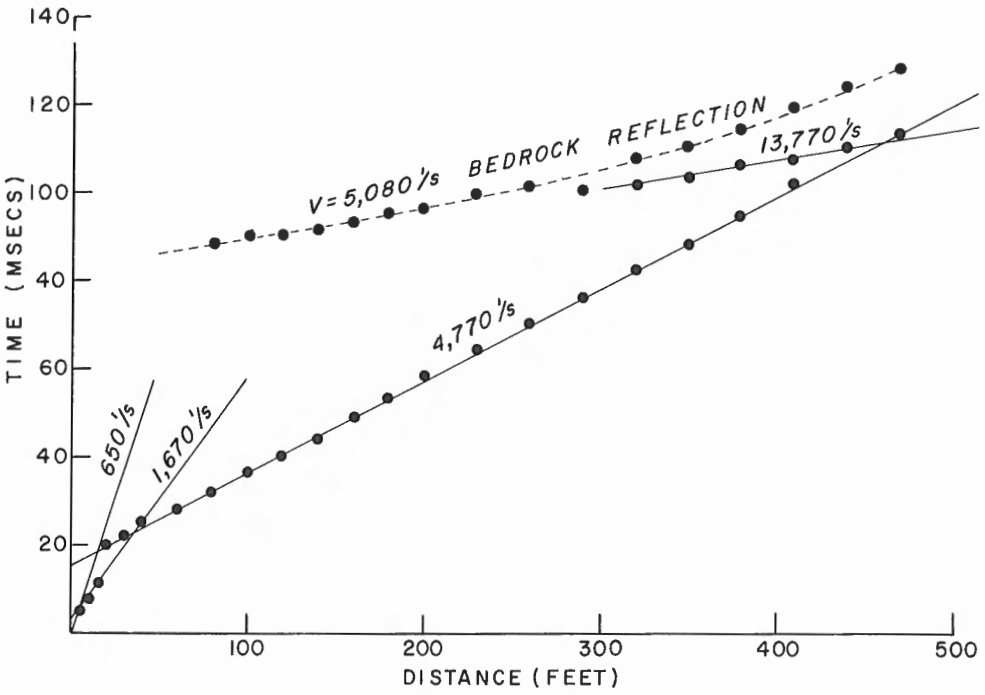

Figure 4(b). Time-distance plot for profile No. 120.

spacing of 20 feet this gave lower limits of acceptance of events with apparent velocities between 6,600 and 8,000 feet per second. This type of filtering eliminates refracted arrivals from the overburden layers with velocities below this lower limit.

The reflection profile data for line A yielded events which can readily be interpreted as bedrock reflections. A portion of the field records is shown in Figure 2. Most events were correlated from hammer spacings between 100 and 300 feet. However, it has been noted that in many cases the arrivals from the 50-foot spacing were apparently overriden by a strong event which did not correlate with the extrapolated reflection time. This strong event has been interpreted as the air-coupled ground wave, a wave that attenuates rapidly with distance so that data from beyond 150 feet are largely unaffected by it.

A sectional plot of the interpretations for reflection line A is also given in Figure 2 along with results obtained from the conventional shallow refraction survey. The data have been interpreted and plotted in the following ways:

a) using the average travel-time and velocity obtained from each reflection profile assuming a single overburden layer least squares travel-time fit,

b) using the reflection travel-times from the reflection profiles and the average overburden velocity as determined from the refraction profiles,

c) using the refraction first arrival times and computing depths from the refraction method, and

d) using a least-squares reflection wave fit to later arrivals picked from the refraction profiles as the bedrock reflection.

Good correlation is shown in general between various reflection interpretations and the refraction results; however, differences as much as 80 feet sometimes do occur. Depths to bedrock range between 225 feet at the south to 300 feet near the north end as one approaches the Gatineau Escarpment. An abrupt rise has been interpreted at the north end of the section.

Of the various interpretations given in Figure 2, the most accurate reflection method appears to be that using the arrival times from the reflection survey in conjunction with the velocity obtained from the refraction survey. The reasons for this conclusion are:

1) The reflection geophone configuration in conjunction with the velocity filter minimizes interference from low velocity events, and

2) The overburden velocity obtained from the refraction profiles is based on many points and is statistically the more accurate velocity measurement obtained compared to that obtained from the reflection profiles.

The reflection data from line B using the split spread method were poor compared to those of line A. This is attributed to a change in geological conditions between the two lines rather than the difference in the method. Figure 3 is a sectional plot of the reflection interpretations in conjunction with the refraction results. The three interpretation methods used were:

a) least squares velocity fit and depth computation of reflection results assuming a single layered overburden,

b) depth computations from refraction results, and

c) depth computation from reflected events on the refraction profiles.

The refraction records from the area suggest an intermediate reflection horizon above the bedrock which appears as a hidden refractor in the first arrival plots. This interpretation is based on the position of reflected later events with respect to the first arrivals on the refraction profiles. Comparison between interpretive methods as shown by Figure 3 suggest that all methods indicate the same depth trends along the section but differ as much as 50 feet at some locations.

For line B, the interpretation based on reflections observed as later arrivals on the refraction profiles may be the best indicator of the subsurface structure. Here the interpreter is guided by the position of the overburden first arrival times and the bedrock refractor times extrapolated back to the origin. Later events in this region can be interpreted as infra-overburden reflections and multiples of same. A reflector tangent to the extrapolated refractor travel-time may be interpreted as the bedrock reflection. Many cases arise in shallow refraction prospecting where the bedrock refractor first arrivals are weak and insufficient to give a reliable velocity but may be usable as a guide to the bedrock reflection.

The average depth values computed from the reflection profiles were obtained under the assumption of a single-layered overburden. To test the effect of low velocity layering on the travel time of a reflection, a refraction profile from the Quyon area (No. 120) showing a clear reflection event was selected. The profile location was close to line B, Figure 1. The field record is shown in Figure 4(a) and the time-distance plot in Figure 4(b). The

first arrival times suggest layers with velocities of 650, 1,670 and 4,770 feet per second. Also, the bedrock refractor was interpreted as a secondary arrival with velocity of 13,770 feet per second.

The bedrock reflector interpreted from profile No. 120 gives an average velocity of 5,080 feet per second and a depth of 222 feet to bedrock as compared to 183 feet from refraction data. In an attempt to resolve the differences by the two methods, layered reflection models were designed and travel-times were computed using an iterative solution of the parametric form of the travel-time and distance equations:

$$T_K = \sum_{i=1}^{k} (2Zi) / (Vi.(1-p^2Vi^2))^{1/2}$$

$$X_K = \sum_{i-1}^{k} (2Zi.Vi\ p) / (1-p^2Vi^2)^{1/2}$$

where T_k = two way travel time of a reflection from the k^{th} interface

X_k = distance between source and receiver

$p = \frac{\sin \alpha i}{Vi}$ = the ray parameter

αi = the incident angle at the i^{th} interface

Vi = the velocity within the i^{th} layer.

Three models which fit the travel times of the reflector within 2 milliseconds are given in the following table:

Model	Layer Velocity (feet per second)	Layer Thickness (feet)
a)	5080	222
b)	1670	10
	5300	200
c)	1670	10
	4770	160
	8000	25

These are not the only best-fitting models available (since many more may be obtained by adding intermediate layers) but rather they are the most probable based on reflection and refraction data. Model (a) is simply the model as given by the reflection results. Model (b) assumes a 10-foot-thick surface low velocity layer and was obtained by trial and error fitting of overburden velocity and depth. Model (c) assumes the 10-foot low velocity layer and the overburden velocity as given by the refraction results. To obtain a good fit with the model, a third layer of high velocity (8,000 feet per second) was added. This suggests a velocity increase at the base of the overburden and

may be correlated with a basal high velocity drift layer interpreted in the Quyon area. A further indication of this lower layer comes from weak events in the region of 230 feet to 410 feet on the profile closely following the first arrival from the 4,770 feet per second layer which may be interpreted as reflections.

Model (c) of those considered appears to be the best interpretation since model parameters are bounded by the refraction results. The work with model studies has demonstrated that multilayered overburden models can substantially alter the travel-time of reflections. Least-squares velocity and depth fits assuming a single layered case may only be approximate. However, reflection observations combined with refraction results may lead to better interpretation in seismic studies of overburden.

---

[1]Hobson, G.D.: Seismic methods in mining and groundwater exploration, in Geol. Surv. Can., Econ. Geol. Rept. No. 26, pp. 148-176, ed. L.W. Morley (1970).

[2]Paterson, N.R. and T. Meidev: Geophysical methods in highway engineering; Presented at 48th Ann. Conv. Can. Good Roads Assoc., Saskatoon, Saskatchewan (1967).

[3]Meidev, Tsvi: Hammer reflection seismics in engineering geophysics; Geophysics, vol. 34, No. 3, pp. 383-395 (1969).

---

18. ELECTRICAL ROCK PROPERTIES

Project 630049

T.J. Katsube and L.S. Collett

Research on the electrical rock properties is carried out with the intention of aiding geological mapping and solving many geophysical problems concerned with industry, by laying a basis for development and improvement of new and existing geophysical exploration equipment and techniques.

Measuring systems have been set up for measuring electrical properties of rocks under various conditions[1, 2, 3] for the frequency range of 10^{-2} to 10^{7} Hz. The systems for the frequency range of 10^{3} to 10^{7} Hz have been standardized. This makes it possible to study the electrical characteristics of rocks in relation to the petrology in the 10^{3} to 10^{7} Hz range. Studies are being made below 10^{3} Hz, but measurement precision will have to be considered before these systems can be standardized. A theoretical study that has been made on the electrical properties of earth materials in general is in the completion stage[4]. This study was necessary for setting up the measuring system, and to lay the basis for electrical characterization study of rocks.

Measurement of various igneous rocks and major rock forming minerals has begun, with the intention of clarifying their electrical

characteristics. A set of measurements on sedimentary and metamorphic rocks is planned to follow the measurement of the igneous rocks. After characterizing the various types of rocks, it is intended that measurement will begin on rocks from various formations across Canada.

A set of measurements on lunar samples from Apollo 11 and 12 has been carried out during the last year, and the results[5] have been presented at the Second Annual Lunar Science Conference in Houston in January, 1971. A paper[6] on the same subject has already been submitted for publication. These results seem to be accepted and are being used by scientists and engineers who are concerned with the EM soundings of the moon.

At present an attempt is being made to standardize the measuring systems in the frequency range of 10^{-2} to 10^{3} Hz. The main object of this attempt is to begin production of measurements in order to study the electrochemical polarization in rocks, including rocks disseminated with sulphide minerals. This study should relate the electrical characteristics of rocks, at these frequencies, to the petrology and geology of various kinds and types of ore-bearing zones across Canada. This study, if successful, should produce significant results for use by scientists and engineers related to mining exploration techniques.

Another subject of industrial importance, which has to be taken up in the near future, is the development of measuring systems for frequencies above 10^{7} Hz. Study of earth material in this frequency range is required in relation to permafrost and electromagnetic subsurface sounding in soils.

Good quality data and a theoretical understanding of measurements are essential for this study of electrical rock properties, and these are the aspects in which most effort has been concentrated during the development stages of the measuring systems. Such effort will be continued besides increasing the quantity of data production. This work may have an important relation to future developments in exploration geophysics in Canada.

---

[1] Katsube, T.J. and Collett, L.S.: Measuring techniques for electrical properties of rocks (in preparation).

[2] Katsube, T.J. and Collett, L.S.: Variable air-gap technique for measuring electrical properties of rocks (in preparation).

[3] Katsube, T.J.: Electrical rock properties; in Report of Activities, Part B, November 1969 to March 1970; Geol. Surv. Can., Paper 70-1B, pp. 39-41 (1970).

[4] Katsube, T.J. and Collett, L.S.: Theoretical discussion on the electrical characteristics of lunar and terrestrial rocks (in preparation).

[5] Collett, L.S. and Katsube, T.J.: Electrical properties of Apollo 11 and 12 lunar samples; presented at the Second Annual Lunar Science Conference, Houston, Texas (1971).

[6] Katsube, T.J. and Collett, L.S.: Electrical properties of Apollo 11 and 12 lunar samples; submitted for publication in Proceedings of the Apollo 12 Lunar Science Conference, Mass. Inst. Technol. Press.

19. A SEISMIC REFRACTION INVESTIGATION IN THE ST. JOSEPH ISLAND, SAULT STE. MARIE AREA (41 J/4 WEST HALF), ONTARIO

Project 670075

H.A. MacAulay

Recent geological mapping[1] on St. Joseph Island has cast some doubt upon the presence of Silurian strata at the southern extremity of the island as previously mapped[2]. The seismic investigation was therefore proposed as an aid to the mapping of bedrock formations beneath the drift covered areas of this part of the island[3].

Contours on bedrock surface, Figure 1, are interpolated from drift thickness calculations based on refraction seismic profiles. The fence diagram of the same figure was constructed from a combination of subsurface geological and seismic data, and a general assumption that Paleozoic strata dip uniformly southward at about 40 feet per mile.

Under the reversed profile between shot points 9 and 10 a short distance north of Tenby Bay Post Office, thickness of drift (unit 4) and the combined Wekwemikongsing, Sheguiandah and Collingwood Formations (unit 2, predominantly shale) were calculated. Further southward where carbonate rocks (unit 3) overlie the shales, depths to the top of the shale (unit 2) could not be determined because shale velocities being generally less than the velocities in carbonate rocks (unit 3) create a velocity inversion problem which the seismic refraction method does not resolve. Southward from shot point 11, near Tenby Bay Post Office where shales are capped by carbonate rocks of unit 3, only that part of the fence diagram of Figure 1 penetrating the top of the upper carbonate sequence is seismically derived. The approximate positions of the underlying stratigraphic units are extrapolated from the Henery Fremlin No. 1 well applying a regional southward dip of 40 feet per mile. The four rock units recognized in the seismic profiles exhibit good velocity contrasts, therefore assuring reliable correlation throughout the area of seismic survey. The velocities of the various units are diagramatically illustrated in Figure 1 and correlated with the rock stratigraphic units which form the southern part of St. Joseph Island.

The bedrock surface at shot point 1, about 3,300 feet northwest of the Henery Fremlin No. 1 well is interpreted as limestone (unit 1). The overlying shales (unit 2) which were encountered in the Fremlin well apparently terminate and form an escarpment at some point between the well and shot point 1. The same phenomenon occurs to the southwest where the change from shale (unit 2) to limestone and/or dolomite (unit 1) of the bedrock surface between shot points 9 and 8 determined seismically, indicates a generally north-facing buried escarpment with a relief of approximately 200 feet. Within the area of seismic control, the drift cover averages 100 feet in thickness above the escarpment, but increases abruptly to 300 feet thick north of the buried limits of the escarpment.

The absence of Silurian strata on St. Joseph Island as recently interpreted by Liberty is puzzling in light of their presence on immediately adjacent Lime Island in the state of Michigan, U.S.A. Ehlers and Kesling have correlated strata encountered in wells penetrating the Silurian rocks of

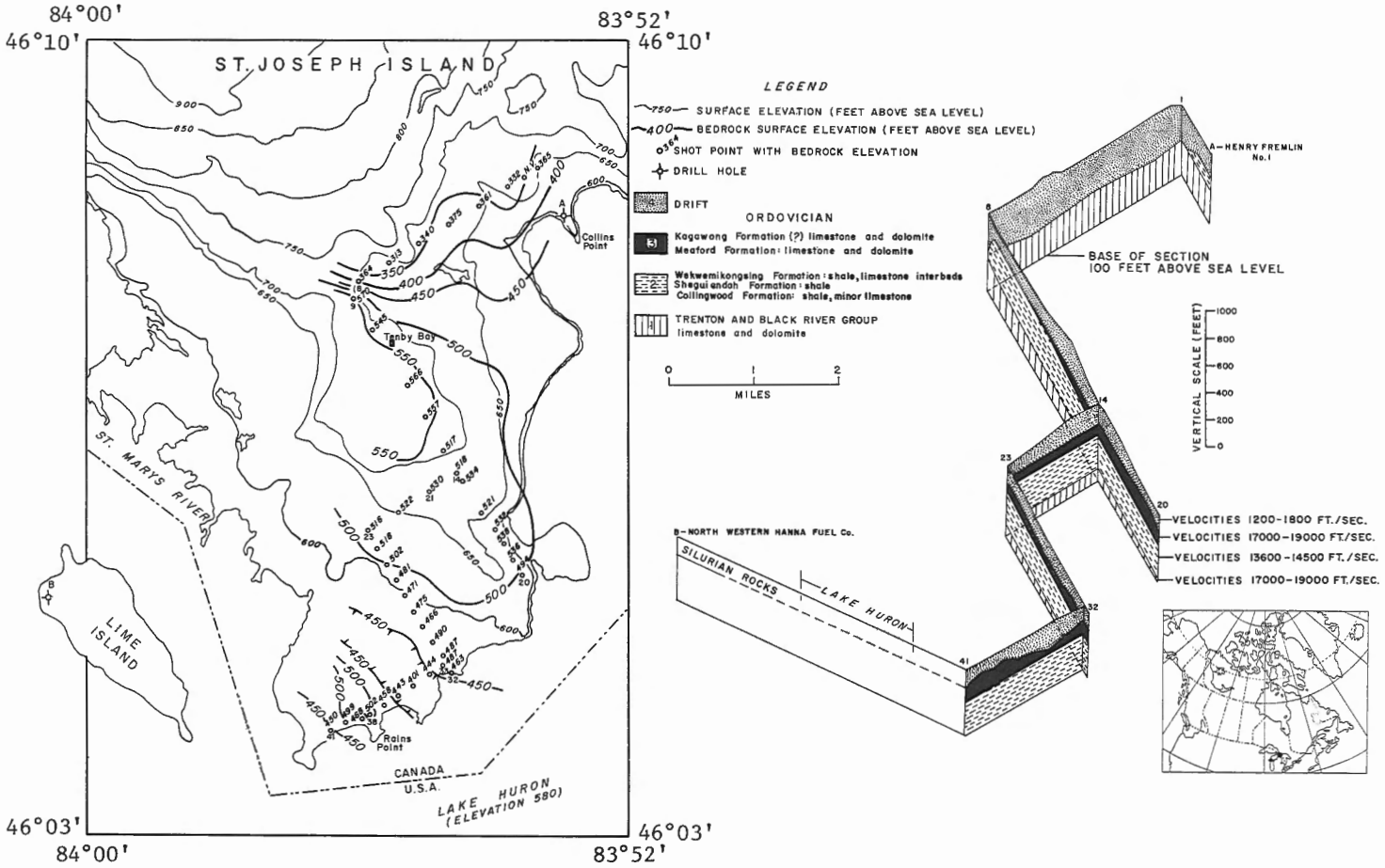

Figure 1. St. Joseph Island area, Ontario.

the Northern Peninsula of Michigan and Cockburn Island, Ontario[4]. One of the wells which provided data for their correlation was drilled by the North Western Hanna Fuel Co. on Lime Island. Although this well was bottomed in the Silurian Moss Lake Formation their correlation shows the stratigraphic succession postulated below the formations penetrated. Ehlers and Keslin's interpretation indicates the presence of approximately 130 feet of Silurian strata extending below lake level at this Lime Island location. At shot point 38 near Rains Point, St. Joseph Island the seismic data indicate a depth of bedrock surface of 80 feet below the level of Lake Huron. This depth to bedrock at Rains Point is along strike with Silurian rocks of Lime Island and suggest that up to 50 feet of Silurian strata may be present under the drift cover at the south end of St. Joseph Island.

It should also be pointed out that a southeast trending buried stream channel approximately 100 feet in depth can be observed in Figure 1 to cross the southern tip of St. Joseph Island and this could very well have developed coincident with the unconformable Silurian-Ordovician boundary.

In conclusion, it has been determined that Silurian formations are not as widely distributed on St. Joseph Island as previously mapped; they are, in all probability, present but confined to the extreme southwestern part of the island which lies adjacent to Lime Island, U.S.A.

---

[1] Liberty, B.A.: Stratigraphic studies of Middle Ordovician and Cambrian strata in the St. Joseph Island-Sault Ste. Marie area; Geol. Surv. Can., Paper 67-1, Part A, pp. 154-155 (1967).

[2] Hewitt, D.F.: Paleozoic geology of southern Ontario; Ont. Dept. Mines, Map 2117 (1966).

[3] MacAulay, H.A. and Hobson, George D.: Seismic refraction, St. Joseph Island, Ontario (41 J/4 West Half); in Report of Activities, Part A, May to October, 1967; Geol. Surv. Can., Paper 68-1, Part A, pp. 85-86 (1968).

[4] Ehlers, G.M. and Kesling, R.V.: Silurian rocks of the Northern Peninsula of Michigan; Mich. Geol. Soc., Guidebook for Annual Field Conference (1967)

---

20. ROCK MAGNETISM AS A GEOLOGICAL TOOL

Project 700054

E.J. Schwarz

The conventional role of rock magnetism is to provide a physical background for paleomagnetism by considering the magnetic mineralogy and mechanisms of acquisition of various types of remanent magnetization under different natural conditions. However rock magnetism has applications to geology apart from paleomagnetism.

The most abundant magnetic minerals are oxides of iron which have been under study for many years. However, sulphide minerals such as pyrrhotite have been avoided in paleomagnetic work because their occurrence is limited essentially to sulphide (ore) deposits and some rock types, and because the complexity of their magnetic properties has been indicated by the few studies conducted on these minerals. Grant and West (ref. 1, p. 363) state that "The properties of pyrrhotites in sulphide ores are completely unstudied". From a practical point of view, these minerals are obviously of great interest. It is for these reasons that the magnetic properties of pyrrhotite are being investigated at the Geological Survey. Pyrrhotite is the only common magnetic sulphide to occur in nature. As a result of this work, some new techniques of analysis have been developed. To illustrate possible applications of these techniques and to encourage further applications the following examples are given.

Figure 1A shows a thermomagnetic curve for a pyrrhotite sample from the Strathcona Mine, Sudbury. The magnetization (J) decreases continuously during heating in a normal manner. The Curie temperature (T_c) indicates that the composition of the pyrrhotite is Fe_7S_8. Figure 1B, however, shows an abnormal curve. This curve has been split into two parts (1) a normal curve due to Fe_7S_8 (T_{c1}) and (2) an abnormal curve due to Fe_9S_{10} (T_{c2}). J before heating yields the relative abundance of both phases if the sample is relatively pure. The reasons behind this interpretation fall outside the scope of the present account but are discussed in earlier papers[2]. The distribution pattern of these phases in the mine (Fig. 2) shows an abrupt break at the lower contact of the norite which must be of significance in unravelling the formation of these deposits. The advantage of this thermomagnetic technique of analysis is that it is generally applicable however finely intergrown both phases may be (superior to the electron microprobe) and that it avoids possible bias due to grinding and other difficulties as in X-ray diffraction. These results can be augmented by a study on the fabric of the orebody which is very easily carried out on the basis of the extraordinary crystalline magnetic anisotropy of pyrrhotite. This method also has definite advantages over X-ray diffraction and interference from other minerals in the samples is negligible owing to the high contrast in this intrinsic anisotropy.

The second major component of the program is the attempt to unravel the NRM as to components of magnetization acquired at some stage(s) in the history of a rock. For instance, a rock may cool through the Curie temperature in a magnetic field H_1 and at some other time be reheated to a temperature (T_R) below the Curie point and cooled in a field H_2 causing a superposition of two magnetizations of the same type. The results shown on Figure 3A may be interpreted in this manner. If reheating results in a different magnetic mineral (e.g. exsolution in an original titanomagnetite) at a temperature below the Curie point of the new mineral (e.g. purified magnetite), a chemical magnetization above the temperature of (magnetic) metamorphism will be acquired and subsequent cooling will result in another type of magnetization. The results shown on Figure 3B may reflect such events. The temperature (T_R) of metamorphism would be around 450°C. This method is elaborate but should find applications in paleomagnetic work on, in particular, Precambrian rocks that may well have undergone metamorphism. Furthermore the determination of temperatures reached in metamorphism is possible on the basis of magnetochemical changes in selected cases[3].

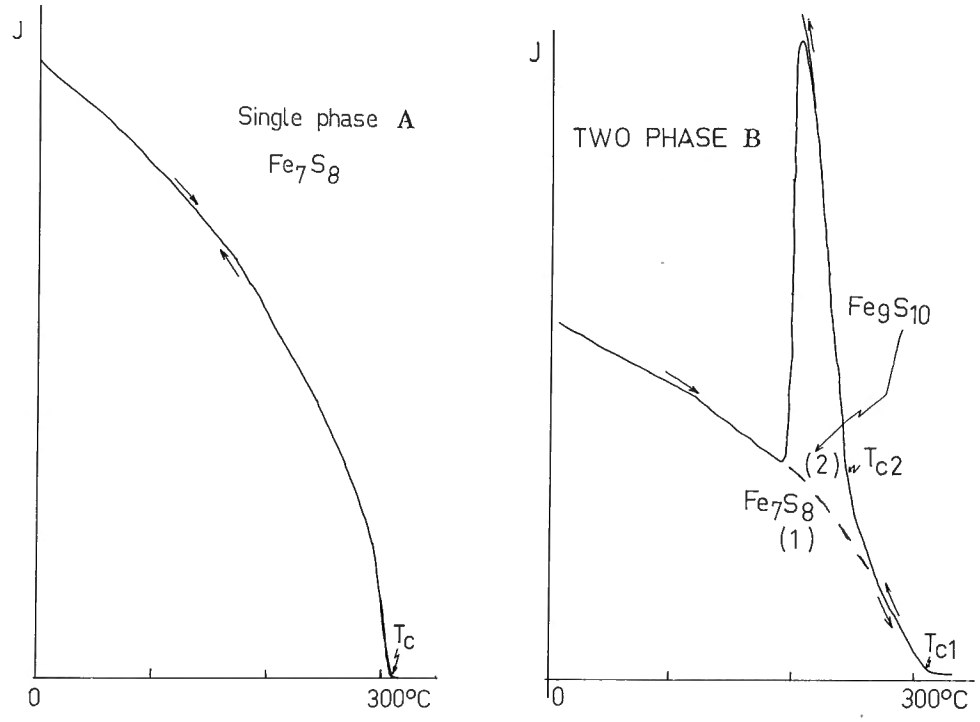

Figure 1. Thermomagnetic curves for single phase (A) and two phase pyrrhotite (B). J. indicates magnetization and T_c represents the Curie point (of phases 1 and 2).

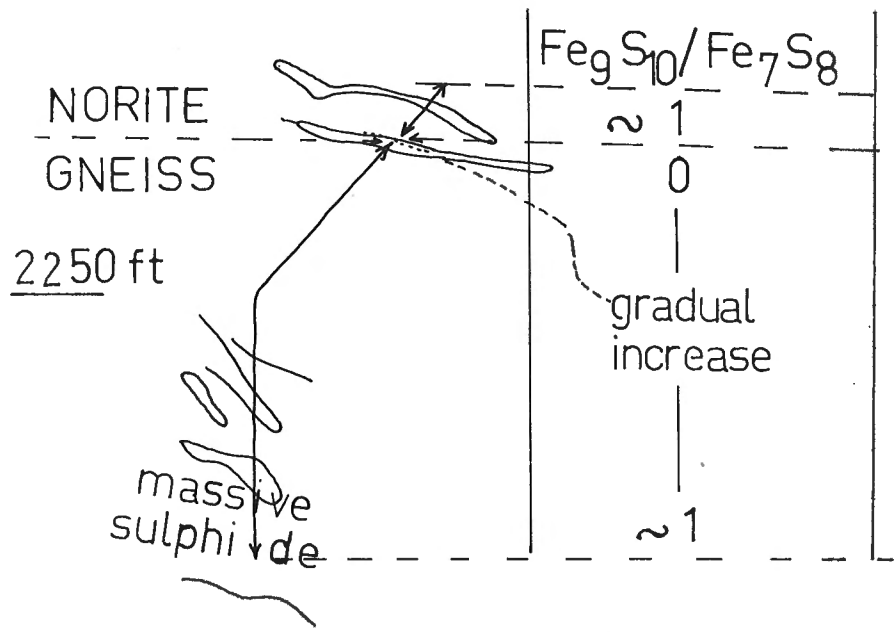

Figure 2. Distribution pattern of Fe_7S_8 and Fe_9S_{10} in the Strathcona Mine, Sudbury.

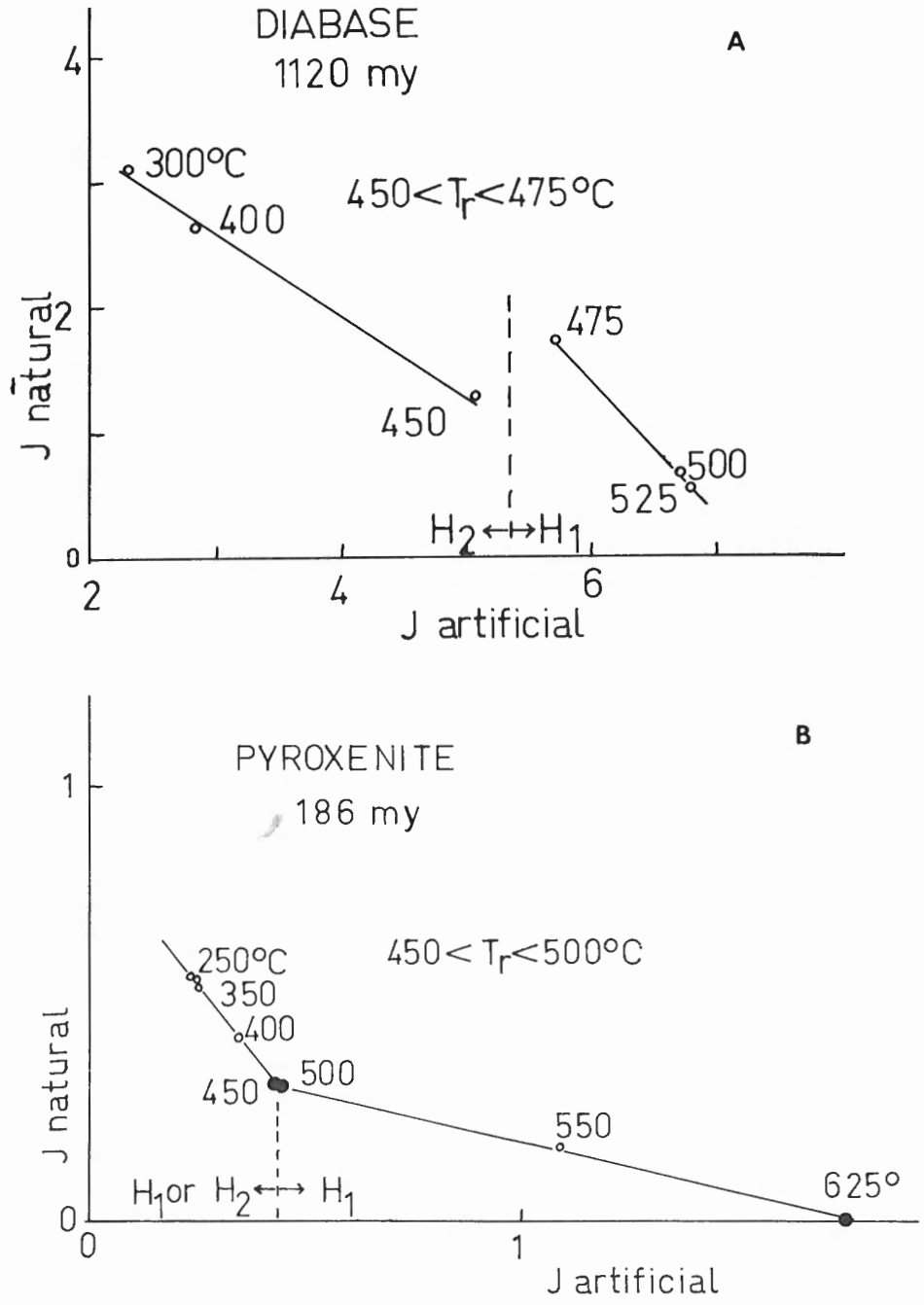

Figure 3. Superposition of components of remanent magnetization of the same type (A) and of different types (B). T_m indicates the upper limit of the temperature reached in (magnetic) metamorphism. J and T_R represent respectively magnetization and temperature of metamorphism.

Techniques and facilities are now available for the following purposes:

1. Quantitative determination of $Fe_{1-x}S$ phases in any pyrrhotite associated with sulphide ores (50 mg samples).
2. Determination of fabric in sulphide bodies (magnetocrystalline anisotropy of pyrrhotite) and in rocks (mainly shape anisotropy of magnetite). This requires oriented samples.
3. Determination of temperatures reached in magnetic metamorphism (only below Curie temperature).

The paleomagnetic investigation of sulphide orebodies in relation to their wall rocks is attractive from a practical point of view but remains a difficult problem. However, the work on pyrrhotite is beginning to provide some answers in this matter.

---

[1]Grant, F.S. and West, G.F.: Interpretation theory in applied geophysics; McGraw Hill, N.Y. (1965).

[2]Schwarz, E.J.: Magnetic phases in natural pyrrhotite; J. Geomag. Geoelect., vol. 20, pp. 67-74 (1968).

[3]Kobayashi, K. and Schwarz, E.J.: Magnetic properties of the contact zone between Upper Triassic red beds and basalt in Connecticut; J. Geophys. Res., vol. 71, pp. 5357-5364 (1966).

---

21. AN ASSESSMENT OF THERMAL INFRARED SCANNING

Project 670054

V.R. Slaney

The Remote Sensing Section of Exploration Geophysics Division has been involved in assessing potential applications of thermal infrared scanners for more than 3 years. Most of the work has been with a Reconofax IV scanner, manufactured by H.R.B. Singer.

The investigations have taken place in association with Inland Waters Branch and therefore have included hydrological studies as well as studies more strictly attributable to the earth sciences. Undoubtedly the most useful application of the scanner lies in the hydrological sciences - the study of currents and water disturbances, thermocline phenomena, harbour studies, groundwater seepage into lakes, rivers or the sea, and the location and the dispersion patterns of coolants and industrial and municipal wastes into rivers and lakes. In each of these areas, a high thermal sensitivity is required, while spatial sensitivity (resolution) is relatively unimportant. The reverse holds true for most, if not for all, investigations over land.

Most of the land areas flown were, for practical reasons, close to Ottawa. Subject areas are generally soil covered and contain a variety of vegetation types. Outcrops are usually scattered and occupy relatively small areas relative to the resolution of the system. There were repeated flights over a test strip near Almonte, which was flown at all times of the year during the day and at night.

The scanner is best applied to the solution of specific problems involving a limited subject area, and allowing for maximum spatial resolution by flying at altitudes not greater than 3,000 feet. Under these conditions most rock outcrops can be recognized and some evidence is available to show that rocks with different thermal conductivity (i.e. limestone and gneiss) can be separated on the imagery. Near surface soil moisture patterns can be distinguished, particularly when the vegetation cover is thin (grassland or crops) or absent. Fractures can often be recognized, particularly when they have topographic expression or when they are outlined because of a distinctive vegetation or soil moisture pattern. Differences in image texture may allow separation of alluvium from glacial drift and from areas underlain by a thin soil cover.

For geological purposes the value of the imagery must be judged with reference to four classes of information: a) the nature of the subject
b) the instrument used
c) timing of flight
d) flight conditions.

(a) The nature of the subject. The most important factors here are the vegetation cover and the effect of air and water.

The vegetation cover is rarely the prime subject of study. Where a vegetation cover exists, and particularly a shrub or tree cover, it acts as a thermal blanket to radiation emanating from the underlying soils. Thermal patterns relating to soils and to scattered outcrops beneath a vegetation cover are usually totally obscured.

The movement of cold air along valleys or into hollows (= frost hollows), and of warm air which often accumulates in vegetation foliage, will modify the radiation from the ground or vegetation surface.

Rain showers during the day preceding a flight will reduce the thermal contrast of the subject area.

(b) The instrument used. The Reconofax IV scanner has a number of limitations which were understood only after a fairly prolonged association with it. Basically the scanner is a military instrument which is being applied to problems for which it was not designed. There is no fixed or measurable relationship between changes in ground radiation received at the detector and changes in image density on the recording film. This is because of an automatic gain control and to the lack of D.C. restoration in the scanner electronics.

The recording system (a modulating lamp scanning 70 mm film) had been designed so that hot, point-source anomalies show up prominently on the film. Subjects colder than average merge into their surroundings. The imagery, once recorded on film, cannot easily be corrected for radial or along track distortion.

(c) The timing of flight. Daytime flights are considered to provide very little useful information because of the irregular and ephemeral effect of solar radiation on the ground. Of all night-time periods, that between sunset and loss of skylight is generally most useful. This is the period of maximum thermal contrast. The length of the survey, 1 1/2 - 2 hours, is limited by the need for accurate visual navigation procedures.

For some subjects, almost any time of year is acceptable e.g. studies of industrial and municipal effluents. For many subjects the timing of the survey may determine whether the technique will be successful in its aim.

Spring - immediately spring floods have subsided is the best time for tracing groundwater infiltration into rivers, since the groundwater being warmer, will float.
- for soil moisture and drainage studies.
- for the greatest thermal contrast between various species of fresh growing vegetation.

Summer - best for differentiating rock types and outcrop from soil or drift.

Autumn - micrometeorology studies, particularly the movement and accumulation of warm or cold air at near-ground levels.

(d) Flight conditions. Many of the requirements for flying have been mentioned already. Given briefly, they are, altitudes below 3,000 feet to maintain ground resolution (aircraft speed is not critical); sufficient light for visual navigation; no rain 24 hours preceding flight; no cloud during flight; high winds and turbulence should be avoided because of need for accurate in-flight measurement of drift and ground speed.

In conclusion, any new sensing system particularly one requiring heavy capital funding, must compete successfully with established sensing systems by providing information not otherwise available, or, by providing the same information at a cheaper price.

Our experience with one particular scanner in a temperate part of Canada would indicate that for geological purposes thermal infrared imaging does not compete successfully with techniques such as aerial photography. While one accepts that the imagery represents a thermal response, there is generally little information on the imagery which can be regarded as unique. In part this is because of the nature of the particular scanner used for the investigations, and in part to the areas chosen for investigation, areas which would now be regarded as being generally unfavourable. Most of the publications claiming a successful application for thermal infrared sensing relate to poorly vegetated, arid environments. The Canadian Shield represents a different environment.

In the summer of 1970, some 300 line miles of thermal imagery was obtained from the area about Fort Smith in the Northwest Territories, using a scanner (manufactured by Daedelus Corporation) specifically designed for natural resource studies.

The imagery produced by this survey has not yet been properly assessed, although from an early examination, it is clear that a number of lithological units can be recognized.

GEOCHEMISTRY

22. DEVELOPMENT OF INSTRUMENTATION FOR VAPOUR SENSING

Project 700087

Q. Bristow

The sensing and measurement of vapour concentrations is receiving increasing attention as an aid in geochemical surveying. Work is proceeding on the development of suitable instrumental techniques for this purpose which it is hoped will enable a number of vapours, e.g. mercury and iodine, to be detected both at ground level and from the air.

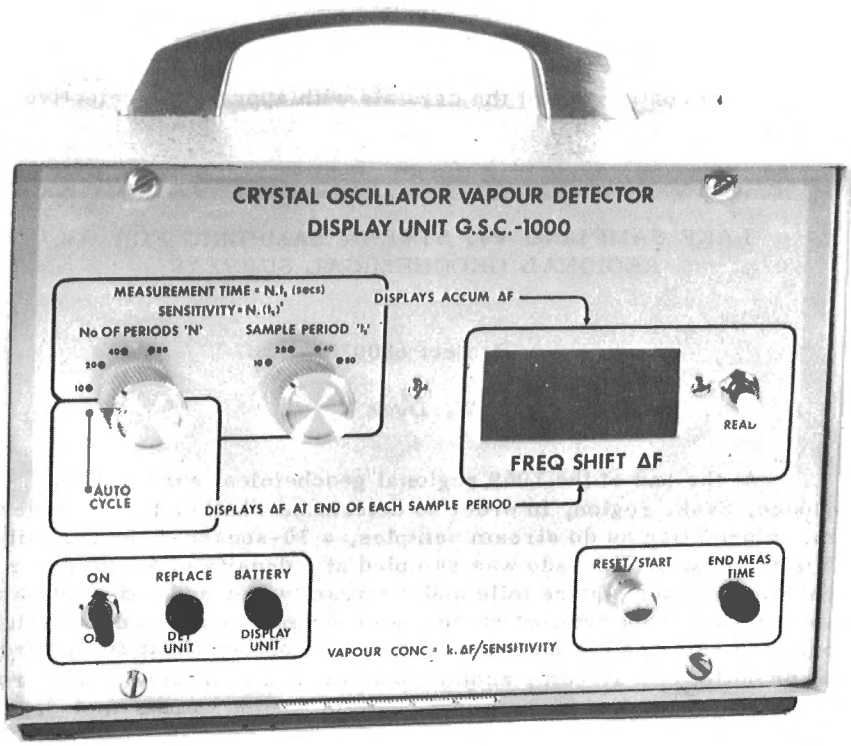

The first objective is the development of a light weight portable instrument for the determination of mercury in soil gases. The photograph (Fig. 1) shows the prototype version of a unit which employs two conventional quartz radio crystals connected as highly stable electronic oscillators with nominal frequencies of 15 MHz. One crystal has aluminum or nickel electrodes and the other has gold electrodes. Both crystals are exposed to the soil gas under investigation and are therefore subject to the same environmental

conditions. Gold has a high affinity for mercury so that if mercury vapour is present in the soil gas it will be adsorbed. The increase in the mass of the crystal lowers its natural frequency by approximately 2.6 cycles/sec per nanogram of additional mass; the other reference crystal frequency is virtually unaffected. The difference between the two frequencies "F_D" is then fed to a mini-computer contained in the display unit (shown in the photograph). As the measurement proceeds and mercury continues to be adsorbed, the value of F_D increases continusouly. The shift is automatically monitored and displayed at predetermined intervals on a digital readout, the accumulated shift over a preset measurement time is a measure of the concentration of mercury vapour in the soil gas.

The crystals and associated oscillator circuits are contained in a detector unit about one-tenth of the volume of the display unit. The equipment is battery operated from four 1.5V "D" cells and two smaller 5.4V cells. An analogue output for driving a strip chart recorder is provided.

The quantity price of gold electrode crystals is of the order of $2.50 and it is anticipated that each crystal will be good for about 10 determinations before its ability to adsorb mercury has deteriorated to the point where it affects the accuracy of the result.

This approach is still in the development stage and has yet to undergo field tests. However, if successful, it may well have application to other vapours by coating one of the crystals with appropriate selective absorbents.

23. LAKE SAMPLING vs. STREAM SAMPLING FOR REGIONAL GEOCHEMICAL SURVEYS

Project 680028

W. Dyck

At the end of the 1969 regional geochemical survey of the Beaverlodge, Sask. region, in order to determine whether lake samples give the same information as do stream samples, a 30-square-mile area situated about 5 miles east of Eldorado was sampled at a density of 4 lake water and sediment samples per square mile and 4 stream water and sediment samples per square mile. This detailed sampling program was carried out as follows: while one man sampled the lake-bay from a helicopter, about 20 feet from the inlet or outlet of a stream, another man took two stream samples roughly 200 feet apart. A total of 63 such lake-stream groups were sampled; another 62 lake sites alone were sampled and included 33 inactive bays. The following variables were determined: temperature, uranium, radon, pH, and alkalinity in waters and uranium, radium, zinc, copper, lead, and nickel in sediments. Except for radon and uranium in water, all variables give significant positive correlations between the lake bay sites and the stream sites. Radon and uranium correlate only weakly, with probabilities of significance of 44 and 77 per cent respectively.

Comparison of the geometric means of element concentrations leads to several interesting observations and rough but useful generalizations.

As was already observed in the regional survey, the pH and temperature was lower, and the radon alkalinity and uranium higher, in stream waters. Analysis of sediments from the detailed survey show that the concentration of U, Cu, Pb, Ni, and Ra is roughly 25 per cent higher in streams than in lakes; Zn shows just the opposite trend. Also, sediments from outflow bays and from streams near outflow bays contain roughly 25 per cent more U, Zn, Cu, Pb, and Ni than do sediments from inflow bays or from streams near inflow bays; in this case Ra shows the opposite trend. It is believed that the organic content, which is about 40 per cent higher in stream sediments than in lake sediments and about 15 per cent higher in outflow sites, and the relative mobility of the elements are responsible, either directly or in combination with iron and manganese hydroxides, for the observed differences in trace element contents.

The results indicate the following relative mobility of trace elements in the Beaverlodge surface environment: Zn>U>Cu>Ni>Pb>Ra.

The results suggest that lake waters are a good medium for geochemical reconnaissance of large regions. However, sampling and analytical problems limit this approach at present. Adsorption on containers and desorption from suspended matter, when acid is added to prevent adsorption, are the toughest problems to overcome. Nevertheless, the regional uranium survey of the Beaverlodge area showed that with the detection of definite amounts of uranium in about 30 per cent of the lake and stream waters out of a total of 1,300 samples, uraniferous zones can be outlined sucessfully. In contrast, out of 350 lake and stream water samples only 16 per cent had Zn contents above the detection limit and none had detectable amounts of Cu and Ni using direct atomic absorption analytical methods. Even with preconcentration of 90 samples, only 70 per cent contained detectable amounts of Zn and 13 per cent detectable amounts of Cu and Ni.

Apart from confirming the existence of three uranium 'highs' detected during the regional survey, the detailed sampling program also showed that sediment sampling of small lakes near the inflow or outflow of streams will give essentially the same information as stream sampling. In rugged terrain like that encountered in the Beaverlodge area where landing on land is practically impossible, lake sampling can result in considerable savings to the exploration geochemist.

Considering the present state of methods of sampling and analysis of geochemical materials, it appears that sediment sampling by helicopter of inflow and outflow lake bays offers the most economical method of assessing the mineral potential of large regions of the Canadian Shield. For U and Zn lake water sampling should suffice.

GEOCHRONOLOGY

24. LEAD ISOTOPIC EVIDENCE ON AGE OF MINERALIZATION, GREAT BEAR LAKE, DISTRICT OF MACKENZIE (Including a New Model for Certain Anomalous Leads)

Project 680060

R.I. Thorpe

Lead isotopic results have been received from the Geochronology Laboratory of the Geological Survey of Canada for 6 galena samples from the silver veins of the Great Bear Lake area, and preliminary results have been received from Isotopes Inc. for an additional 5 samples. The following notes give a tentative interpretation of the available isotopic data; further documentation will be presented in a paper now in preparation.

Seven of the above samples are composed of ordinary lead, as were three of the galena samples from Port Radium that were analyzed by Jory[1]. The preliminary data from Isotopes Inc. give points falling far below any accepted model curve, but the remaining 8 ordinary galenas on a plot of Pb^{206}/Pb^{204} ratio versus Pb^{207}/Pb^{204}, the so-called x-y plot, are closely scattered about a Pb^{204} error line. If it is considered that the data for these 8 galenas indicate a single lead composition then, on the basis of the assigned analytical errors, lead with a Pb^{207}/Pb^{206} ratio of 0.963 to 0.966 and an age of 1623 $\pm$ 17 m.y. satisfies the analytical results. The Geological Survey of Canada data fit closely the model curve suggested by Stacey et al.[2] This model uses, as primordial lead isotope ratios, the absolute values determined by Oversby[3] on meteorites. However, on a plot of Pb^{206}/Pb^{204} ratio against Pb^{208}/Pb^{204} ratio, the so-called x-z plot, the model of Stacey et al. is not entirely satisfactory. The authors have used a decay constant of 4.99×10^{-11}/yr. for Th^{232}, although they do not specify this. Change of the decay constant will not, however, improve the agreement of the apparent x-z age with that indicated by the x-y plot, but an increase in the value for the present Th^{232}/Pb^{204} ratio from 34.75 to a value in the range of 35.3 to 36.0 gives good agreement. The calculated Th/U ratio on the basis of this model is approximately 3.88 to 3.96. This is in good agreement with values tabulated by Stacey et al. (ref. 2, p. 22) for leads that are generally considered to be of single-stage origin.

Four anomalous galenas have been analyzed for the writer and four were done by Jory[1]. In addition two samples analyzed by Jory, one of galena (PR 42) and one of a tetrahedrite-chalcopyrite assemblage (PR 3), were found to consist of a mixture of ordinary lead with radiogenic lead from a very uranium-rich source. These anomalous galenas generate a chord on the x-y plot which apparently merges with the average Port Radium ordinary galena at one end and intersects the model curve again near the zero isochron as it passes into the more radiogenic region of the plot. The radiogenic component for these anomalous galenas have been derived from a source about 1625 m.y. old if the leads resulted from mixing of a radiogenic component with ordinary lead and if deposition of the galena was very recent. Pitchblende

in the veins at Port Radium would be a logical source for radiogenic lead, in fact the amount of uranium lead generated in the veins has been calculated by (ref. 1, p. 175) at 3.5×10^6 pounds on the basis of the quantity of uranium mined. However, the anomalous galenas are not a product of mixing of ordinary lead and uranogenic lead, because the Th/U ratio of the source for the radiogenic component has been calculated to be as great as 2.89 to 4.5%. If recent formation of the anomalous galenas is assumed then a source age of about 1625 m.y. for the radiogenic component is a problem because this is the date of ordinary lead mineralization and the host rocks have been dated as considerably older (refs. 1, 4). The maximum age for formation of the anomalous leads by this mixing model is about 933 m.y., the time at which the instantaneous production ratio Pb^{207}/Pb^{206} was in agreement with that of the radiogenic component.

The writer's first interpretation of the anomalous leads was that they must have formed very recently, probably even in a groundwater regime that persists to the present. This is the interpretation that was arrived at by Tugarinov et al.[5] for a similar suite of anomalous galenas. The writer has now developed a new model for anomalous leads that seems more in line with some of the observed relationships. It is postulated that the anomalous galenas were formed at the same time as ordinary galena and other vein minerals, but that they have been subjected to continuous addition of radiogenic lead, probably by diffusion from their relatively immediate environment, until the present. This best explains why in a number of cases (for example: the present study; refs. 5, 6) where the ordinary galena composition is closely defined, the model age for the ordinary lead is in good agreement with a Pb^{207}/Pb^{206} slope age for the source of the radiogenic component when recent formation of the galena is assumed. The slope of a suite of anomalous galenas on an x-y plot can thus be used to confirm the age indicated by ordinary galena in the veins, and a less certain technique would be to use the "anomalous lead age" of vein galenas as the age of mineralization even when the ordinary lead composition has not been defined.

Jory's leads which contain a uranogenic component yield some interesting evidence on the age of mineralization. Sample PR 42 contains only a small radiogenic component and this makes calculations subject to considerable error. Jory (ref. 1, p. 190) assigned a Pb^{207}/Pb^{206} ratio of 0.15 ± 0.04 to the uranogenic lead component in this sample. However, a ratio as low as 0.0815 can be calculated using his assigned error limits and taking sample S 207 as representative of the ordinary lead. This removes the minimum age of 750 m.y. suggested by Jory for this galena. Sample PR 3 was found (ref. 1, p. 189) to contain some uranium, and the ordinary lead content was very low in the tetrahedrite-chalcopyrite material analyzed, and these facts together suggest that the uranogenic lead has been generated in situ in this case. On the basis of this assumption an age for the source uranium mineral can be calculated using Jory's sample S 207 for the composition of the ordinary lead component. This age is 1579 to 1630 m.y. and indicates that some uranium was deposited in the veins in association with sulphides at the time of ordinary lead mineralization. This date is not in agreement with Jory's date of 1445 ± 20 m.y. for the time of pitchblende deposition.

Jory's data for pitchblendes was obtained on seven samples of various size taken from three specimens from the Port Radium mine. He concluded from his work that the pitchblende in carbonate gangue was deposited at 1445 ± 20 m.y. However, this age was based so heavily on a single

sample, which could have been subjected to later redeposition, that he could not rigidly conclude that a single age of uranium mineralization was represented, although he considered his results to favour this conclusion (ref. 1, p. 173). If one combines the results of earlier isotopic analyses on radiogenic lead from pitchblende at Port Radium with Jory's data, any lingering doubts about his apparent age for pitchblende mineralization are eliminated. Data from Cumming et al.[7] for 18 lead isotopic determinations on an x-y plot, together with Jory's data, define an isochron at 1451 ± 12 m.y., in excellent agreement with the age based on Jory's data alone.

The possibility that pitchblende mineralization at about 1450 m.y. was superimposed on an earlier sulphide mineralization at about 1625 m.y. seems remote, in view of the paragenetic evidence from microscopic study of textures that the reverse sequence of deposition was the case[1,8]. It therefore seems necessary to conclude that the pitchblende in the Port Radium veins has been updated from 1625 to 1450 m.y., possibly by mobilization and redeposition at the latter date. There is evidence of an event in the area at this approximate date. Wanless et al.[9] report a K-Ar age of 1400 ± 75 m.y. for a biotite-hornblende mixture from a sample collected by W.F. Fahrig from a diabase sheet or "sill" on Hogarth Island, about 16 miles northeast of Port Radium. Such a diabase sheet or sill about 150 feet thick cuts through the veins at Port Radium. Magnetite-actinolite veins, sometimes containing apatite, pyrite and other minerals, are closely associated spatially with the diabase sheet. Robinson[4] concluded that there is probably a genetic relationship between the magnetite-actinolite veins and the diabase sheet and he reports an age for the veins of 1420 ± 60 m.y. on the basis of K-Ar analysis of two actinolites and one hornblende from the veins (loc. cit., p. 61). The obvious mobility of iron oxides at the time these veins were formed may be a factor in favour of the suggestion that pitchblende was mobilized and redeposited at this time, although such remobilization appears to be contradicted by the textural evidence unless all vein minerals were remobilized and sulphides redeposited slightly later than pitchblende.

For those who may be reluctant to accept the idea that pitchblende can be completely updated by postdepositional events some further evidence should be cited. It is, of course, widely accepted that pitchblende and other uranium-bearing minerals undergo episodic and/or continuous diffusion loss of radiogenic lead. U-Pb dating of pitchblende in the Beaverlodge area, Saskatchewan, by Koeppel[6] resulted in the definition of an apparent age of mineralization at 1780 m.y. and a redeposition of some of the pitchblende at 1110 m.y. The lead isotopic data obtained by Koeppel on galenas and clausthalites suggest, by the writer's interpretation, an original age for the mineralization of 2500 to 2560 m.y. Indeed, Koeppel's suite of galenas included one that is apparently an ordinary galena with a model age of 2450 to 2500 m.y. (or a little order if there is a very slight radiogenic contamination), in very good agreement with the age suggested above on the basis of anomalous galenas. Thus Koeppel's U-Pb date of 1780 m.y. for the pitchblende would appear to also represent an updating event. Not all of Koeppel's lead isotopic data can be readily interpreted, and possibly after further consideration the updating events recorded by the pitchblendes can be identified in the galenas. Knipping[10] has reported that U-Pb dating work on pitchblende from the Rabbit Lake deposit, within the Wollaston Lake fold belt, "indicates primary emplacement of pitchblende 1,200 million years ago with leaching and redeposition at stages between 1,200 and 200 million years ago". However, one sample

recently analyzed from the same deposit for H.W. Little (pers. comm.) at the Geological Survey of Canada suggests a minimum age of about 1610 m.y., and the writer would suggest that the 1200 m.y. date represents an updating event, possibly the same event as that interpreted at 1110 m.y. in the Beaverlodge area by Koeppel.

---

[1]Jory, L.T.: Mineralogical and isotopic relations in the Port Radium pitchblende deposit, Great Bear Lake, Canada; Ph.D. thesis, Calif. Inst. Technol., 275 pp. (1964).

[2]Stacey, J.S., Delevaux, M.H. and Ulrych, T.J.: Some triple-filament lead isotope ratio measurements and an absolute growth curve for single-stage leads; Earth Planet. Sci. Letters, vol. 6, No. 1, pp. 15-25 (1969).

[3]Oversby, V.M.: The isotopic composition of lead in iron meteorites; Geochim. Cosmochim. Acta, vol. 34, pp. 77-88 (1970).

[4]Robinson, B.W.: Studies on the Echo Bay silver deposit, Northwest Territories, Canada; Ph.D. thesis, Univ. Alberta (Edmonton), 229 pp. (1971).

[5]Tugarinov, A.I., Bibikova, E.V. and Zykov, S.I.: Age of rocks of the Kursk magnetic anomaly; Geochemistry International, No. 5, pp. 945-950 (1964) (Transl. from Geokhimiya, No. 10, pp. 988-994, 1964).

[6]Koeppel, V.: Age and history of the uranium mineralization of the Beaverlodge area, Saskatchewan; Geol. Surv. Can., Paper 67-31 (1968).

[7]Cumming, G.L., Wilson, J.T., Farquhar, R.M., and Russel, R.D.: Some dates and subdivisions of the Canadian Shield; Proc. Geol. Assoc. Can., vol. 7, Pt. 2, pp. 27-79 (1955).

[8]Kidd, D.F. and Haycock, M.H.: Mineragraphy of the ores of Great Bear Lake; Bull. Geol. Soc. Am., vol. 46, pp. 879-959 (1935).

[9]Wanless, R.K., Stevens, R.D., Lachance, G.R. and Delabio, R.N.: Age determinations and geological studies, K-Ar isotopic ages, Report 9; Geol. Surv. Can., Paper 69-2A (1970).

[10]Knipping, H.D.: Geology and uranium metallogenesis, Wollaston Lake area, Saskatchewan (Abstract); Can. Mining Met. Bull., vol. 64, No. 707, p. 51 (1971).

---

25. COMMENTS ON ROCK AGES IN THE YELLOWKNIFE AREA, DISTRICT OF MACKENZIE

Project 680060

R.I. Thorpe

During the course of compilation of Pb-Pb and U-Pb isotopic data for the Bear and Slave provinces in connection with this project, some interesting conclusions were reached with regard to the age of rocks at Yellowknife, primarily on the basis of U-Pb data recorded by Green[1] for 15 zircon concentrates. His extensive Rb-Sr and K-Ar age data are not reviewed. Green's data were examined on plots of Pb^{207}/Pb^{204} ratio against Pb^{206}/Pb^{204} ratio and Pb^{207}/Pb^{208} ratio versus Pb^{206}/Pb^{208} ratio. On such plots the Pb^{207}/Pb^{206} ratio for the radiogenic component added to a zircon since its formation is derived as the slope of the resulting[2, 3, 4] line if the points define a well-controlled line. The result is independent of any recent chemical loss of lead from the zircons since chemical fractionation of the Pb^{206} and Pb^{207} isotopes is generally considered to be insignificant. Past loss of lead would result in an age that is too young and, since uniform loss would be unlikely for a suite of samples, should result in some scatter of the analytical points. A significant point to be made is that such plots should always be prepared in zircon dating work, in addition to the standard Concordia plot, in order to avoid errors in interpretation.

In the calculation of ages used in the following discussion the decay constants employed for U^{238} and U^{235} were 1.537×10^{-10}/yr. and 9.722×10^{-10}/yr., respectively. A value of 1/137.8 was used for the present atomic ratio of U^{235} to U^{238}. Green (ref. 1, Appendix, pp. 29, 39) used the same values for these constants. The limits of error assigned to the ages refer to the uncertainty of the slope defined by the data points and do not account for possible errors in age due to uncertainties in the constants listed above.

Green's 12 analytical points, including spiked values, for zircons from the Southeastern Granodiorite give an excellent lead isochron or "Houterman's" isochron at 2610 ± 10 m.y. on a Pb^{207}/Pb^{204} - Pb^{206}/Pb^{204} plot. This includes the Ross Lake sample which is considerably more radiogenic than the other samples, but which does appear to be part of the suite. The single zircon Pb^{207}/Pb^{206} age for the sample, given by Green as 2640 ± 10 m.y., also suggests this affinity. The lead isochron age of 2610 ± 10 m.y. is in excellent agreement, as should be the case, with the Concordia age of 2618 ± 20 m.y. given by Green.

In the case of the Western Granodiorite, however, the lead isochron age is considerably greater than for the Southeastern Granodiorite while Green arrived at a slightly younger age. A plot of Pb^{207}/Pb^{204} ratio versus Pb^{206}/Pb^{204} ratio gives an age of 2699 ± 20 m.y. if the Stock Lake sample is ignored, and an age of 2675 ± 40 m.y. if it is included. A plot of Pb^{206}/Pb^{208} ratio against Pb^{207}/Pb^{208} ratio for Green's unspiked data gives a good isochron at approximately 2713 m.y., but this is not completely satisfying since the slope is controlled by the point for the Stock Lake specimen. However, a plot of Pb^{207}/Pb^{208} ratio against Pb^{206}/Pb^{208} for Green's results when a Pb^{208} spike was employed, yields an excellent isochron at 2690 ± 20 m.y. (Fig. 1). There is no essential disagreement in these various ages,

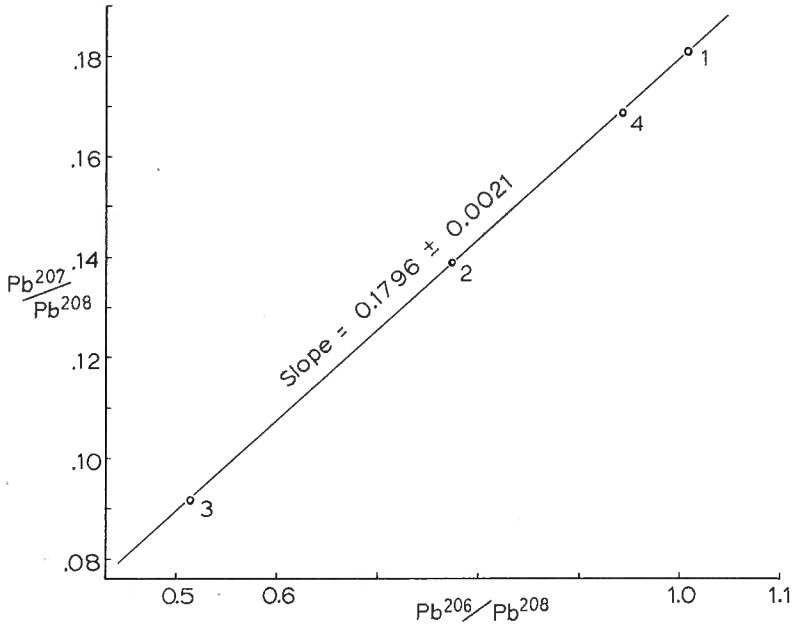

Figure 1. Lead isotopic plot of zircon data for the Western Granodiorite, Yellowknife area. Data from Green (1968).

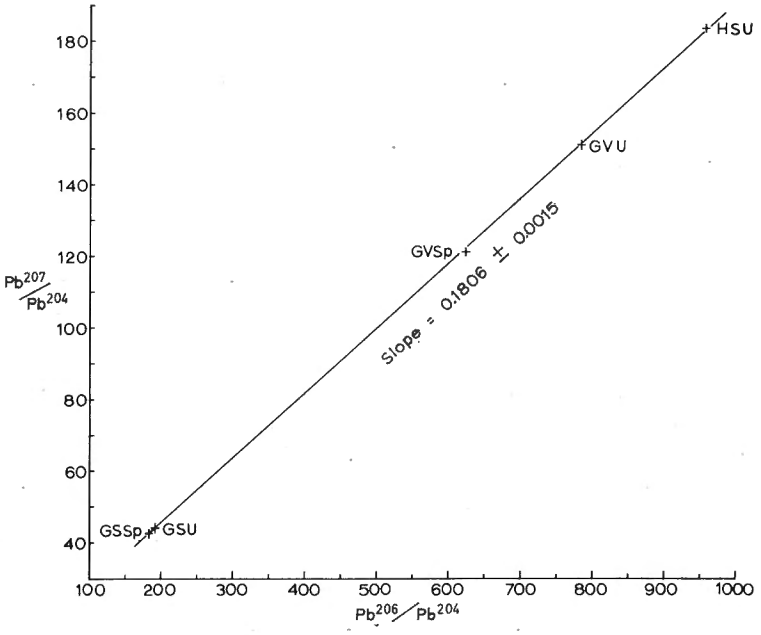

Figure 2. Lead isotopic data for zircons from sediments and volcanics of the Yellowknife Group. H = Henderson, G = Green, S = sediments, V = volcanics, U = unspiked, Sp = spiked.

but the latter date is accepted as the data points show less scatter on this plot. Figure 1 shows that the point for the Stock Lake sample falls on the line generated by the other three samples, suggesting that the Stock Lake intrusion is essentially coeval with the main Western Granodiorite mass. This age of 2690 ± 20 m.y. for the Western Granodiorite is not in agreement with the Concordia age of 2596 ± 16 m.y. given by Green, and the reason for the lack of agreement is not obvious. The problem most likely lies in the fact that Green's chord on the Concordia plot is controlled by a single point for a specimen from the Fort Rae highway. The other points on his Concordia plot could be on a chord intersecting the curve at 2725 ± 45 m.y. This age, although the error limits are broad, is in reasonable agreement with the 2690 ± 20 m.y. date deduced above. The chord gives a lower or secondary Concordia intersection of about 860 m.y. for an age of 2690 m.y. or of about 1000 m.y. if the age is assumed to be as great as 2725 m.y. The lower intersection could represent the time of an episodic lead loss from the zircons. It has been found by a number of workers, however, that the lower intersection on a Concordia diagram does not necessarily have geological significance[5].

Green's data for two zircon samples, one from Yellowknife Group sediments and one from Yellowknife Group volcanics, have been considered together with the data obtained at the Geological Survey of Canada for a zircon concentrate from Yellowknife Group sediments collected by J.B. Henderson. With Green's spiked data, five points are then available for defining an isochron on a Pb^{207}/Pb^{204} - Pb^{206}/Pb^{204} plot at 2700 ± 14 m.y. (Fig. 2). This age is in close agreement with the single zircon Pb^{207}/Pb^{206} age of 2685 m.y.[6] for the Henderson sample. The detrital zircon suite in the Yellowknife Group sediments, which have greywacke affinities, have been derived, at least in part, from the Yellowknife Group volcanics according to Henderson (ref. 7, p. 6, and pers. comm.). Thus the isochron could be indicating the age of the Yellowknife Group volcanics. This latter reasoning also provides the justification for using zircon lead isotope data on both sediments and volcanics in a single plot. On a Concordia plot a chord joining the analytical points for the two sediment samples intersects the curve at about 2702 m.y., but the point for the volcanic sample plots some distance from the line. It must be noted that this possible age for the Yellowknife Group "volcanics" is indistinguishable from that derived above for the Western Granodiorite. Whether or not intrusion of the Western Granodiorite followed extrusion of the volcanics very closely is not known, but the alternate possibility that zircons in the sediments have been largely derived from the Western Granodiorite and that the (considerably older?) volcanics have not been dated by the above technique, must still be entertained. This is especially so in view of the divergence of the point for the volcanic sample from the chord generated by the sediment samples on a Concordia plot. More samples of Yellowknife Group volcanics should be investigated for age dating, possibly using lead isotopic analysis of mixed heavy mineral concentrates to avoid the problems inherent in attempting to derive a high-purity zircon concentrate from zircon-poor lavas and in carrying out quantitative U and Pb analyses.

---

[1] Green, D.C.: Precambrian geology and geochronology of the Yellowknife area, N.W.T.; Ph.D. thesis, Univ. Alberta (Edmonton), 166 pp. (1968).

[2]Houtermans, F.G.: Die Isotopenhäufigkeiten im natürlichen Blei und das Alter des Urans; Naturwissenschaften, vol. 33, pp. 185-186 (1946).

[3]Houtermans, F.G.: Das Alter des Urans: Zeitschr. Naturforschung; vol. 2a, pp. 322-328 (1947).

[4]Stieff, L.R., Stern, T.W. and Eicher, R.N.: Algebraic and graphic methods for evaluating discordant lead-isotope ages; U.S. Geol. Surv., Prof. Paper 414E, 27 pp. (1963).

[5]Steiger, R.H. and Wasserburg, G.J.: Comparative U-Th-Pb systematics in 2.7 x 10^9 yr. plutons of different geologic histories; Geochim. Cosmochim. Acta, vol. 33, pp. 1213-1232 (1969).

[6]Wanless, R.K.: Isotopic age map of Canada; Geol. Surv. Can., Map 1256A (1970).

[7]Henderson, J.B.: Stratigraphy of the Archean Yellowknife Supergroup; Yellowknife Bay-Prosperous Lake area, District of Mackenzie; Geol. Surv. Can., Paper 70-26 (1970).

MINERALOGY

26. PARTLY-FUSED PHLOGOPITE FROM ECLOGITE NODULES AND ITS RELATION TO DIAMOND-BEARING KIMBERLITE AND RELATED ROCKS

Project 700067

J. Rimsaite

Chemical and optical properties of the partly-dehydrated phlogopite and the host eclogite (Ec) from kimberlite were studied and compared with those reported for South African diamond-bearing kimberlites (K), their cognate inclusions, and Canadian kimberlites, lamprophyres (L), carbonatite (C) and metasomatic limestone. The distinctive features of the partly dehydrated phlogopite and associated pyroxene from the eclogite nodules in kimberlite are their partly fused edges and glass particles, which indicate that the mica and the pyroxene were affected by thermal alteration after crystallization (Figs. 1, 2).

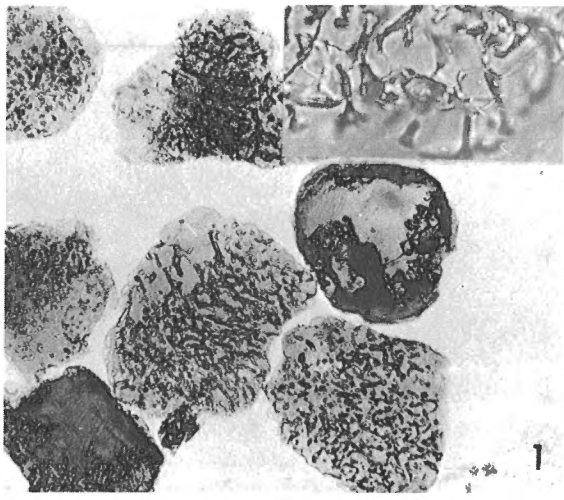

Figure 1.
Phlogopite flakes with glass particles, x40. Area containing glass particles is illustrated in the upper right field, x500.

Figure 2.
Partly-fused and recrystallized phlogopite and pyroxene in eclogite nodule from South African kimberlite.

The results show that the host rocks are ultrabasic with Niggli values for si between 25 and 100, and k between 0.7 and 1.0. The Niggli values for a phlogopite-rich nodule and for the phlogopites fall also in the field of the ultrabasic rocks. As can be seen from Figure 3, the phlogopite is the principal

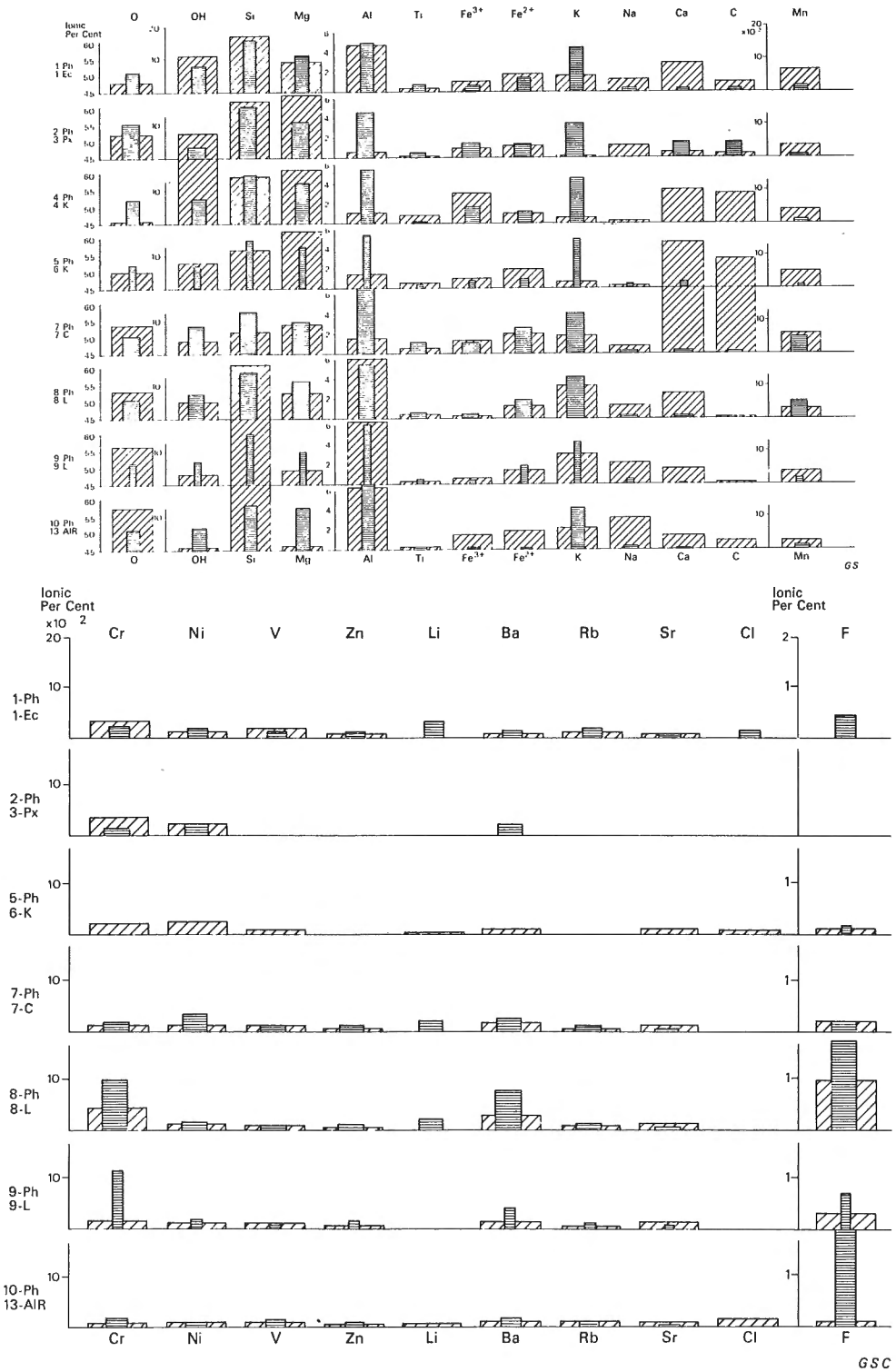

Figure 3. Ionic percentages of major and minor constituents in phlogopite (Ph) and in ultrabasic host rocks.

carrier of potassium, rubidium, aluminium, and of primary magmatic water in kimberlite and in carbonatite. Some minor elements, such as fluorine, chlorine, lithium, barium, nickel, chromium, titanium and zinc are also present mainly in the phlogopites. The magmatic phlogopite differs from the metasomatic phlogopite in its lower aluminium and fluorine contents, and in the abundance of some trace elements. The phlogopite is of geochemical and petrological interest because it reflects chemical composition of the parent ultrabasic magma, including its water and alkali contents which are altered in the host rocks during subsequent serpentinization and weathering.

27. EXAMPLES OF SPINEL-MICA ASSOCIATIONS IN CANADIAN ULTRABASIC ROCKS AND IN NICKEL DEPOSITS

Project 700067

J. Rimsaite and G.R. Lachance

Two hundred ultrabasic rocks and specimens from Cu-Ni deposits of Coppermine, Lynn Lake, Shebandowan, Timmins, Malartic, and Ungava areas, and from Eastern Townships of Quebec were examined under a petrographic microscope for their mica contents. It was found that these rocks contain fresh, altered, primary and secondary micas associated with fresh and/or altered spinels. Chemical properties of the micas and of the associated spinels and some other minerals were studied by an electron microprobe and a few examples of spinel-mica associations from the ultrabasic rocks, massive Cu-Fe-Ni sulphides, and from selvages between the sulphides and wallrocks are given in this summary:

An example of the mica-olivine-spinel association in an ultrabasic rock is illustrated in Figure 1. The spinels and micas are zoned. The early phlogopite and olivine phenocrysts, cogenetic with red chromite, contain relatively high concentrations of nickel (0.1-0.3%). The chromium contents of the zoned phlogopite and spinel decrease from the core towards the rim, as can be seen from the changes in structural formulae of the spinel: $(Mg_{.7}Fe''_{.3})(Fe''_{.2}Al_{.6}Cr_{1.2})O_4$ for the core, to $(Mg_{.6}Ti_{.1}Fe_{.3})(Fe_{.6}Al_{.3}Cr_{1.1})O_4$ for the inner rim, and to $(Mg_{.1}Ti_{.6}Fe''_{.3})(Fe_{1}''_{.8}Al_{.2}Cr_{.02})O_4$ for the outer rim. The chromium content in the early phlogopite phenocrysts is 1.5% Cr_2O_3 and decreases in the rim of zoned crystals to 0.05% Cr_2O_3. Similar red Cr-spinels associated with micas were found in ultrabasic rocks from the Eastern Townships of Quebec, from Shebandowan and Bird River areas and from the Thompson Nickel Belt. In some drill core samples from the southwest part of the Manitoba Nickel Belt, the phlogopite is partly altered to bright-green chlorite which contains less chromium than the original mica. It is concluded that the early phlogopites which are cogenetic with chromite contain relatively high concentration of chromium which decreases in later generations of the phlogopite and during its alteration to chlorite.

The metaperidotite of the Manitoba Nickel Belt, described by Zurbrigg[1] and metaperidotites from the Werner Lake Ni-deposit contain phlogopite in intergrowths with green and olive-brown Al-Fe-spinels which contain 5 to 30 per cent Cr_2O_3 (Fig. 2).

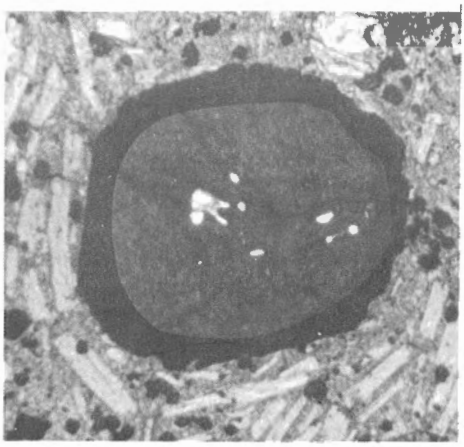

1

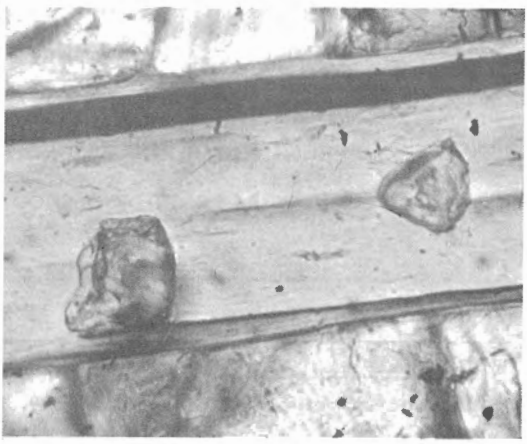

2

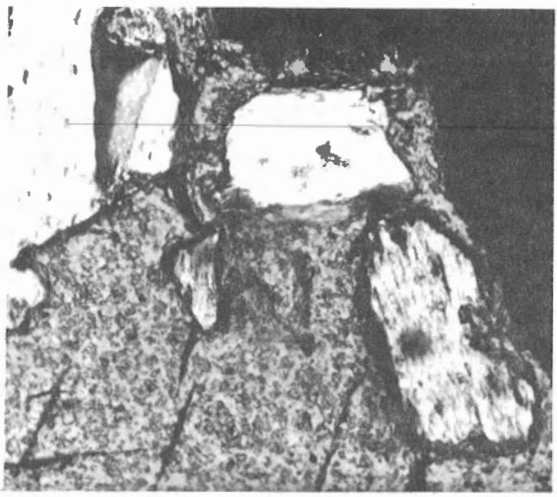

3

4

Figure 1. Chromite rimmed by titaniferous magnetite and surrounded by mica flakes in kimberlite, x40.

Figure 2. Phlogopite with opaque bands and green spinel (two grains having high relief) in the metaperidotite from the Manitoba Nickel Belt, x100.

Figure 3. Zincian spinel with mica inclusions (white) adjacent to massive Fe-Ni sulphides (black), x100.

Figure 4. Zoned Cr-rich granules in massive Fe-Ni-sulphides from the Megantic area in Quebec, x100.

Selvages between massive Cu-Fe-Ni sulphides and the wall-rocks in the Ni-deposits of the Manitoba Nickel Belt consist of brown-red chromian biotite, greenish chromian muscovite, and mottled yellow-brown-red spinels (Fig. 3). The spinel varies in colour and chemical composition from a yellow zincian variety $(Mg_{.05}Fe_{.55}Zn_{.4})(Al_{1.6}Cr_{.4})O_4$ to red chromite

TABLE 1.

DISTRIBUTION COEFFICIENTS K_D^{m-s} FOR SEVEN OXIDES BETWEEN FRESH MICAS AND ASSOCIATED SPINELS, AND SOME ALTERED AND SECONDARY MINERALS

Host rock	Al_2O_3	TiO_2	FeO	Cr_2O_3	MgO	MnO	Ni
in Ultrabasic rock, Fig. 1:							
Phlogopite-chromite core	.7	49.	.2	.04	1.8	.03	1.
Biotite-spinel rim	3.6	.2	.2	.08	4.	.4	1.
Thompson Nickel Belt in Serpentinite:							
Phlogopite-red spinel	5.	.5	.08	.02	19.	.03	1.
Phlogopite altered-olive spinel	1.	.9	.08	.02	5.	.04	.5
in Metaperidotite : Phlogopite-green spinel	.3	1.8	.25	.04	4.	.4	1.
Cu-Fe-Ni sulphides in Selvages:							
Biotite-red spinel	2.	4.	.7	.03	24.		3.
Muscovite-yellow spinel	1.2	.4	.05	.03	5.		3.
Sericite-red spinel	2.3	.2	.06	.00	2.		.0
In Spinel:							
Biotite-yellow spinel	.3	5.	1.	.08	6.	2.3	4.
In Po-Pn Ore:							
Biotite-brown spinel	.5	5.	.7	.03	6.	4.	2.
Werner Lake Area in Serpentinite							
Phlogopite-olive green spinal	.3	2.	.3	.08	3.5	.2	.4
Phologpite altered green spinel	.4	.25	.1	.07	4.6	.2	.4
Chlorit. mica-olive spinel	.3	1.6	.2	.02	2.6	.07	1.
in Po-Pn Ore							
Biotite-Zoned Cr-grains	.3	10.	.8	.02	.7	.1	1.
Fe-Oxide vein-host spinel	.05	0.0	3.	.00	.0	.4	7.

$(Mg_{.04}Fe''_{.82}Zn_{.14})(Al_{.9}Cr_{1}Fe'''_{.1})O_4$. Micas and spinels, which are present in massive Cu-Fe-Ni sulphides of the Thompson Nickel Belt, are similar in chemical composition to those from the selvages. Some of the biotite flakes are partly altered and replaced by greenish chlorite, some of the spinels are partly replaced by carbonates and hydrous silicates, and fractures contain secondary sericitic mica. No chromium or nickel was detected in the secondary mica. Fresh and altered micas and zoned concentric granules containing about 15 per cent Cr_2O_3 were found in massive Fe-Ni sulphides of the Werner Lake and Megantic deposits (Fig. 4). The chromian grains from the Werner Lake deposit contain about 1.5 per cent vanadium. Economic and genetic significances of uncommon elements in micas and associated spinels will be investigated.

The results of the electron probe microanalyses indicate that the chromium contents of phlogopite, biotite and muscovite vary with those of the associated spinel, and that micas associated with nickeliferous pyrrhotite and pentlandite contain up to 0.3 per cent nickel. Nickel and chromium contents of micas can be used for distinguishing between micas that are related to Cr-Ni-rich minerals and those which are not related. Examples of chemical relationships between phlogopite, biotite, and muscovite, and associated spinels are illustrated as distribution coefficients for seven oxides (between the mica and the associated spinel) in Table 1.

---

[1] Zurbrigg, H.F.: Thompson Mine geology; Bull. Can. Inst. Mining Met., vol. 56, pp. 451-460 (1963).

28. PALYNOLOGIC EVIDENCE FOR A VERY LATE CRETACEOUS AGE OF LITTLE BEAR AND EAST FORK FORMATIONS, DISTRICT OF MACKENZIE

Project 500029

Wayne W. Brideaux

Significant palynomorphs have been identified in four of six samples collected by C. J. Yorath in 1968, from a stratigraphic section at the type locality of the Little Bear Formation[1] on Little Bear River, 24 miles southwest of Fort Norman, at 68°34'N, 126°19'W. Recent work by C. J. Yorath shows that this section comprises 310 feet of Little Bear Formation overlain unconformably by about 20 feet of the East Fork Formation, and that the contact of the Little Bear and the underlying Slater River Formation, is not exposed. Tassonyi[2] has pointed out that the stratigraphy of this area is by no means clearly understood. The thickness of 780 feet given for the Little Bear Formation[1] and later quoted by Hume[3], probably should be considered as an estimate. All three formations were assigned previously to the Cretaceous, but little concrete evidence existed to support a more refined determination.

Table 1. Palynomorphs recovered from the Little Bear and basal East Fork Formations from a section on Little Bear River. Datum base of section.

EAST FORK FORMATION 306-310 feet – Unit 5 of section GSC Loc. C-8720	Cingulatisporites radiatus Stanley Cingutriletes spp. Stereisporites spp. Cicatricosisporites spp. Hamulatisporis amplus Stanley Lycopodiumsporites sp. cf. L. papillaesporites (Rouse) Srivastava Deltoidospova sp. Gleicheniidites senonicus (Ross) Skarby Zlivisporis sp. cf. Z. blanensis Pacltova Osmundacidites wellmannii Couper Laevigatosporites ovatus Wilson & Webster Polypodiisporites sp. cf. P. favus (Potonié) Potonié Inaperturopollenites hiatus (Potonié) Thomson & Pflug

Liliacidites sp.
various trilete apiculate spores
Marcellopites sp. cf. M. tolmanensis Srivastava
Tetracolpites sp.
Retitricolporites sp.
Triporopollenites sp.
Extratriporopollenites sp.
Triatriopollenites costatus Norton
Aquilapollenites trialatus Rouse
Aquilapollenites sp. cf. A. oblatus Srivastava
"Mancicorpus" sp.
Aquilapollenites clarireticulatus (Samoilovich) B. D. Tschudy
Tenua? sp. *

UNCONFORMABLE CONTACT OF LITTLE BEAR AND EAST FORK FORMATIONS AT 306 FEET

LITTLE BEAR FORMATION

280-306 feet – Unit 4 of section
GSC Loc. C-8719

Cingulatisporites radiatus Stanley
Stereisporites spp.
Cingutriletes spp.
Hamulatisporis amplus Stanley
Gleicheniidites senonicus (Ross) Skarby
Osmundacidites spp.
Abietineaepollenites sp.
Inaperturopollenites hiatus (Potonié) Thomson & Pflug
Psilatricolpites sp.
Retitricolpites sp.
Marcellopites sp. cf. M. tolmanensis Srivastava
Aquilapollenites sp. cf. A. dentatus B. D. Tschudy
Aquilapollenites sp. cf. A. steilckii Srivastava
Aquilapollenites trialatus Rouse
Hystrichosphaera sp. *
Baltisphaeridium sp. *

274-280 feet - Unit 3 of section
GSC Loc. C-8718

Osmundacidites sp.
unidentifiable bisaccate grains
unidentifiable trilete spores

239-246 feet – Unit 2 of section
GSC Loc. C-8717

Barren of microfossils

229-239 feet – Unit 2 of section GSC Loc. C-8716	Barren of microfossils
Unit 1 of section Thickness 229 feet Sample taken within Unit 1. Stratigraphic position uncertain	Deflandrea sp. cf. D. spectabilis Alberti* Deflandrea spp.* Spinidinium sp.* various unidentified dinoflagellates* Baltisphaerdium spp.* Veryhachium reductum forma trispinoides (de Jekhowsky) de Jekhowsky* Gleicheniidites senonicus (Ross)' Skarby various trilete spores Inaperturopollenites dubius (Potonié) Thomson & Pflug Aquilapollenites trialatus Rouse Aquilapollenites sp. cf. A. decorus Srivastava

* Microplankton species

The pollen and spore assemblages recovered from samples of Units 1, 4 and 5 of Yorath's measured section on Little Bear River comprise both long ranging species and those with more restricted ranges. Some species with published ranges restricted to the Maestrichtian have been described only from the Edmonton Formation by Srivastava[4] and their basal ranges have not been determined. Certain other species have been widely reported and possess ranges restricted to the Campanian. Few palynological studies have been published on the Cretaceous of northwestern Canada and it is possible that these ranges extend into the Early Maestrichtian in this region.

The assemblage of angiosperm pollen from Units 1, 4 and 5 includes abundant specimens of the genus Aquilapollenites Rouse. Ranges of species

Legend for Plate I (opposite)
All figures x1200 unless otherwise noted.

Figure 1. Aquilapollenites sp. cf. A. oblatus Srivastava. Polar diam. 29μ. 27816
Figure 2. Tetracolpites sp. Max. diam. 33μ. 27817
Figure 3. Triporopollenites sp. Equat. diam. 13μ. 27818
Figure 4. Aquilapollenites sp. cf. A. clarireticulatus (Samoilovich) B.D. Tschudy. Polar diam. 38μ. 27819
Figure 5. Deflandrea sp. Length 43μ. 27820
Figure 6. Deflandrea sp. cf. D. spectabilis Alberti (x500). Length 96μ. 27821
Figures 7-9. Aquilapollenites trialatus Rouse. 7. Polar diam. 52μ. 27822. 8. Polar diam. 38μ. 27823. 9. Polar diam. 37μ. 27824.
All specimens from basal bed, East Fork Formation, except Figures 5 and 6 from the Little Bear Formation.

PLATE I


1

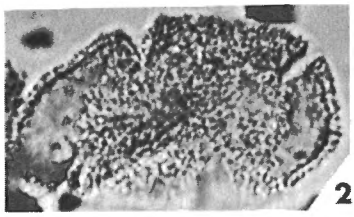
2


3

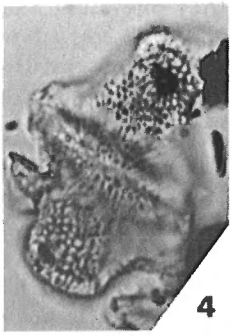
4

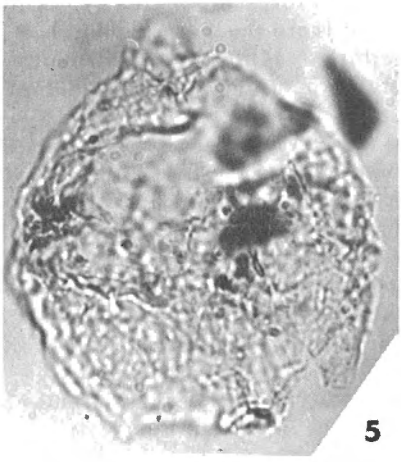
5


7

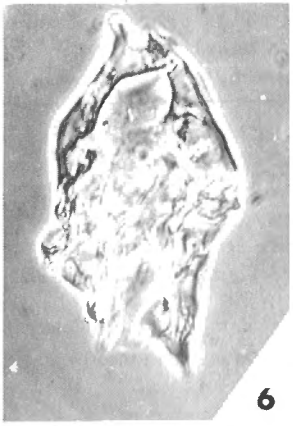
6

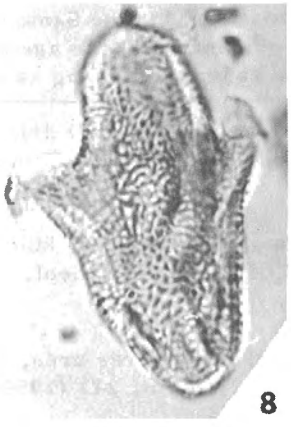
8

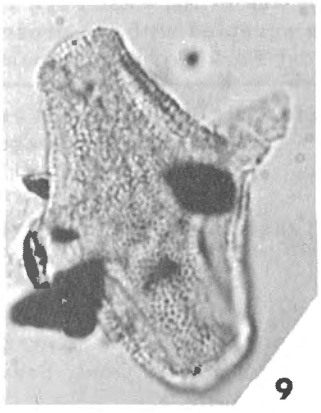
9

of this genus determined in the Rocky Mountain region are assumed to hold for the District of Mackenzie. Reports in the literature of Aptian-Albian and other pre-Late Santonian occurrences of this genus have never been substantiated. A very few speciments have been recorded from the Late Santonian of Alaska (unpublished information), but the abundance of specimens and the species diversity of the Aquilapollenites assemblage under discussion rules out any possibility of a Late Santonian age assignment.

Aquilapollenites trialatus Rouse has been reported only from deposits of Campanian age in the Rocky Mountain regions of Canada and the United States.[5] The presence of this species in abundance in Units 1, 4 and 5 therefore strongly supports assignment of a Campanian age for the Little Bear and basal East Fork Formations. Other species of Aquilapollenites cited in this report have been recorded from the Maestrichtian. A Campanian age assignment is not contradicted by the absence of the genus Wodehouseia Stanley, species of which are common in the Maestrichtian, but occur only rarely in older rocks.

The sample taken from Unit 1 also contains several species of the cavate dinoflagellate cyst, Deflandrea Eisenack, notably one species very similar to D. spectabilis Alberti, a species recorded from the Late Senonian of Germany. The presence of a marine dinoflagellate assemblage in this sample contrasts with the almost exclusively continental aspect of the samples from Units 3 to 5.

The proposal of a Campanian or possibly Early Maestrichtian age for the Little Bear Formation and the basal portion of the East Fork Formation is in conflict with several sources. Tassonyi[2] (p. 135), summarizing available evidence, suggested that the Little Bear Formation is probably Late Turonian or younger. He pointed out, however, that this determination was tentative and based on insufficiently documented paleontological data. Mountjoy and Chamney[6] (pp. 20-22 and Fig. 4) speculated that the Little Bear Formation may be in part equivalent to the Arctic Red and Trevor Formations of Albian age, but emphasized the need for confirmatory studies. Douglas et al.[7] (p. 455 and Chart III, prepared prior to Tassonyi[2] and Mountjoy and Chamney[3]) tentatively suggested a Late Albian age for the Little Bear and East Fork Formations based on published and unpublished evidence advanced by earlier workers. Finally, Jeletzky[8] (p. 58) reported an occurrence, brought to his attention by C.R. Stelck, of a "... 2-foot long Santonian Inoceramus ex. gr. cardissoides - pinniformis ..." which was "... presumed to have been collected from the East Fork shale ...", and suggested from this evidence that the age of the East Fork Formation could be Santonian. This premise cannot be accepted with the present evidence that the age of the basal beds of the East Fork Formation must be at least as young as Campanian.

---

[1] Stewart, J.S.: Recent exploratory deep well drilling in Mackenzie River valley, Northwest Territories; Geol. Surv. Can., Paper 45-29 (1945).

[2] Tassonyi, E.J.: Subsurface geology, Lower Mackenzie River and Anderson River area, District of Mackenzie; Geol. Surv. Can., Paper 68-25 (1969).

[3] Hume, G.S.: The Lower Mackenzie River area, Northwest Territories and Yukon; Geol. Surv. Can., Mem. 273 (1954).

[4]Srivastava, S.K.: Pollen biostratigraphy and paleoecology of the Edmonton Formation (Maestrichtian), Alberta, Canada; Palaeogeogr. Palaeoclim. Palaeoecol., vol. 7, pp. 221-276 (1970).

[5]Tschudy, B.D. and Leopold, E.G.: Aquilapollenites (Rouse) Funkhouser-selected Rocky Mountain taxa and their stratigraphic ranges; Geol. Soc. Am., Spec. Paper 127, pp. 113-167 (1970).

[6]Mountjoy, E.W. and Chamney, T.P: Lower Cretaceous (Albian) of the Yukon: Stratigraphy and foraminiferal subdivisions. Snake and Peel Rivers; Geol. Surv. Can., Paper 68-26 (1969).

[7]Douglas, R.J.W., Gabrielse, H., Wheeler, J.O., Stott, D.F. and Belyea, H.R.: Geology of western Canada, in Geology and economic minerals of Canada; Geol. Surv. Can., Econ. Geol. Rept. No. 1, 5th ed., pp. 367-488 (1970).

[8]Jeletzky, J.A.: Marine Cretaceous biotic provinces and paleogeography of western and Arctic Canada: illustrated by a detailed study of ammonites; Geol. Surv. Can., Paper 70-22 (1971).

92E

29. TERTIARY STRATIGRAPHY AND MICROFAUNAS FROM THE HESQUIAT-NOOTKA AREA, WEST COAST, VANCOUVER ISLAND (92E)

Project 690075

B.E.B. Cameron

Analyses of microfossil assemblages collected during the summer of 1969 on Nootka Island and samples provided for study from Hesquiat Peninsula by J.A. Jeletzky have resulted in the recognition of a sequence of foraminiferal zones and additional information on the depositional environments of the Tertiary succession in this area. In general the superpositional relations of the molluscan assemblages as recognized by Jeletzky have been proven correct. The ages and biostratigraphic correlation of these rocks have been more refined on the basis of the rich foraminiferal assemblages and are shown on the accompanying table.

Foraminiferal Ages and Depositional Environments

1) Bulimina schencki/lower Sigmomorphina schencki zones

The coarse conglomeratic and sandstone lithologies mapped by Jeletzky[1] in 1954 as Division A (= Escalante Formation) contain Foraminifera

of the Sigmomorphina schencki zone of Washington State (Rau[2], 1958). Rather than a Middle Oligocene age assignment as suggested by Jeletzky, the unit is now assigned to the late Upper Eocene. The late Narizian (Upper Eocene), Bulimina schencki zone may also be represented in the basal part of the Escalante Formation. The depositional environment indicated by the foraminiferal assemblages in one of deep water, continential slope (ca. 2, 000 feet) deposition. The conglomerates of this unit are therefore probably parts of deep-water turbidite sequences.

2) Upper Sigmomorphina schencki zone

This biostratigraphic zone of lower Refugian (late Upper Eocene) is represented in stratigraphic Division B of Jeletzky on Nootka Island and in Division C of Hesquiat Peninsula. The fine-grained clastic sequence on Nootka Island is a facies equivalent of the generally coarser conglomeratic-sandstone-shale sequence on Hesquiat Peninsula. Both facies represent deep-water depositional environments.

3) Eponides kleinpelli zone

This zone is present both in the upper part of Jeletzky's stratigraphic Division B on Nootka Island and Division C on Hesquiat Peninsula. These rocks are assigned a late Refugian (Lower Oligocene) age rather than late Zemorrian (Upper Oligocene) as suggested by Jeletzky. Depositional environments of these rocks are interpreted as deep water on the basis of the contained foraminiferal assemblages.

4) Later Oligocene - Zemorrian

The uppermost parts of stratigraphic Division B on Nootka Island and Division C on Hesquiat Peninsula as mapped by Jeletzky contain Foraminifera indicative of early and middle Zemorrian of the Oligocene. The sequence on Hesquiat Peninsula may become somewhat younger in the Oligocene than on Nootka Island.

5) Upper Miocene/Lower Pliocene Assemblage

The western edge of Nootka Island exposes a shallow water Tertiary sequence in the vicinity of Bajo Point. The lower part of the sequence was mapped by Jeletzky[1] as stratigraphic Division C. Foraminiferal evidence indicates a much younger age for this unit than assumed by Jeletzky and indeed the Bajo Point section appears to have no biostratigraphic equivalence to Division C as mapped by Jeletzky on Hesquiat Peninsula. The overall composition of the foraminiferal assemblage is closely similar to the Miocene Montesano Formation and possibly to part of the Astoria sensu lato of Washington (Rau[3, 4]). The following forms were recorded:

Globigerina bulloides d'Orbigny
Quinqueloculina sp.
Nonionella miocenica Cushman
Globobulimina sp. cf. G. ovata (d'Orbigny)
Pseudonodosaria sp. indet.
Haplophragmoides sp.
Reophax sp.

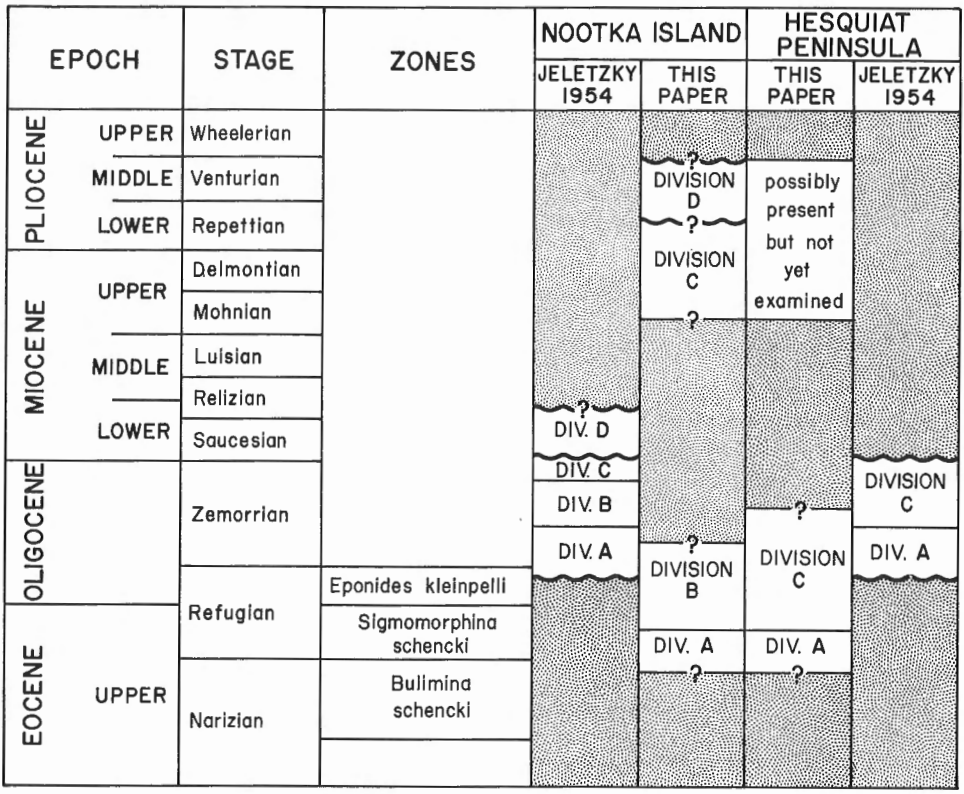

Figure 1. Correlation of Tertiary rocks, Nootka-Hesquiat Area, west coast of Vancouver Island, B.C. Stratigraphic Nomenclature after Jeletzky, 1954.

The oldest recorded occurrence of G. bulloides d'Orbigny is Tortonian (Mohnian in West Coast sense) or Upper Miocene (N-16 zone, Blow[5], p. 316). A very shallow water depositional environment is indicated for most of this sequence.

6) Lower to Middle Pliocene Assemblage

The sequence at Bajo Point, Nootka Island is capped by a sandstone and conglomerate unit which has been mapped by Jeletzky as Division D. Two significant species of Foraminifera were found there.

Protelphidium depressulum matagordanum (Kornfeld)
Elphidiella hannai (Chshman and Grant)

These shallow water foraminifers are characteristic of the upper part of the Quinault Formation of Washington State and suggest a late Lower to early Middle Pliocene age for this sequence (Rau[4]). Elphidiella hannai is not known from deposits older than Pliocene.

The microfaunas of Divisions C and D of Jeletzky (1954) as exposed on Bajo Point of Nootka Island have not yet been encountered in any of the available samples from Hesquiat Peninsula. It is planned, however, to systematically sample the Hesquiat Peninsula rocks during the summer of 1971.

[1]Jeletzky, J.A.: Tertiary rocks of the Hesquiat-Nootka area, west coast of Vancouver Island, British Columbia; Geol. Surv. Can., Paper 53-17 (1954).

[2]Rau, W.W.: Stratigraphy and foraminiferal zonation in some of the Tertiary rocks of southwestern Washington, U.S. Geol. Surv., Oil and Gas Investigations, Charts OC 57 (1958).

[3]Rau, W.W.: Tertiary foraminifera from the Willapa River valley of southwest Washington, J. Paleontol., vol. 25, No. 4, pp. 417-453 (1951).

[4]Rau, W.W.: Foraminifera, stratigraphy, and paleoecology of the Quinault Formation, Point Grenville-Raft River coastal area, Washington; Wash. State Div. Mines Geol., Bull. 62 (1970).

[5]Blow, W.H.: Late Middle Eocene to recent planktonic foraminiferal biostratigraphy; Proc. First Intern. Conf. Planktonic Microfossils, Geneva, 1967; vol. 1, pp. 199-421 (1969).

92J

30. MIDDLE TRIASSIC CONODONTS FROM THE FERGUSSON GROUP, NORTHEASTERN PEMBERTON MAP-AREA (92J), BRITISH COLUMBIA

B.E.B. Cameron and J.W.H. Monger

The Fergusson Group[1] is a thick complexly deformed succession of thin-bedded chert with interbedded locally graphitic pelite, cherty argillite, locally altered, pillowed, basic volcanic rocks and minor lenses and pods of carbonate. Previously, the Fergusson Group had been assigned to the Permian[1] on the basis of its lithologic similarity to part of the Cache Creek Group. No specifically identifiable fossils had been recovered from these rocks up to this time.

Locality and Lithology

G.S.C. Locality 86300

Conodonts were recovered from the unit as insoluble acetic acid residues of a partly recrystallized limestone pod collected by J.W.H. Monger. The limestone grades from oolitic calcarenite to aphanitic carbonate. The collection was made on the east side of Tyaughton Creek immediately above the Bridge River road (latitude 50°53'N, longitude 122°36'W, NTS 92J).

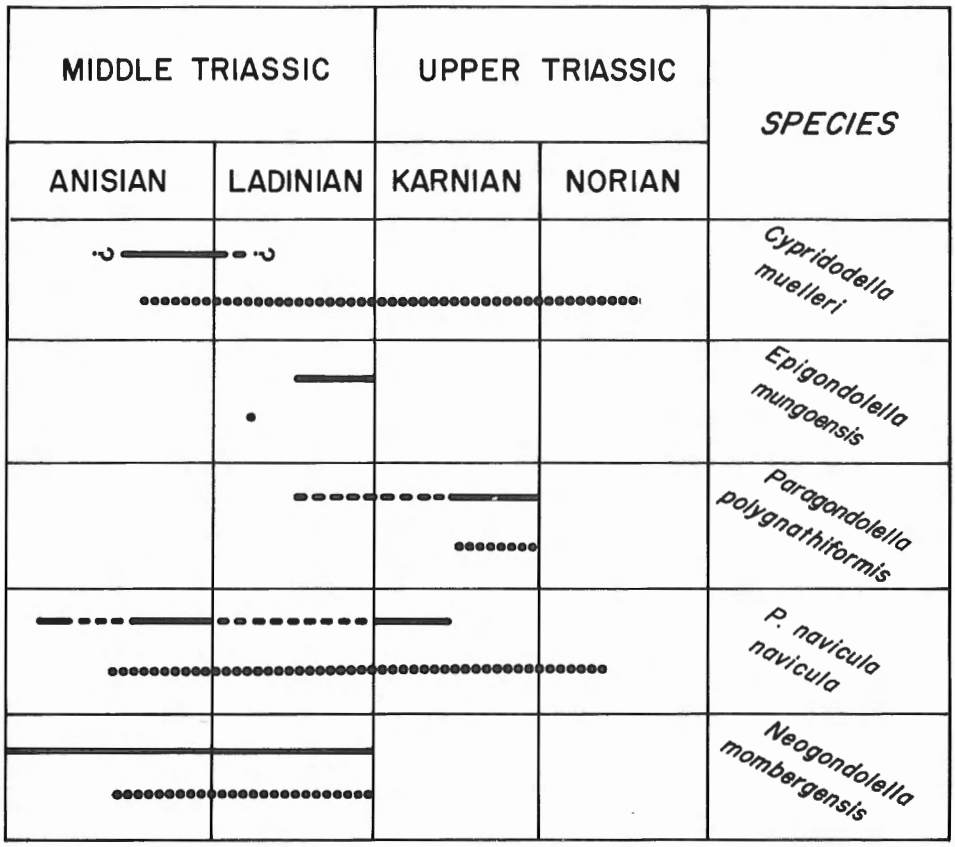

Species ranges (Mosher, 1968, 1970)

known — inferred ------ North America

•••••••••• Europe

Conodonts

The very rich conodont assemblage recovered from this locality includes the following forms:

Hindeodella spp.
Cypridodella sp. cf. C. muelleri (Tatge)
C. ? sp.
Prioniodina sp.
Epigondolella mungoensis (Diebel)
Paragondolella polygnathiformis (Budurov and Stefanov)
P. navicula navicula (Huckreide)
cf. Neogondolella mombergensis (Tatge)

Age Assignment

The accompanying range chart derived principally from publications of L.C. Mosher[2,3] indicates the ranges of the species pertinent to this discussion. The overall composition of the assemblage clearly indicates a late Middle to early Upper Triassic age for these rocks. If, as Mosher suggests, Epigondolella mungoensis is restricted as indicated in the chart, the assemblage can be dated precisely as late Ladinian of the Middle Triassic. Triassic conodont studies are at a relatively early stage of development, however, and further documentation of these ranges is desirable.

The possibility that Triassic conodonts are more generally distributed in the Western Cordillera may provide a method of solving other similar stratigraphic problems.

Correlation

These rocks may be correlated with the probable Middle Triassic Pavilion Group (ref. 4, p. 34) that is exposed only twenty miles to the east. On the basis of lithologic similarity, the undated Hozameen Group (ref. 5, p. 1205) outcropping 120 miles to the south-southeast is possibly an equivalent. Finally, this discovery raises the possibility that parts of the extensive upper Paleozoic Cache Creek Group of the Intermontane Belt may be as young as Middle Triassic.

---

[1] Cairnes, C.E.: Geology and mineral deposits of Bridge River Mining Camp, British Columbia; Geol. Surv. Can., Mem. 213 (1937).

[2] Mosher, L.C.: Triassic conodonts from western North America and Europe and their correlation; J. Paleontol., vol. 42, No. 4, pp. 895-946 (1968).

[3] Mosher, L.C.: New conodont species as Triassic guide fossils; J. Paleontol. vol. 44, No. 4, pp. 737-742 (1970).

[4] Trettin, H.P.: Geology of the Fraser River valley between Lillooet and Big Bar Creek; B.C. Dept. Mines Petroleum Resources, Bull. 44 (1961).

[5] McTaggart, K.C. and Thompson, R.M.: Geology of parts of the Northern Cascades in southern British Columbia; Can. J. Earth Sci., vol. 4, pp. 1199-1228 (1967).

---

31. PRELIMINARY ECOLOGICAL COMMENTS ON ALBIAN MICROFLORAS FROM THE CANADIAN ARCTIC ISLANDS

Project 680068

W.S. Hopkins

Introduction

This paper presents some preliminary data and conclusions on Albian floras of the Arctic Islands, based on palynological analysis. Ultimately, it is hoped that this total project will lead to a fuller understanding of Cretaceous floras throughout the Sverdrup basin. Panarctic Oils Ltd. supplied the samples and stratigraphic information from Ellef Ringnes and Melville Islands on which this work is based.

Geology

Samples were obtained from the Christopher Formation, a sequence of marine shales that lies between the Isachsen Formation below and the Hassel Formation above. This is a widespread formation in the Sverdrup basin with a highly variable thickness ranging from 130 feet on Prince Patrick Island[1] to 4,600 feet on southern Axel Heiberg Island[2]. It is about 400 feet thick on the Sabine Peninsula of Melville Island. Consequently, samples come from both a compressed section on Melville Island and from a much expanded, and presumably more complete section on Ellef Ringnes Island. Although marine invertebrate fossils are rare, there is general agreement that the Christopher is Albian in age[1,3]. Spore and pollen evidence also supports an Albian age.

Palynology

Samples were examined in stratigraphic succession from youngest to oldest, in order to determine whether there were significant range or frequency changes in the palynomorph distribution. The total number of samples examined was 21; 13 from Melville Island and 8 from Ellef Ringnes Island.

Maceration followed standard techniques: solution of the rock in hydrochloric and hydrofluoric acids; oxidation of the organic residue in either Schultzes solution or bleach and treatment with potassium hydroxide. This was followed by staining, and then mounting in glycerine jelly as a permanent mount.

The palynomorphs that have been identified and to which formal names have been applied follow. Insofar as possible they are classified into the natural botanical system.

Family Sphagnaceae

Cingulatisporites cf. radiatus Stanley 1965
Sphagnum antiquasporites Wilson and Webster 1946
Sphagnum buchenauensis (Krutzsch) Elsik 1968
Sphagnum psilatus (Ross) Couper 1958

Family Locopodiaceae

Lycopodiumsporites austroclavatidites (Cookson) Pocock 1962
Lycopodium cerniidites (Ross) del. and Sprum. 1965
Lycopodiacidites irregularis Brenner 1963
Lycopodiumsporites marginatus Singh 1964
Lycospora sp.
Hamulatisporis hamulatis Krutzsch 1959
Foveosporites cyclicus Stanely 1965

Family Selaginellaceae

Acanthotriletes varispinosus Pocock 1962
Leptolepidites verrucatus Couper 1953

Family Osmundaceae

Baculatisporites comaumensis (Cookson) Potonié 1956
Osmundacidites wellmanii Couper 1953

Family Matoniaceae

Matonisporites phlebopteroides Couper 1958

Families Cyatheaceae or Dicksoniaceae

Cyathidites australis Couper 1958
Cyathidites minor Couper 1953
Kuylisporites lunaris Cookson and Dettmann 1958

Family Gleicheniaceae

Gleicheniidites senonicus (Ross) Skarby

Family Schizaeaceae

Appendicisporites tricornitatus Weyland and Greifeld 1953
Appendicisporites perplexus Singh 1964
Cicatricosisporites australiensis (Cookson) Potonié 1956
Cicatricosisporites dorogensis Potonié and Gelletich 1933
Cicatricosisporites hallei Delcourt and Sprumont 1955
Cicatricosisporites perforatus (Baranov, Nenkova and Kondratiev) Singh 1964
Cicatricosisporites pseudotripartitus (Bolkhovitina) Dettmann 1963
Cicatricosisporites sp.
Lygodiumsporites (Potonié, Thomson and Thiergart) Singh 1964
Neoraistrickiea cf. N. robusta Brenner 1963
Plicatella erdtmanii (Pocock) Ameron 1965

Filicales – Incertae sedis

Aequitriradites sp.
Concavissimisporites parkinii (Pocock) Singh 1964
Concavissimisporites variverrucatus (Couper) Singh 1964
Concavissimisporites verrucosus Del. and Sprum 1955
Contignisporites cooksonii (Balme) Dettmann 1963
Converrucosisporites saskatchewanensis Pocock 1962
Deltoidospora hallii Miner 1935
Deltoidospora junctum (Kara-Murza) Singh 1964
Hymenozonotriletes mesozoicus Pocock 1962
Laevigatosporites ovatus Wilson and Webster 1946
Pilosisporites versus Del. and Sprum. 1955
Pilosisporites sp.
Rouseisporites laevigatus Pocock 1962
Rouseisporites reticulatus Pocock 1962
Trilobosporites appiverrucatus Couper 1958
Trilobosporites canadensis Pocock 1962
Trilobosporites trioreticulosus Cookson and Dettmann 1958
Trilobosporites sp.
Verrucosisporites rotundus Singh 1964

Spores – Incertae Sedis

Apiculatisporis sp.
Lycopodiacidites ambifoveolatus Brenner 1963
Microreticulatisporites sp.
Reticulatisporites sp.
Schizosporis sp.
Triplanosporites sinuosus (Pflug) Thomson and Pflug 1953
Undulatisporites sp.
T2

Cycadophyta and/or Ginkophyta

Monosulcites sp. A
Monosulcites sp. B

Coniferales

Araucariacites australis Cookson 1947
Calassopollis classoides (Pflug) Pocock and Jansonius
Eucommiidites troedssonii (Erdtman) Hughes 1961
Laricoidites magnus (Potonié) Potonié, Thomson and Thiergart 1950
Podocarpidites sp.
Tsugaepollenites mesozoicus Couper 1958
Taxodiaceae – Cupressaceae
Bisaccate miscellaneous

General Remarks in Regard to Flora

In general the recovered palynomorphs are comparatively well preserved and moderately numerous. Dinoflagellates and other phytoplankton are present in most samples, occasionally up to as much as 8 per cent of the total. These, however, are beyond the scope of this report. Representative coniferales are treated in a general way, being classified into six more or less easily identified genera; i. e. Araucariacites, Classopollis, Eucommiidites, Laricoidites, Podocarpidites, and Tsugaepollenites. Another less distinctive group is referred to the Taxodiaceae-Cupressaceae. The remaining saccate forms, because of their almost endless variation in morphology, size and preservation, are simply assigned to "miscellaneous bisaccate conifers". Most would probably be considered members of the Pineaceae.

Composition

Excluding the phytoplankton, and the large variation present in the bisaccate conifers, a total of sixty-nine species were identified. According to the writer's interpretation of affinities this breaks down to 4 species of bryophytes, 9 lycopods, 18 ferns, 19 filicales Incertae Sedis, 8 spores Incertae Sedis, 2 probable cycadophytes and 7 conifers.

Range charts were drawn up for each of the stratigraphic sections studied but no variation of significance was noted, i. e. the environment apparently remained comparatively constant during Christopher time and no particular evolution or plant migration took place. Generally, the flora of the surrounding country during deposition of the sediments was a conifer-fern complex. These two broad groups are the most common by far of the spore and pollen types. Virtually all of the conifer genera, as well as large numbers of miscellaneous bisaccates, are well represented in nearly every sample. Of those identified at a generic level, Tsugaepollenites seems to be the most abundant. Conversely, Araucariacties, Classopollis, and Eucommiidites, appear to be the least common. All of this suggests a complicated and varied coniferous forest.

Among the ferns, spores of the Gleicheniaceae are overwhelmingly dominant, as they seem to be throughout the Cretaceous rocks of the Arctic Islands. Next in abundance are members of the family Schizaeaceae of which at least six species of Cicatricosisporites are present. Other fern families identified are considered representatives of the Cyatheaceae, Matoniaceae and Osmundaceae. Abundant genera of other probable filicales are present also. Finally, though limited in number, there are representatives of the Sphagnaceae, Lycopodiaceae, and Selaginellaceae.

Monocolpate pollen grains are conspicuous by their rarity, only a very few specimens being found. The large size of these specimens suggests they may belong to the Cycadales or Bennettitales. Several smaller monocolpate grains doubtfully belong to the Ginkgoales. Finally, and significantly, no evidence of angiosperm pollen was found.

In short then, we have represented in the Christopher Formation a fern-conifer forest made up of a large number of species, and no evidence of the presence of angiosperms.

Climatic Interpretations

As in all Mesozoic palynology, environmental interpretations are difficult, and can be made only generally, utilizing groups of families, always with the hope that ecologic requirements haven't changed too much in a 100 ± million years. Below follows a brief synoptic outline of the climatic requirements of modern families which can be related to microfossils from the Albian Christopher Formation.

SPHAGNACEAE – Cosmopolitan family in ponds and bogs, lives from the Arctic to the tropics. Usually rare in the Christopher.

LYCOPODIACEAE – Cosmopolitan family in moist areas, from the tropics to the Arctic. Usually present, but never an abundant form in the Christopher.

SELAGINELLACEAE – Cosmopolitan family in moist areas, tropical to temperate. Rare in the Christopher.

OSMUNDACEAE – A family found in swampy or damp regions in tropical to temperate climates. Moderately abundant form in the Christopher.

CYATHEACEAE – Mostly tropical to warm temperate tree ferns. A rare family in the Christopher.

GLEICHENIACEAE – A tropical family normally, but does extend into warm temperate areas, such as along the coast of the southern United States. A very abundant family in the Christopher.

SCHIZAEACEAE – A tropical family normally, but certain members do occur in temperate regions such as Nova Scotia and Ontario. Comparatively abundant in the Christopher Formation.

CYCADACEAE – An exclusively tropical to subtropical family. Only doubtfully present in the Christopher, but even if present is very rare.

ARAUCARIACEAE – Subtropical to warm temperate in southern hemisphere. Rare in the Christopher.

CUPRESSACEAE – TAXODIACEAE – Cosmopolitan, mostly subtropical to warm temperate. Rare in the Christopher.

PINACEAE – Mostly temperate throughout the northern hemisphere. Exceedingly abundant throughout the Christopher.

PODOCARPACEAE – Essentially a southern hemisphere family, present in tropical to temperate climates. Comparatively rare in nearly all samples.

The overwhelming abundance of the Pinaceae would suggest strongly that we are not dealing with anything warmer than a temperate climate. The apparent lack (or rarity) of cycadales, which is strictly a tropical to subtropical form, is probably significant because it is present in most Albian microfloras elsewhere. Ephedraceae, a common constituent of arid parts of the tropics and subtropics is absent also. However, the various fern families would suggest a damp climate, and comparatively warm conditions. In short, the microflora would seem to indicate a moist, warm, temperate climate. This would be in keeping with Smileys[4] interpretation of a humid warm temperate climate for northern Alaska in Albian time.

[1]Tozer, E.T. and Thorsteinsson, R.: Western Queen Elizabeth Islands, Arctic Archipelago; Geol. Surv. Can., Mem. 332 (1964).

[2]Tozer, E.T.: Mesozoic and Tertiary stratigraphy, western Ellesmere Island and Axel Heiberg Island, District of Franklin; Geol. Surv. Can., Paper 63-30 (1963).

[3]Tozer, E.T.: Mesozoic and Tertiary stratigraphy, in Fortier, Y.O. ed., Geology of the north-central part of the Arctic Archipelago, Northwest Territories (Operation Franklin); Geol. Surv. Can., Mem. 320, pp. 74-95 (1963).

[4]Smiley, C.J.: Floral zones and correlations of Cretaceous Kukpowruk and Corwin Formations, northwestern Alaska; Am. Assoc. Petrol. Geol., vol. 53, pp. 2079-2093 (1969).

32. CRETACEOUS AND/OR TERTIARY ROCKS, NORTHERN SOMERSET ISLAND, DISTRICT OF FRANKLIN

Project 680068

W.S. Hopkins

Introduction and Geology

In July 1970, through the kind cooperation of a Sproule and Associates field party headed by Mr. Ken Neile, the writer had the opportunity of visiting briefly several localities along the Cunningham Inlet Fault on northern Somerset Island. The purpose was to collect several grab samples for palynological analysis. This aim was achieved during the course of five hours during the night of July 27th, 1970. Time was not available to measure sections nor even to look at the rocks in any detail. However, the seven samples collected were sufficient to demonstrate through palynology that latest Cretaceous and/or earliest Tertiary rocks are present along this fault zone.

For a more complete discussion of the geology of northern Somerset Island, the reader is referred to Fortier et al. and to Map 1098A which accompanies that report. Briefly, northern Somerset Island is composed of essentially flat-lying Ordovician, Silurian and ? Devonian limestones and dolomites. Some conglomerates, sandstones, and siltstones are present in the Silurian and/or Devonian Peel Sound Formation on the northwesternmost part of the Island.

The Cunningham Inlet Fault zone lies entirely within the Middle and Upper Silurian Read Bay Formation, which is dominantly a massive, fossiliferous limestone. This fault zone, which extends east-southeast from the head of Cunningham Inlet, is marked topographically by a comparatively deep, narrow and straight-sided valley in which a river runs west-northwest into Cunningham Inlet.

In the bottom of this valley sporadic outcrops of a very different rock type occur. This succession appears to be comparatively thin, but detailed work will be necessary to determine its geographic and vertical extent.

The unit appears to be completely clastic with fine- to medium-grained sandstones dominating, but pebble-conglomerates are present as are carbonaceous siltstones. Cross-bedding is common in both the sandstone and pebble conglomerates. Many of the sandstones contain abundant but poorly preserved plant remains, mainly material that appears to be small stems, twigs or rootlets. The remains of carbonized leaves, present also on some sandstone bedding planes, are impossible to identify. There is little doubt, however, that they are the remains of angiosperms. In short, this unit is very different from the massive Silurian limestone which borders it to the north and south.

Palynology

Two of the examined samples came from about two miles above the head of Cunningham Inlet, the remaining five samples are from about ten miles farther up the fault zone.

Palynological analyses of these samples produced some rather interesting results. Although the samples yielded palynomorphs of varying numbers and of uneven quality, the florules from all samples appear to be essentially the same, and probably represent rocks of the same age. The more abundant and conspicuous forms include the following:

Laevigatosporites sp.
Verrucosisporites sp.
Hamulatisporis amplus Stanley 1965
Osmundacidites sp.
Baculatisporites sp.
Gleicheniidites senonicus Ross 1949
Sphagnum antiquasporites Wilson and Webster 1946
Sphagnum sp.
Lycopodiumsporites cf. L. austroclavatidites (Cookson) Pocock 1962
Lycopodium sp.
cf. Cyathidites sp.
Cicatricosisporites cf. C. australiensis (Cookson) Potonié 1956
Undifferentiated bisaccate conifer pollen
Taxodiaceae
Glyptostrobus-type
cf. Sequoia sp.
Podocarpidites sp.
Cycadopitys sp.
Schizosporis cf. S. microfoveatus Stanley 1965
cf. Liliaceae
cf. Typha sp.
cf. Ericaceae
cf. Carya sp.
Extratiporopollenites spp.
Betula sp.
Alnus verus (Potonié) Martin and Rouse 1965

cf. Pterocarya sp.
cf. Corylus sp.
cf. Salix sp.
Wodehouseia spinata Stanley 1961
Tricolpites spp.
Tricolporopollenites sp.

The dominant element of this flora, in terms of numbers of palynomorphs and variety of types, seems to be angiosperms, many of which are of comparatively modern aspect. Spores of ferns and lycopods are next in abundance. Present, but least common in all samples, are pollen grains representing the conifers.

In spite of the comparatively large flora from these samples, most of the listed palynomorphs are indicative of either the uppermost Cretaceous or lowermost Tertiary. Wodehouseia spinata and Schizosporis microfoveatus have been found, as far as the writer is aware, only in Maestrichtian rocks in North America, although the former has been found in Danian rocks of the Soviet Union. This would suggest a very late Cretaceous age for these rocks.

Summary and Conclusion

This brief study indicates that Late Cretaceous and/or Early Tertiary rocks are present in at least one east-southeast - west-northwest trending linear band at the north end of Somerset Island. A very elongated but narrow graben apparently developed along the Cunningham fault zone, and this resulted in the preservation of younger rocks. This faulting probably took place in the Tertiary. Furthermore, the lithology and age of these rocks indicate that they belong to the Eureka Sound Formation which was evidently widespread at one time throughout the Arctic Archipelago.

---

[1] Fortier, Y.O., and others: Geology of the north-central part of the Arctic Archipelago, Northwest Territories (Operation Franklin); Geol. Surv. Can., Memoir 320 (1963).

PETROLEUM GEOLOGY

33. SOURCE ROCK ANALYSIS IN ALBERTA AND THE NORTHWEST TERRITORIES, UTILIZING BOREHOLE CUTTINGS

Project 680134

L. R. Snowden

Preliminary analyses have been run on samples from selected boreholes in Alberta, Saskatchewan, and the Northwest Territories including all wells drilled on the Arctic Islands. The purpose of the project was (1) to establish a procedure for the identification of petroleum source rocks, (2) to provide data for determining the level of diagenesis of sediments in selected areas and (3) to initiate organic geochemical reconnaissance in the Arctic in order to aid in basin studies and to correlate with other geochemical information generated by petroleum companies operating in the Northwest Territories.

Using the simple extraction technique of hermetic, mechanical disintegration, light hydrocarbon gases (methane through butane) from borehole cuttings collected and canned at drilling sites were quantitatively analyzed on a flame ionization gas chromatograph. The results were keypunched and printer plotted on a downhole log (100 feet to 1 inch); total gas and methane concentrations were plotted on the same grid so that methane anomalies and so called "wet" gas (C_2, C_3, iC_4 and nC_4) anomalies could be distinguished.

Complementary to the gas analysis, the total carbon and total organic carbon content of the samples were determined using a conventional high temperature combustion apparatus. By correlation of the total extractable gas and its composition (wet or dry) with the organic content of the cuttings, potential source rocks have been identified for several areas in Alberta and the Arctic. As well as source material, low grade reservoir rocks have been tentatively identified.

The method serves as a rapid and reasonably accurate tool for the initial stages of identification of source material because a large number of samples can be handled.

No specific wells, areas or facies have been mentioned here because most data which have been collected to date are still confidential.

PRECAMBRIAN GEOLOGY

34. A CONTRIBUTION TO THE STRUCTURAL GEOLOGY AT YELLOWKNIFE, DISTRICT OF MACKENZIE

Project 670006

John B. Henderson

The structural geology of the Yellowknife area has been described in considerable detail by Campbell[1], Henderson and Brown[2], and Boyle[3] among others. In the course of a sedimentological study of the Archean Yellowknife Supergroup at Yellowknife certain aspects of the structure were considered.

The main structural element is a north-northeasterly trending syncline through Yellowknife Bay and the lakes to the north (Figs. 1, 2). A smaller subsidiary anticline on the east limb occurs just north of the large granitic area southeast of Yellowknife. The west limb of the major syncline consists of the steeply dipping Kam Formation of some 35,000 feet of predominantly mafic massive to pillowed volcanics and related intrusions that are unconformably overlain by the basal conglomerates and volcanic lithic sandstones of the Jackson Lake Formation. On the east limb of the major fold in the core of the subsidiary anticline occurs the volcanic Duck Formation which is believed to be an eastward extension of the upper part of the main volcanic sequence to the west. It is conformably overlain by the greywacke-mudstone turbidites of the Burwash Formation. The Banting Formation, a felsic volcanic unit of varied thickness, occurs on both east and west limbs of the syncline as do the greywacke-mudstones of the Walsh Formation that conformably overlies the Banting or in places the Burwash Formation.

The whole area is offset by a series of sharply defined, essentially vertical, left lateral strike slip faults of which the West Bay Fault just east of Yellowknife is a well known example. Figures 1 and 2 are respectively sketches of the geology at Yellowknife and of the same area with the displacements due to the late faulting removed.

Economic interest in the area has centred on gold deposits associated with major shear zones in the Kam Formation. Three of these major systems, the Con, the Giant, and the Campbell systems are indicated in the figures. These shear zones have been described in considerable detail[1, 2, 3] and the suggestion made that the shear zones have developed along major thrust faults of which the Campbell-Giant system is the most important. The offset on these early shears is evident in Figure 2. The Con system as well as others not plotted represent subsidiary zones to the main Campbell-Giant system.

It is suggested that a second major subsidiary shear zone occurs east of the Giant system underlying the west side of the north part of Yellowknife Bay and extending north between the Jackson Lake Formation and the Banting Formation. Nowhere can these two formations be seen in normal contact but are typically separated by a narrow outcrop-free area with the outcrops in the contact being typically more sheared than those more removed from the contact. The Jackson Lake Formation along the west shore of the bay exhibits

a zone of shearing parallel to the trend of the hypothesized fault. As in the shear zones in the Kam volcanics there are horses of undeformed rock with, in this case, perfectly preserved primary sedimentary structures between which are zones where the original features of the sediment have been completely obliterated. In this same area is a zone of tectonic breccia which varies along strike from sharp, angular, tightly packed to sheared stretched clasts of the Jackson Lake Formation sandstone. Adjacent outcrops stratigraphically above and below this breccia zone are essentially undeformed. This brecciation may be related to the formation of a shear zone in this area. A similar breccia occurs further north near the contact between the Jackson Lake and Banting Formations. The strike of the shoreline in the northwestern part of the bay parallels the shoreline in the southwestern part of the bay which is apparently controlled by the Campbell shear zone. The presence of the suggested subsidiary shear zone may similarly govern the position of the northwesterly shoreline as well.

The occurrence of this branch of the Yellowknife shear zone system to the east of the main mafic volcanic sequence may be of economic interest.

---

[1] Campbell, N.: Regional structural features of the Yellowknife area; Econ. Geol., vol. 42, pp. 687-698 (1947).

[2] Henderson, J.F. and Brown, I.C.: Geology and structure of the Yellowknife Greenstone Belt, District of Mackenzie; Geol. Surv. Can., Bull. 141 (1966).

[3] Boyle, R.W.: The geology, geochemistry and origin of the gold deposits of the Yellowknife district; Geol. Surv. Can., Mem. 310 (1961).

Note: Figures 1 and 2 for this report are on pages 108 and 109.

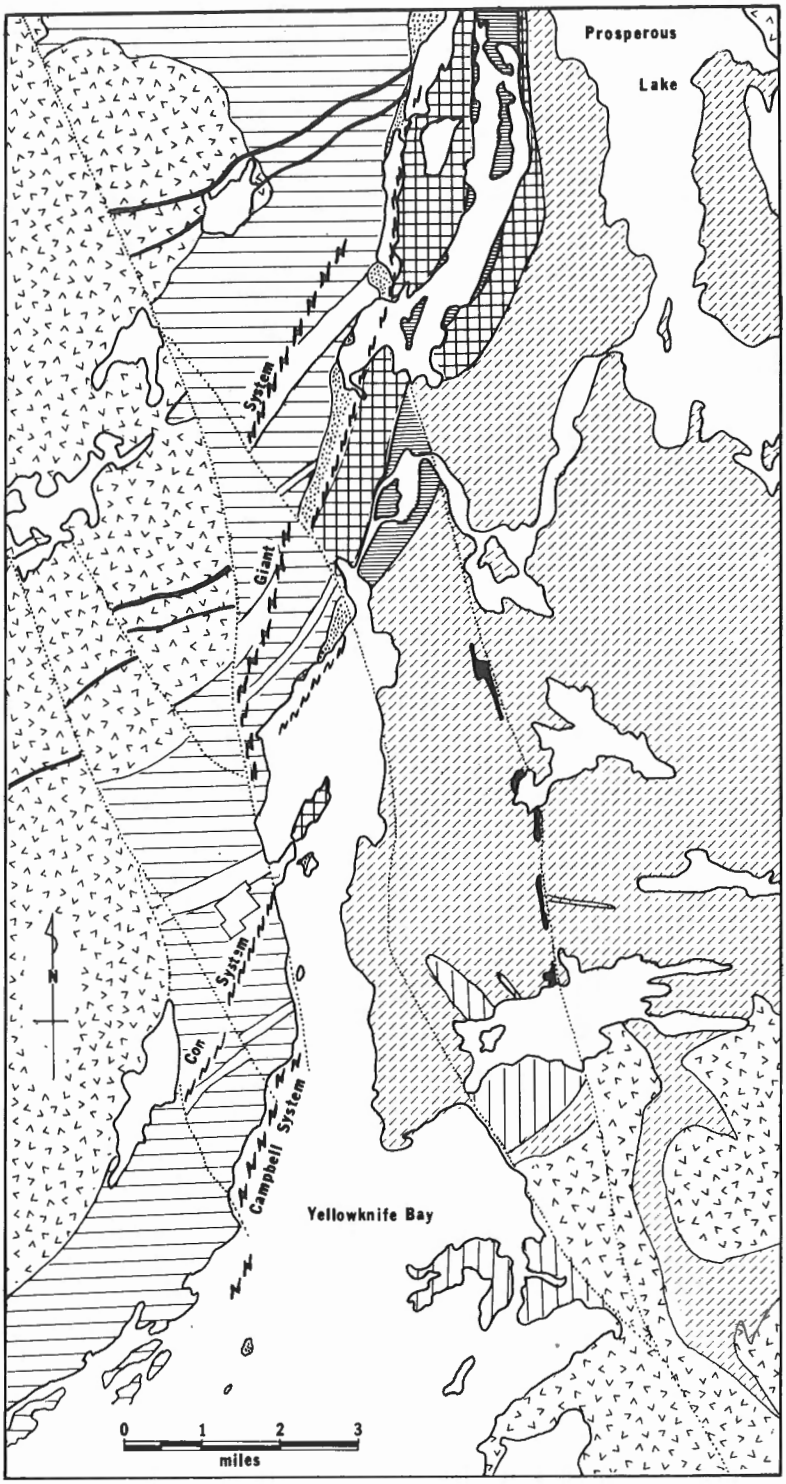

Figure 1. General geology of the Yellowknife area. Legend as for Figure 2.
#34 Henderson

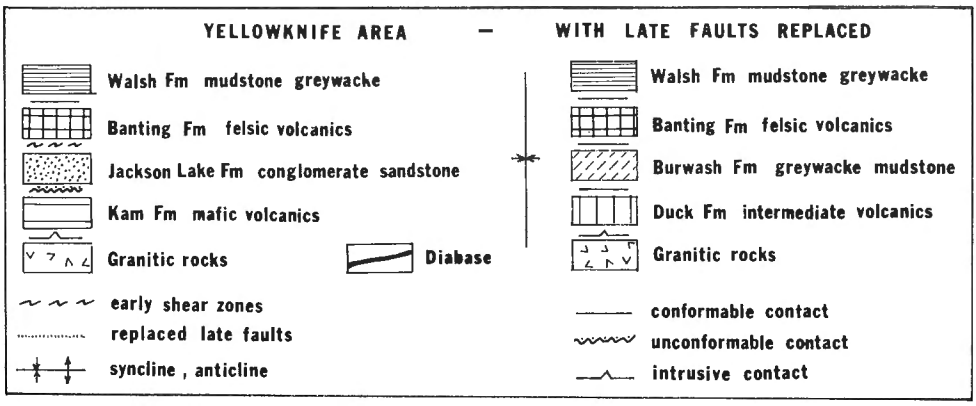

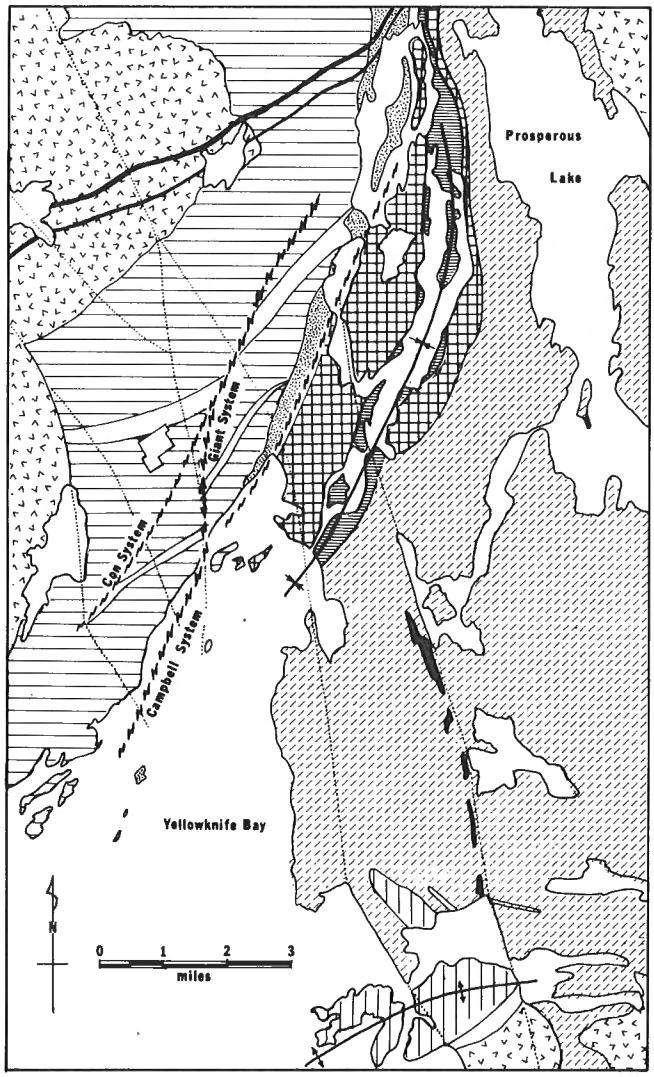

Figure 2. General geology of the Yellowknife area with late faults replaced.
#34 Henderson

35. GLACIAL DEPOSITS, SEA LEVEL CHANGES AND PRE-WISCONSIN DEPOSITS IN SOUTHWEST NOVA SCOTIA

Project 660036

D. R. Grant

Southwestern Nova Scotia possesses a unique combination of evidence of three major Quaternary events: (1) glaciation, including unidirectional ice-flow lineation attributed to a Laurentide phase, as well as radially-oriented features indicating final recession to an upland ice cap, (2) sea level changes, including post-Wisconsin marine overlap better exposed than elsewhere in the Maritimes, as well as recent submergence due to eustatic rise, tidal increase and local subsidence, and (3) a nonglacial warm-water interval of sea level higher than the present, which is thought to date from the Sangamon Interglacial.

Figure 1 depicts evidence for a sequence of glaciation beginning with the earliest ice-flow moving in an easterly and southeasterly direction. This same trend is recorded in northern Nova Scotia and Cape Breton Island; together they point to early centres in New Brunswick–New England. Subsequently, the ice moved southward and left a linear pattern of eskers, drumlins and fluting which characterize the surficial fabric not only of this area but of the entire Atlantic slope of Nova Scotia. This would indicate that, presumably during the Wisconsin maximum, the ice shed lay over New Brunswick and the Gulf of St. Lawrence, if not farther north. Later, during the recession, numerous examples of crossed striations and intersecting drumlins indicate that the movement was in a more southerly to southwesterly direction. This later trend is paralleled by eskers and crossed by belts of corrugated moraine. North of a line through Salmon River, however, quite a different trend is evident. Bold morainal ridges abut the coast, displaying marine-reworked distal slopes and unmodified, ice-scalloped proximal faces, attesting to the synchroneity of moraine-building and the formation of the marine limit. Few southerly drift lineations remain; most have been reworked and appear circular; many are completely reoriented with the stoss side lying to the east. Rock-inscribed features agree and point west also, many crossing earlier striae. The features on Long Island reveal the gradual rotation of ice flow from southwest to northwest. Eskers lie perpendicular to the coast (see Fig. 1), trending west to east and north to south inland over the topographic divide at 500 to 700 feet, and converge on an area around Kejimkujik Lake (K. L. – Fig. 1) at 300 feet. This was apparently the site of the westernmost of several late remnants of the ice shed on the Atlantic Upland.

Prest and Grant[1] explain the flow reversal by drawdown into a calving bay produced by the marine invasion of the Bay of Fundy, the supposition being that a reshaping of the ice front would impose new hydraulic gradients to which eskers would adjust, and might oversteepen the profile sufficiently to reverse former flow directions. North of the Salmon River discontinuity, the marine limit is more erratic and rises less steeply than to the

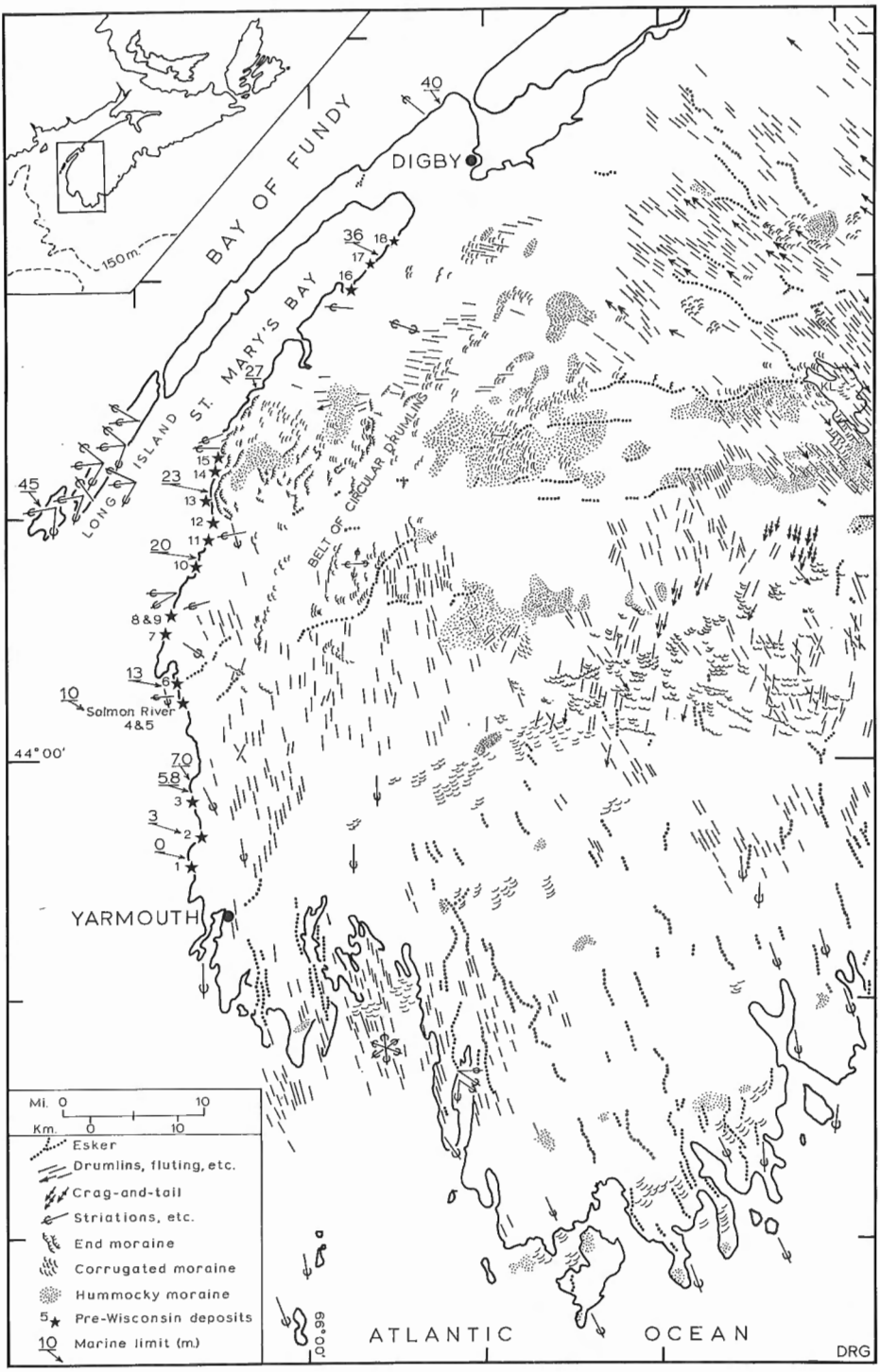

Figure 1. Pleistocene features, southwest Nova Scotia. Some striations from Taylor[4, 5].

south. This, and the greater development of ice-flow features, suggest that the late ice mass was better nourished in this sector and more capable of sustaining ice movement in its redirected course.

The record of sea level change begins with the late Wisconsin sea standing high against the receding ice front. Evidence suggests the sea was highest at deglaciation and fell thereafter; no transgression occurred. Marine overlap is easily determined owing to freshly eroding cliffs of variable height composed of easily reworkable till. In section, overlap deposits appear as wedges of plane-bedded, well-sorted gravel that pinch out upslope against unmodified till. The zero isoline crosses the coast 1 km north of Red Head.

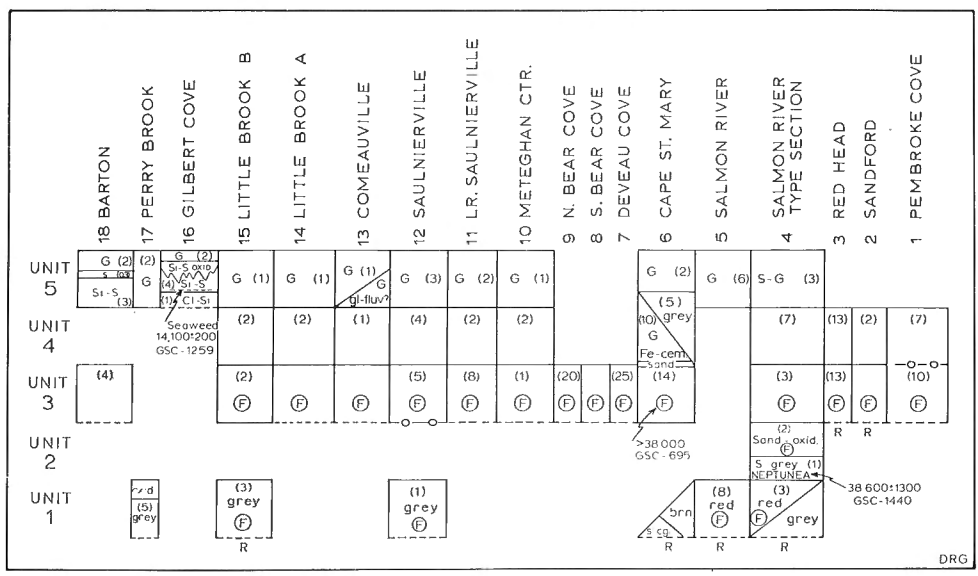

Unit 1: tills of early Wisconsin or pre-Sangamon Laurentide and local glaciation,

Unit 2: sediment with warm water fauna deposited during nonglacial interval of higher sea level (Sangamon?),

Unit 3: reddish brown shell-bearing till with foreign stones deposited by Laurentide ice moving south across red rocks underlying Bay of Fundy,

Unit 4: greyish tills of local derivation deposited by late Wisconsin ice flowing west from Nova Scotia uplands,

Unit 5: post-Wisconsin marine overlap sediment.

Figures in parentheses are thicknesses in metres. Broken lines at base of each section represent high tide level.

R – bedrock; G – gravel; S – sand;
Si – silt; Cl – clay; F – shell fragments.

Figure 2. Correlation chart of Pleistocene deposits exposed along the coast between Yarmouth and Digby (numbered localities indicated on Fig. 1).

The marine limit rises to the north, with the direction of maximum tilt at 160 degrees – nearly parallel the maximum Wisconsin ice-flow direction. The only age determination on this phase (as well as the only indirect age of deglaciation in the area, and the oldest in Nova Scotia) is one of 14, 100 ± 200 years (GSC-1259) on detritus of intertidal seaweed in grey sand at 1 m above high tide in Gilbert Cove. Following the establishment of the marine limit, sea level fell, reached and crossed the present sea level ca. 13, 000 years ago, and continued falling to a level 20 to 30 m below present, judging by the thickness of intertidal sediment aggraded in estuaries. The last 15 m and 4, 000 years of its return to present level have been determined by dating submerged intertidal and supratidal indicators[2].

Deposits predating the locally-derived tills of the last glaciation may be seen in numerous coastal exposures. Figure 2 shows the stratigraphy inferred by correlating two distinctive units common to most exposures – the post-Wisconsin marine overlap gravel and an anomalous red till containing shell fragments. Identification of species by F.J.E. Wagner and A.H. Clarke Jr. show that Venericardia borealis and Mercenaria mercenaria are dominant, Astarte undata and Placopecten magellanicus are common, and that Astarte subequilatera and Balanus spp., among others, are accessory. The red till is assigned to the Wisconsin maximum phase because both its fabric, as well as the striations beneath it, point to the south. At Salmon River (44°03.5'N, 66°10.5'W) the red till overlies a deeply oxidized bed of grey sand containing all the above species plus several others, all largely intact, including a large extinct gastropod – Neptunea stonei – that gave a somewhat questionable age of 38, 600 ± 1, 300 years (GSC-1440). The fauna indicates that the water was as warm as at present and the top of the Neptunea bed, where it is truncated by the overlying till, is fully 6 m above high tide or 9 m a.s.l. For these reasons, the radiocarbon age notwithstanding, the Neptunea bed is assigned to the Sangamon Interglacial, a time when the sea was both warm enough and high enough for this fauna to have been present[3].

---

[1] Prest, V.K. and Grant, D.R.: Retreat of the last ice sheet from the Maritime Provinces–Gulf of St. Lawrence region; Geol. Surv. Can., Paper 69-33 (1969).

[2] Grant, D.R.: Recent coastal submergence of the Maritime Provinces, Canada; Can. J. Earth Sci., vol. 7, No. 2, part 2, pp. 676-689 (1970).

[3] Clarke, A.H. Jr., Grant, D.R. and Macpherson, E.: Notes on the paleoecology of Neptunea stonei; Malacology (1971).

[4] Taylor, F.C.: Reconnaissance geology of Shelburne map-area; Geol. Surv. Can., Mem. 349 (1967).

[5] Taylor, F.C.: Geology of the Annapolis–St. Mary's Bay map-area; Geol. Surv. Can., Mem. 358 (1969).

36. GEOMORPHOLOGY, LAKE MELVILLE AREA, LABRADOR (13 F AND G)

Project 680086

D.R. Grant

This report terminates a surficial geology study for the Labrador Pilot Project of the Canada Land Inventory. The deposits and glacial history have been outlined previously[1].

The geomorphology of the coastal lowland bordering Lake Melville on the southwest was interpreted and plotted on ten sheets at a scale of 1:50,000. Figure 1 is a sample that illustrates most of the geomorphic features including (1) an extensive kettled ridge and terrace, (2) raised marine strandlines as high as 400 feet above sea level, (3) abandoned deltas of the Kenamu River at elevations of 50, 120, 160, and 260 feet, overlapped by (4) a broad alluvial fan spreading from the Mealy Mountains scarp, and (5) numerous flow-slides propagated by failure of the sand and buried marine pelite that deeply mantle the entire area.

Figure 2 is a compilation of this detailed information generalized as contrasting geomorphic units of ecological as well as geological significance. The continuity, topographic prominence and arcuate shape of the dominating kettled ridge and terrace led to its recognition as the largest of a series of interlobate and marginal moraines[2].

With the moraines depicted by Blake[3], a network of ice-marginal ridges was revealed by means of a derived bathy-orographic map (Fig. 3) based on water depths from the Canadian Hydrographic Chart 4728, and published topographic maps, both at the scale of 1:50,000. Subaerial topography has been interpreted to restore the original glacial surface, thus neglecting the distracting effect of postglacial dissection and some marine deposition. The result is believed to reflect the pattern of major morainal elements underlying the mantle of marine sediment.

Figure 4 depicts a sequence of deglaciation inferred from the moraines. The pattern is seen to be largely the result of four tributary sublobes occupying the Melville basin, the most active and latest of which was apparently the one that emanated from Grand Lake valley and excavated a trough in the floor of Lake Melville.

---

[1] Grant, D.R.: Surficial deposits, Lake Melville area, Labrador; in Report of Activities, Part A, April to October, 1968; Geol. Surv. Can., Paper 69-1, Part A, pp. 197-198 (1969).

[2] Bajzak, Denes: Bio-physical land classification, Labrador; Department of Fisheries and Forestry, Forest Research Laboratory, St. John's, Newfoundland, Internal Report N-13 (1969).

[3] Blake, W. Jr.: Landforms and topography of the Lake Melville area, Labrador, Newfoundland; Can. Dept. Mines Tech. Surv., Geog. Bull., No. 9, pp. 75-100 (1956).

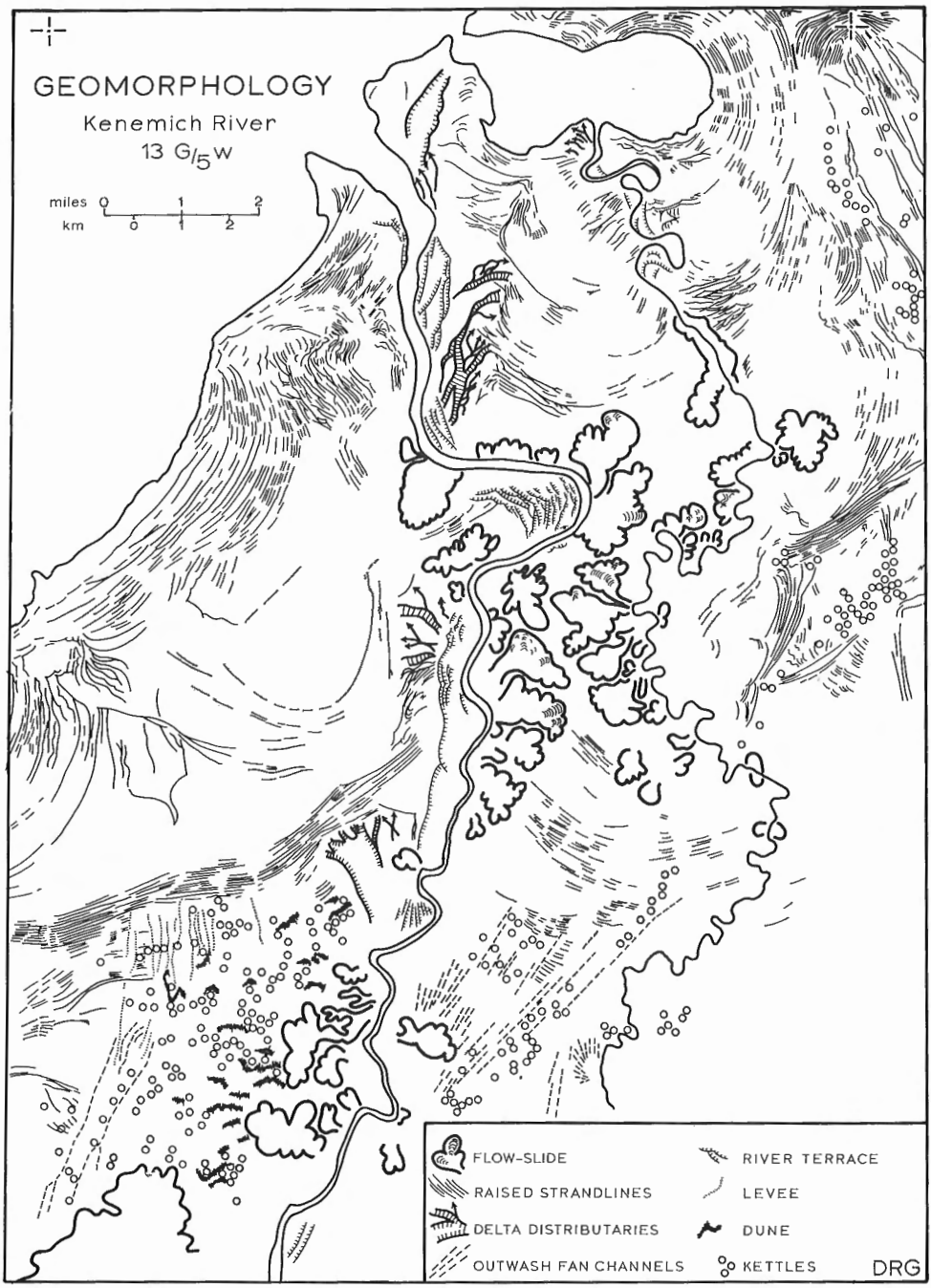

Figure 1. Geomorphological features, Kenemich River map-area, Labrador.
#36 Grant

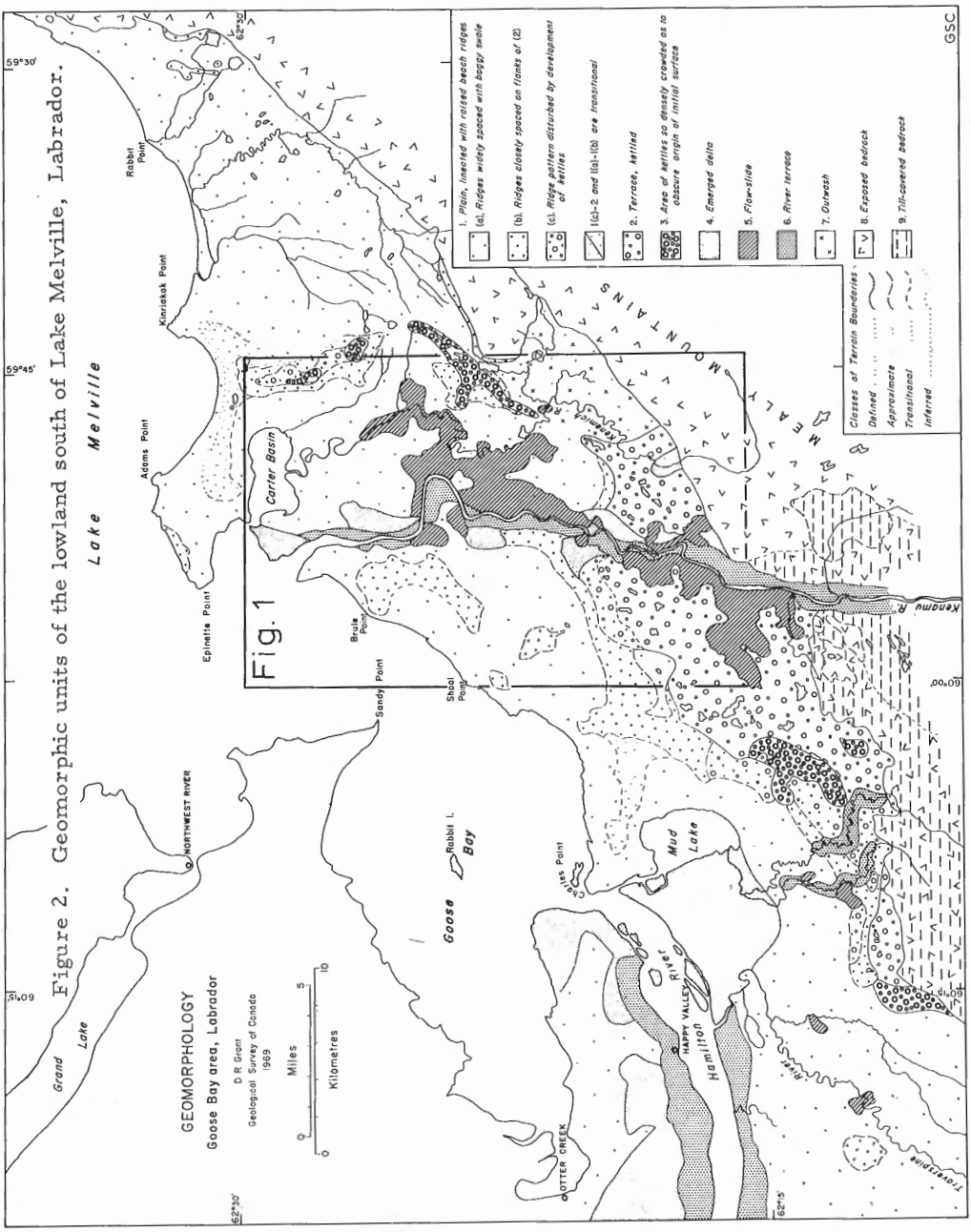
Figure 2. Geomorphic units of the lowland south of Lake Melville, Labrador.
Lake Melville
GEOMORPHOLOGY
Goose Bay area, Labrador
D.R. Grant
Geological Survey of Canada
1969
Miles
Kilometres
Fig. 1
Carter Basin
Grand Lake
NORTHWEST RIVER
Rabbit Point
Kinziakok Point
Adams Point
Epinette Point
Brule Point
Sandy Point
Shoal Point
Rabbit I.
Goose Bay
Otter Point
OTTER CREEK
Mud Lake
HAPPY VALLEY
Hamilton River
LOWER SEBAIE
Kenamu R.
MOUNTAINS
MEALY
1. Plain, lineated with raised beach ridges
(a). Ridges widely spaced with boggy swale
(b). Ridges closely spaced on flanks of (2)
(c). Ridge pattern disturbed by development of kettles
1(a)-2 and 1(a)-1(b) are transitional
2. Terrace, kettled
3. Area of kettles so densely crowded as to obscure origin of initial surface
4. Emerged delta
5. Flow-slide
6. River terrace
7. Outwash
8. Exposed bedrock
9. Till-covered bedrock
Classes of Terrain Boundaries
Defined
Approximate
Transitional
Inferred
GSC

#36 Grant

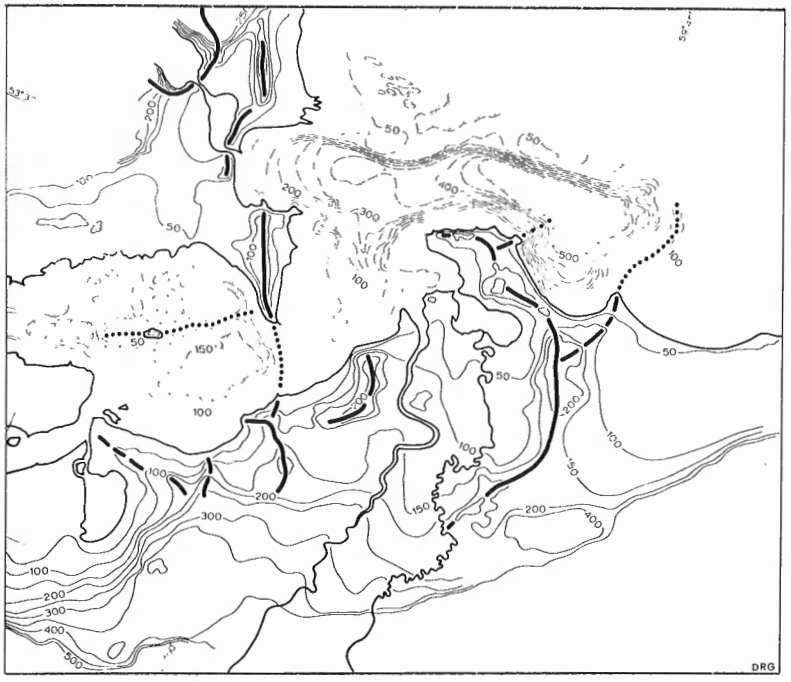

Figure 3. Bathymetry and derived topography showing morainal ridges, southern Lake Melville area, Labrador.

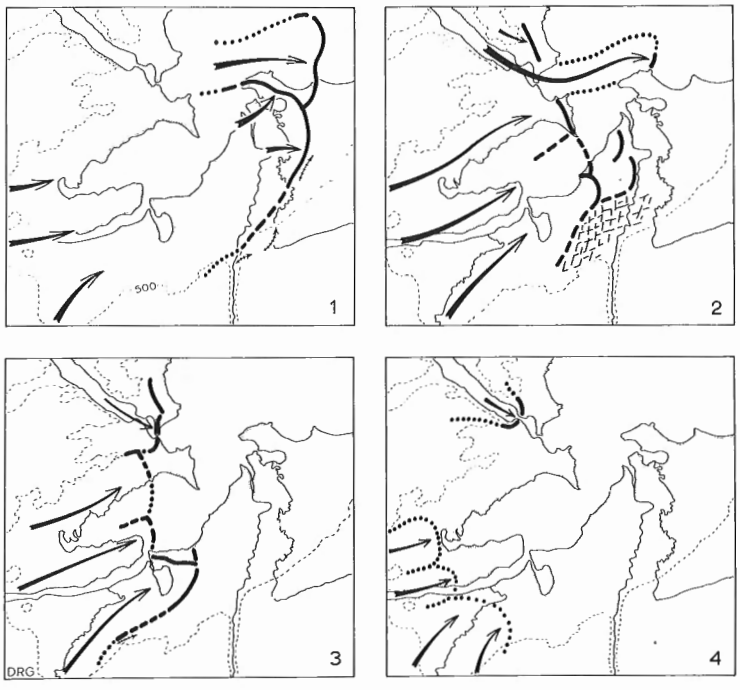

Figure 4. Hypothetical ice-marginal positions, with inferred meltwater escapeways and areas of dead-ice topography.

#36 Grant

37. GLACIATION OF CAPE BRETON ISLAND, NOVA SCOTIA

Project 700056

D. R. Grant

Airphoto study of glacial features in Cape Breton Island corroborates earlier interpretations and provides more uniform knowledge of the entire island. Grant[1] collected evidence in southern Cape Breton of "early, easterly, coastwise and onshore ice flow crossed by later southerly offshore movement". Grant[2] notes that "newly-observed striae support the concept of a radially-spreading, land-locked Bras D'Or lowlands ice mass". Prest and Grant[3] depicted evidence of ice flow throughout the region and portrayed withdrawal to an active lowland centre as well as to a weaker centre on the northern plateau. After detailed mapping, Grant[4] confirmed the early easterly flow and the final retreat to the north, but also provided compelling evidence that main flow had been from south to north over much of the lowlands, apparently from a centre on the continental shelf. Whereas elsewhere on the Atlantic side of Nova Scotia retreat was apparently upslope from south to north from the shelf to the uplands, deglaciation in southern Cape Breton may have been later because of the extra step involved in shifting the ice divide from the shelf to the Bras D'Or area.

Examination of small-scale airphotos at scales of 1:65,000 and 1:86,000 reveals a well-developed lineation in tills, often with directional asymmetry, on both highlands and lowlands alike. Reliable knowledge of the entire island can now be claimed. The patterns are clear and convincing, and generalized flowlines, substantiated by over 400 directional striations, are shown in Figure 1. A feature of this paper is the author's commitment to the previous existence of a full-fledged ice cap on the northern plateau in view of equally well-developed tracts of crag-and-tail hills on the western as well as eastern slopes.

While the patterns are at variance with the popular notion of simple unidirectional movement characteristic of much of Canada overridden by the Laurentide ice sheet, they are actually just what should be expected in a region that is near the Wisconsin limit, that has high relief relative to the tapering ice thicknesses of the marginal zone, and that occupies a windward and maritime position where local accumulation can be enhanced. The observed pattern is regarded as a natural consequence of the following events or processes: (1) before and after possible confluence with Labradorean (Laurentide) ice, the regional flow pattern was dominated by the activity of local dispersal centres, one of which happened to have centred offshore on the formerly emergent shelf, like that indicated by Hoppe[5] for the Barents Sea; (2) movement was topographically directed with local reversals, like that indicated for Victoria Island by Fyles[6]; (3) ice centres and ice divides shifted in response to differential accretion and shrinkage, such as was recognized in the District of Keewatin by Tyrrell[7], and (4) movement in the final stages became essentially radial to the coast occasioned by marine incursion, such as occurred when the Tyrrell Sea invaded Hudson Bay[8].

Thus, the interpretations being proposed for Cape Breton Island are not without precedent, even in Canada. Cape Breton does, however,

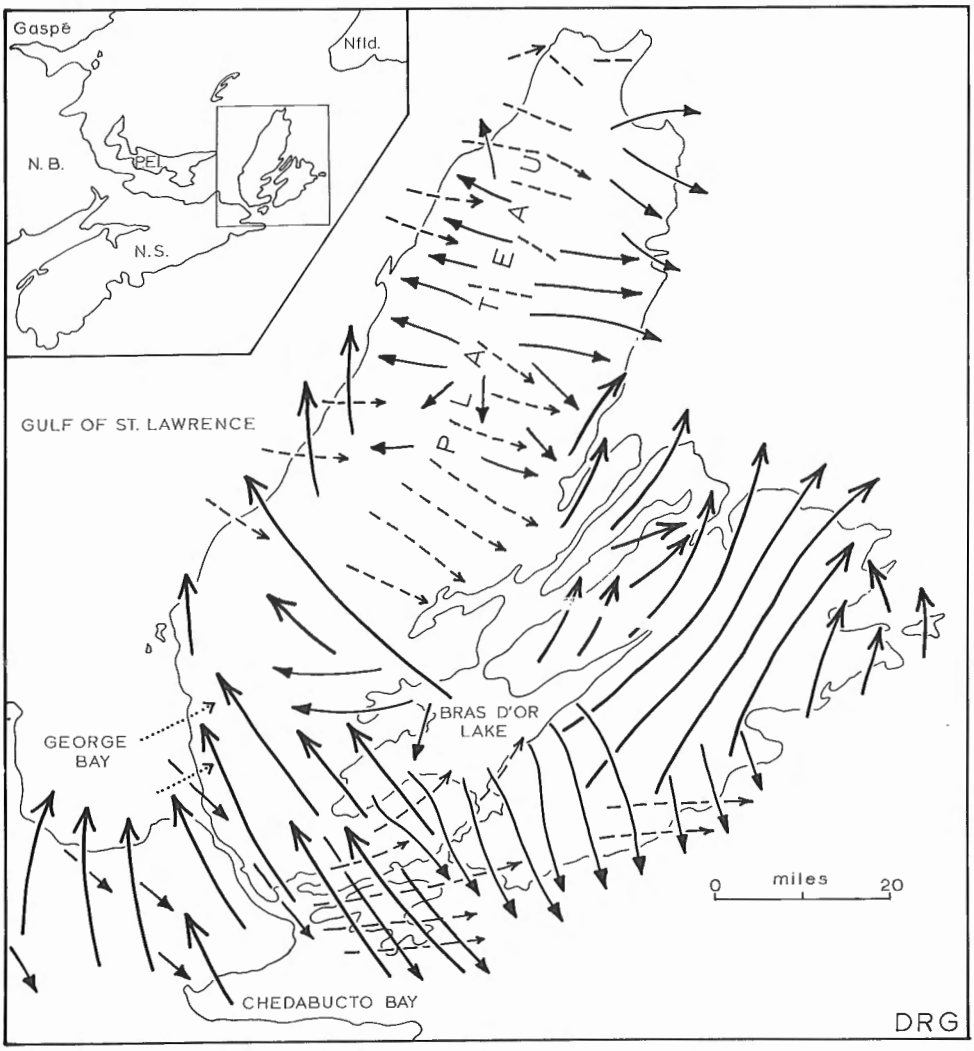

Figure 1. Generalized glacial movements in Cape Breton Island based on field observations and airphoto interpretation. (Dashed arrows denote early flow from distant sources; solid arrows denote flow from several sources on or near the island active during maximum and late Wisconsin phases; dotted arrows denote a late local recession).

commend itself as a type area for these variations in glaciation by virtue of the abundant clear-cut evidence. Arguments are being marshalled to promote this theme during an excursion of the 1972 International Geological Congress.

---

[1] Grant, D. R.: Reconnaissance of submergence phenomena, Nova Scotia; in Report of Activities, Part A, May to October, 1966; Geol. Surv. Can., Paper 67-1, Part A, pp. 173-174 (1967).

[2] Grant, D.R.: Recent submergence in Nova Scotia and Prince Edward Island; in Report of Activities, Part A, May to October, 1967; Geol. Surv. Can., Paper 68-1, Part A, pp. 162-164 (1968).

[3] Prest, V.K. and Grant, D.R.: Retreat of the last ice sheet from the Maritime Provinces-Gulf of St. Lawrence region; Geol. Surv. Can., Paper 69-33 (1969).

[4] Grant, D.R.: Surficial geology, southwest Cape Breton Island, Nova Scotia; in Report of Activities, Part A, April to October, 1970; Geol. Surv. Can., Paper 71-1, Part A, pp. 161-164 (1971).

[5] Hoppe, G.: The Wurm ice sheets of northern and arctic Europe; Acta Geog. Lodz., No. 24, pp. 205-215 (1970).

[6] Fyles, J.G.: Surficial geology of Victoria and Stefansson Islands; Geol. Surv. Can., Bull. 101 (1963).

[7] Tyrrell, J.B.: Report on the Dubawnt, Kazan and Ferguson Rivers and the northwest coast of Hudson Bay; Geol. Surv. Can., Ann. Rept., 1896, Pt. F (1897).

[8] Lee, H.A.: Quaternary geology; in Science, history and Hudson Bay, C.S. Beals, ed., Can. Dept. Energy, Mines Resources, Ottawa, vol. 2, pp. 503-543 (1968).

38. MODIFICATIONS TO RAPID SEDIMENT ANALYSER

Project 680017

D.E. Lawrence

The useful range of the rapid sediment analyser, (Benthos No. 341) used by the Division of Quaternary Research and Geomorphology has been extended by effecting a number of small changes allowing smaller samples to be processed with less background interference. The changes were aimed at limiting vibration, variations in temperature, and pressure from external sources.

The principle of the operation is based on the measurement of pressure differential between two columns of water, one a reference and the other a settling column for the sediment. Introduction of a sample increases the effective column density, which is measured by a pressure transducer located near the bottom of the columns. As the particles fall past the transducer sensor, pressure changes generate a voltage, the output of which is fed to a signal processing network and an X-Y plotter where pressure is plotted against time.

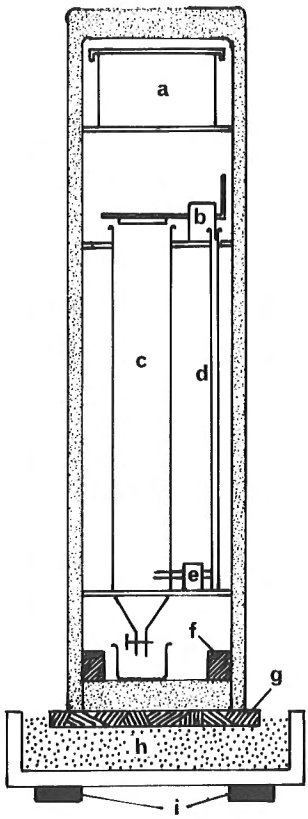

Figure 1 (left)
Diagrammatic sketch of settling column module (not to scale).
(a) water reservoir (removed in modification).
(b) sample introduction mechanism.
(c) settling column.
(d) reference column.
(e) transducer.
(f) lead ballast.
(g) 2-inch concrete levelling platform.
(h) 5 inches of uniform sand.
(i) isomode antivibration pads.

Figure 2 (below)
Base of settling tube module with modifications. GSC Photo No. 20/629-E.
(a) isomode rubber antivibration pads (two only visible) used to decouple instrument from floor.
(b) plywood box containing silica sand. This serves a dual role providing a stable base of high inertia and damping out vibration.
(c) concrete platform.
(d) lead ballast.

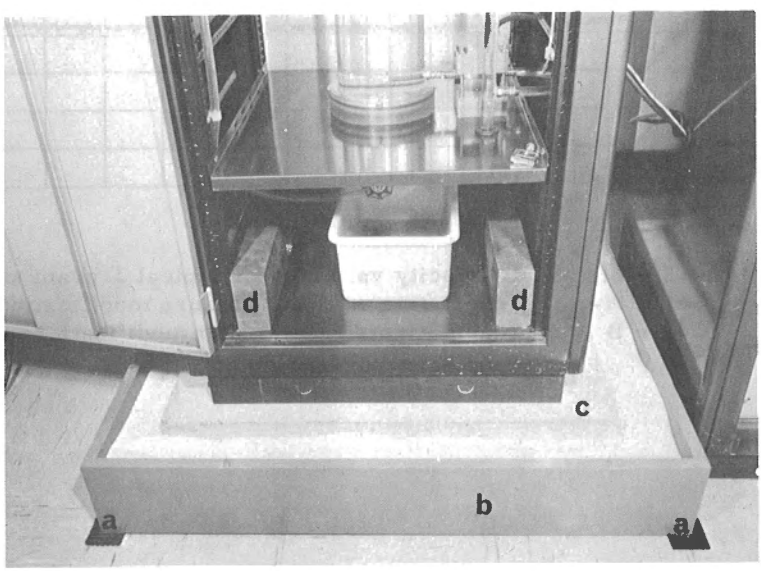

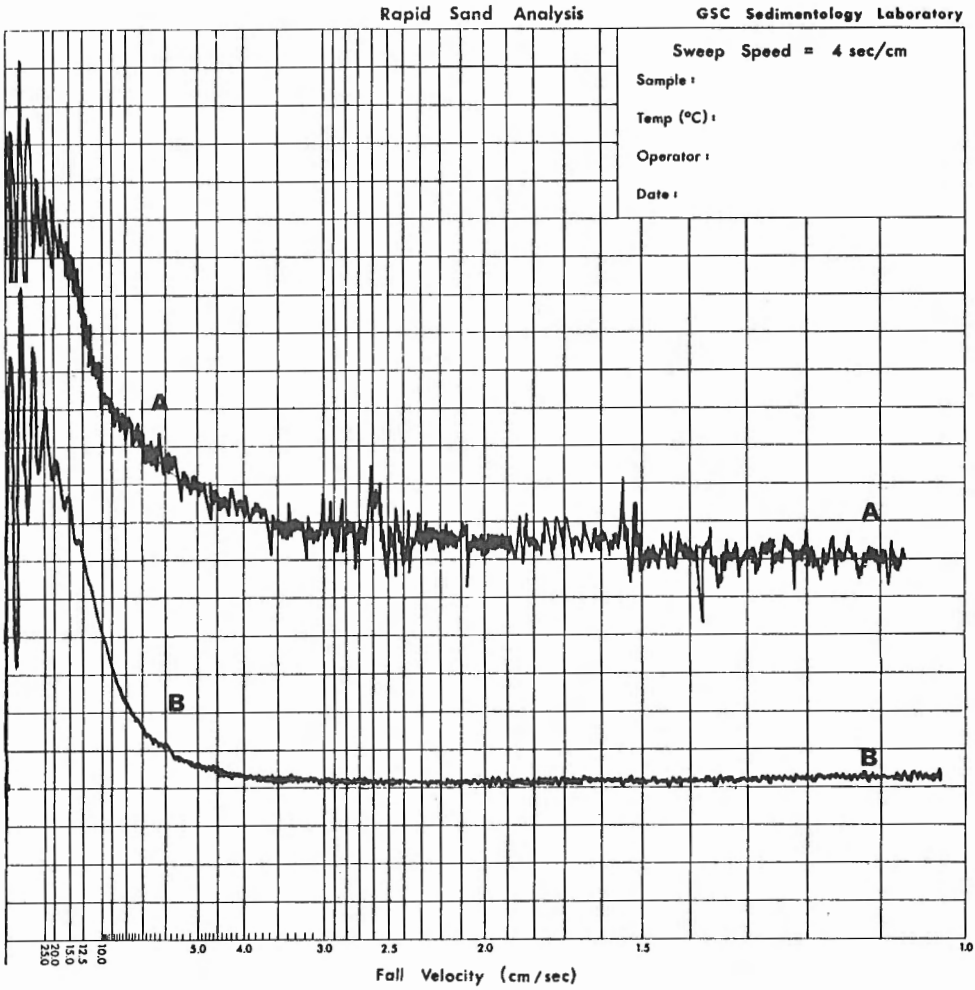

Figure 3. X-Y plots of fall velocity vs. time for typical 3-gram samples. Curve A is representative of results before modifications. Curve B is representative of results after modifications were made.

The following tabulation and figures indicate the nature and effects of the modifications.

TABLE I

MODIFICATIONS TO RAPID SEDIMENT ANALYSER

Problem	Cause	Modifications	Effect
High background and interference	External Vibration	a. Decouple instrument from floor with isomode anti-vibration pads. b. Install high inertia base of sand with concrete levelling pad.	A large portion of the low frequency vibration is reduced or eliminated.
Vibrations within instrument slow to attenuate	a. Vibrations set up waves in reservoir tank. b. High centre of gravity.	a. Remove water reservoir from module and mount on wall bracket. b. Add lead ballast to instrument base.	Vibration is attenuated more quickly.
Instrumental drift	Transducer sensitive to temperature variation.	a. Relocate instrument to draft free location. b. Insulate pressure transducer.	Drift reduced to a minimum.
X-Y plot of fall velocity vs. time does not register the complete sample.	a. May be attributed to temperature drift. b. Complete sample not settling in tube due to surface tension.	Application of wetting agent to sample when placed on introduction mechanism.	All sample is wetted and promptly falls when introduced to the settling column.

The modifications tabulated above can easily be applied to any vibration-sensitive instrument, as no physical modifications to the instrument itself are necessary.

The decoupling method has been in use for some time on an astatic magnetometer located in the same building. Thanks are extended to members of the Rock Magnetism Section of the Exploration Geophysics Division for advice and assistance in this respect.

39. PALYNOLOGY OF A BURIED ORGANIC DEPOSIT, RIVER INHABITANTS, CAPE BRETON ISLAND, NOVA SCOTIA

Project 690064

R.J. Mott

The stratigraphy and palynology of several buried organic deposits from Cape Breton Island have been described by Mott and Prest[1] and Livingstone[2]. During the summer of 1970, Grant[3] rediscovered a buried organic deposit that had originally been noted by Sir William Dawson in 1855[4] on the Northwest Arm Brook, a tributary of River Inhabitants (45°40.57'N, 61°19.58'W), and collected samples for wood identification and paynological study.

The river is exhuming a buried bedrock depression containing a stratigraphic thickness of 15 feet of colluvial lenses interbedded with organic sand, peat and wood that is more than 39,000 years old (GSC-1406)[3], overlain by 10 feet of cobble gravel and 30 feet of reddish till containing shell

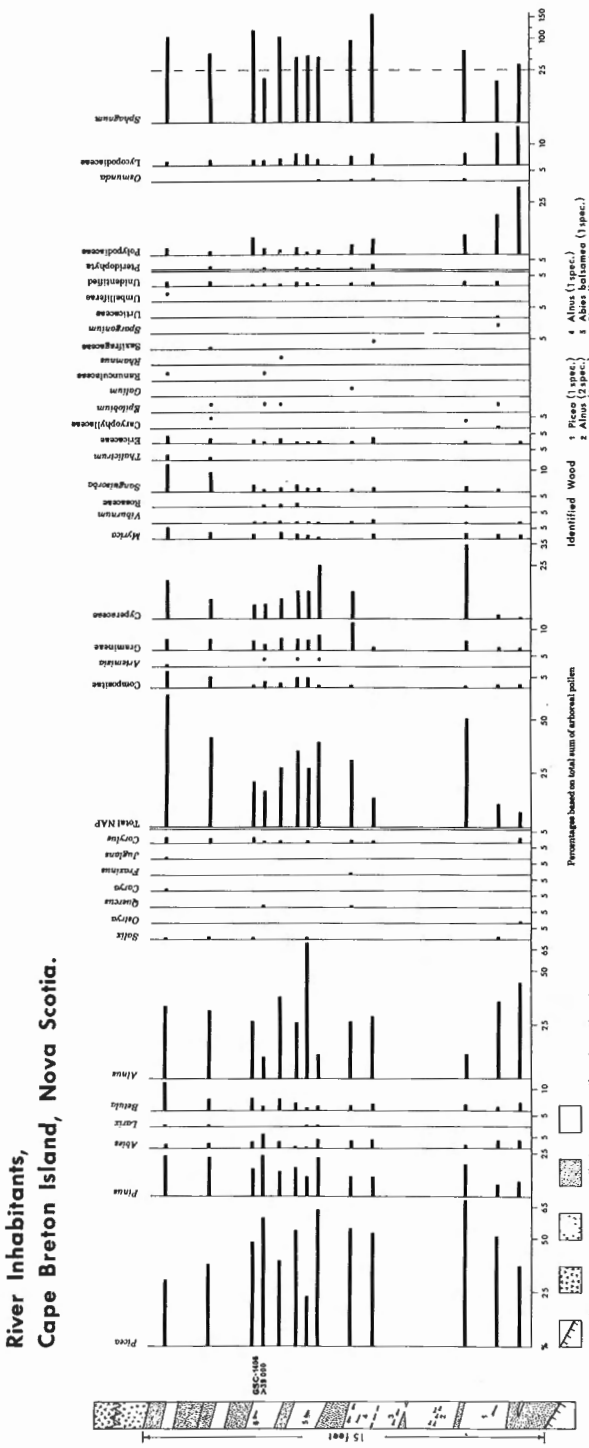

Figure 1. Pollen diagram with schematic outline of stratigraphy and wood identifications.

fragments that, elsewhere, gave an apparently finite age of 32,100 ± 900 years (GSC-1408)[3]. Glacial loading has greatly compressed and depressed the peat and caused the formation of boudins in the colluvial layers by differential stretching at the margins where the beds lap steeply onto bedrock. The sediment sequence is interpreted by Grant[3] to represent: (1) periglacial deposition of colluvium and organic detritus; (2) proglacial deposition of outwash gravel and (3) burial by tills of the last glaciation.

Results of a preliminary palynological study are shown in Figure 1 with a schematic outline of the stratigraphy and wood identifications. The assemblages throughout the sequence, dominated by Picea (spruce) and Alnus (alder), with lesser amounts of Pinus (pine) and small percentages of Betula (birch) and Abies (fir), are boreal forest assemblages which are significantly different from modern pollen spectra and most postglacial spectra from Cape Breton Island[2, 5]. The low Betula percentages and the almost complete lack of Tsuga (hemlock) and thermophilous deciduous genera are the more obvious deviations from the modern spectra. The high, and somewhat erratic, frequencies of Alnus pollen point to over representation due to its local abundance in the vegetation. Numerous pieces of alder wood in the sediments corroborate this interpretation and suggest an alder swamp environment of deposition with frequent inundations and deposition of colluvium. The surrounding region was probably covered by a closed spruce forest with some fir and pine on suitable sites. Some wood of spruce and fir was also found in the sediments. Among the nonarboreal pollen taxa, Cyperaceae (sedges) and Sphagnum are the most abundant, indicating that these plants were plentiful in the local flora together with several other taxa represented by lesser pollen frequencies.

The similarity between the pollen spectra at the River Inhabitants site and those described for other buried organic deposits on Cape Breton Island suggests a tentative correlation between them. Until more evidence of other interglacial or interstadial episodes is brought forth, this deposit is assigned to an early Wisconsin interstade, as suggested previously for other deposits by Mott and Prest[1].

---

[1] Mott, R.J. and Prest, V.K.: Stratigraphy and palynology of buried organic deposits from Cape Breton Island, Nova Scotia; Can. J. Earth Sci., vol. 4, pp. 709-724 (1967).

[2] Livingstone, D.A.: Some interstadial and postglacial pollen diagrams from eastern Canada; Ecol. Monog., vol. 38, No. 2, pp. 87-125 (1968).

[3] Grant, D.R.: Surficial geology, southwest Cape Breton Island, Nova Scotia; in Report of Activities, Part A, April to October, 1970; Geol. Surv. Can., Paper 71-1, Part A, pp. 161-164 (1971).

[4] Dawson, Sir J.W.: Acadian geology (first edition); Edinburgh, 338 pp. (1855).

[5] Livingstone, D.A. and Estes, A.H.: A carbon-dated pollen diagram from the Cape Breton Plateau, Nova Scotia; Can. J. Bot., vol. 45, pp. 339-359 (1967).

40. RADIOCARBON DATES FROM SASKATCHEWAN

Project 650030

R. J. Mott

Four radiocarbon dates on basal organic lake sediments from four lake sites in Saskatchewan were reported previously[1, 2]. These and two new dates from lake sites farther to the north are listed below and are shown in Figure 1.

Site 1.	GSC-648	– 11,560 ± 640
Site 2.	GSC-642	– 11,090 ± 160
Site 3.	GSC-647	– 10,260 ± 170
Site 4.	GSC-643	– 8,520 ± 170
Site 5.	GSC-1446	– 8,640 ± 240
Site 6.	GSC-1466	– 8,230 ± 250

Basal organic sediment from a small unnamed lake about 68 miles north-northeast of La Ronge, Saskatchewan (Site 5, Fig. 1) (55°53'20"N, 104°4'30"W) gave a date of 8,640 ± 240 years B.P. (GSC-1446). The lake, formed in a bedrock basin, has a surface elevation of about 1,570 feet above sea level and a maximum water depth of 30 feet. The sediment core showed 494 cm of dark brown laminated algal gyttja and 6 cm of grey, silty clay overlying coarse bouldery gravel. The radiocarbon date was on a 5 cm interval at the base of the algal gyttja. Some organic material was present in the silty clay but in amounts too small to date.

The second date, 8,230 ± 250 (GSC-1466), is on basal organic sediment from an unnamed lake about 88 miles north-northeast of La Ronge (Site 6, Fig. 1) (56°7'30"N, 104°24'20"W). This lake also occupies a bedrock basin. Because the water depth was too great in the deepest part of the lake (more than 80 feet) the core was taken in a small bay at the eastern end of the lake which was almost cut off from the main part of the lake by a bedrock ridge and esker. However, the bay was not a separate basin as the bottom sloped continuously into the main lake. Elevation of the lake surface was also about 1,570 feet above sea level, and water depth at the coring site was 25 feet. Coring revealed 500 cm of brown algal gyttja, 50 cm of grey-brown silty gyttja and 22 cm of dark brown to black organic silt overlying inorganic silty clay. The interval from 562 to 572 cm depth was used for dating as the underlying silty clay did not contain enough organic matter to yield a date.

Both new dates provide minimum ages for deglaciation, and the date from Site 6 also gives a minimum age for retreat of the ice from the Cree Lake Moraine which is situated less than 5 miles south of the coring site (Fig. 1). Since both lakes are outside the area covered by any phase of Glacial Lake Agassiz or any other known glacial lakes, the beginning of organic accumulation was not delayed, as was probably the case with three of the original four sites dated. For example, Cycloid Lake (Site 4, Fig. 1), which gave a date of 8,520 ± 170 (GSC-643) on basal gyttja, was probably covered by two phases of Glacial Lake Agassiz possibly until as late as 9,000 years ago[3, 4, 5]. Although more than 5 m of organic sediments were recovered from the lake north of the Cree Lake Moraine, the deepest part of the lake

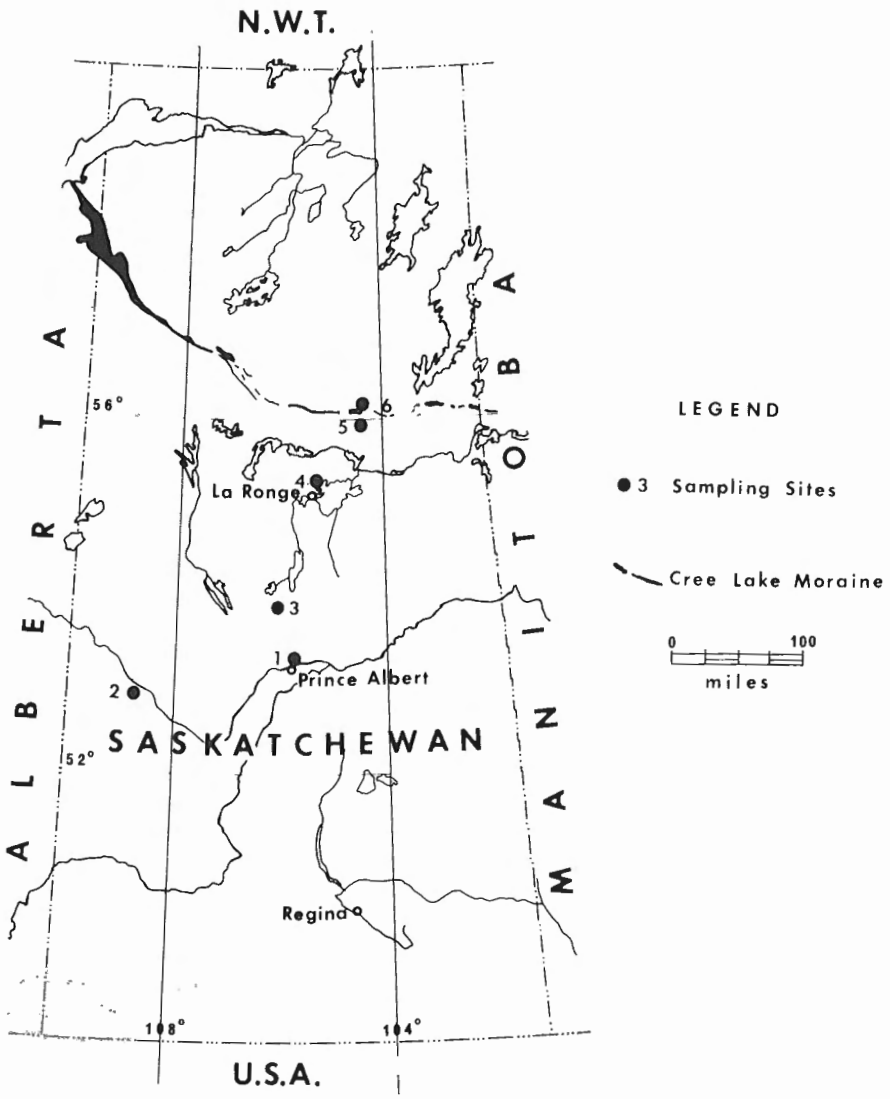

Figure 1. Location map showing lake sites and Cree Lake Moraine.

and, therefore, presumably the oldest sediment, was not sampled. The lag between deglaciation, the invasion of plants into the area, and the accumulation of sufficient organic matter in the sediment for radiocarbon dating are other factors which involve an unknown length of time.

Prest[5] has suggested, somewhat speculatively, that the Cree Lake Moraine is about 10,000 years old. The date from Site 6 is much younger but, because of the factors noted above, the date must be considered a minimum and neither verifies nor negates Prest's suggested age.

[1] Mott, R.J.: Palynological studies in central Saskatchewan; in Report of Activities, Part A, May to October, 1966; Geol. Surv. Can., Paper 67-1, Part A, pp. 122-123 (1967).

[2] Lowden, J.A., Fyles, J.G. and Blake, W. Jr.: Geological Survey of Canada radiocarbon dates VI; Radiocarbon, vol. 9, pp. 156-197 (1967).

[3] Elson, John A.: Geology of Glacial Lake Agassiz; in Life, Land and Water, Proc. 1966 Conf. on Environmental studies of the Glacial Lake Agassiz Region, William J. Mayer-Oakes, ed., pp. 37-95 (1967).

[4] Prest, V.K., Grant, D.R. and Rampton, V.N.: Glacial map of Canada; Geol. Surv. Can., Map 1253A (1967).

[5] Prest, V.K.: Retreat of Wisconsin and recent ice in North America (speculative ice-marginal positions during recession of last ice-sheet complex); Geol. Surv. Can., Map 1257A (1969).

41. GROUND ICE CONDITIONS: YUKON COASTAL PLAIN AND ADJACENT AREAS

Project 690047

V.N. Rampton

Buried massive ice and icy sediments, i.e. sediments containing excess ice, are commonly reported in shot-hole logs and engineering test-hole logs[1] along the Yukon coast and adjacent areas (Fig. 1). These occurrences indicate that massive ice and icy sediments are common in near-surface unconsolidated materials along the Yukon coast, even though previously published observations and maps covering the same area[2, 3] did not acknowledge their presence. Ice-rich till and colluvium, which probably have ice contents typical of icy sediments in the area, can be observed in the sea cliffs along the Yukon coast (Fig. 2). Any disturbance of the landscape causing icy sediments similar to those in Figure 2 or buried massive ice to melt will produce thermokarst depressions whose depths will be proportional to the amount of excess ice the melted sediments contain.

West of longitude 137° more than half the drilled holes on the coastal plain encountered icy sediments or buried massive ice. A comparison of the logs and maps of the surficial geology[3] indicates that all clayey and silty materials, this includes morainal deposits, lacustrine deposits, fine-grained alluvium and colluvium, have high contents of ice. Excess ice is even common

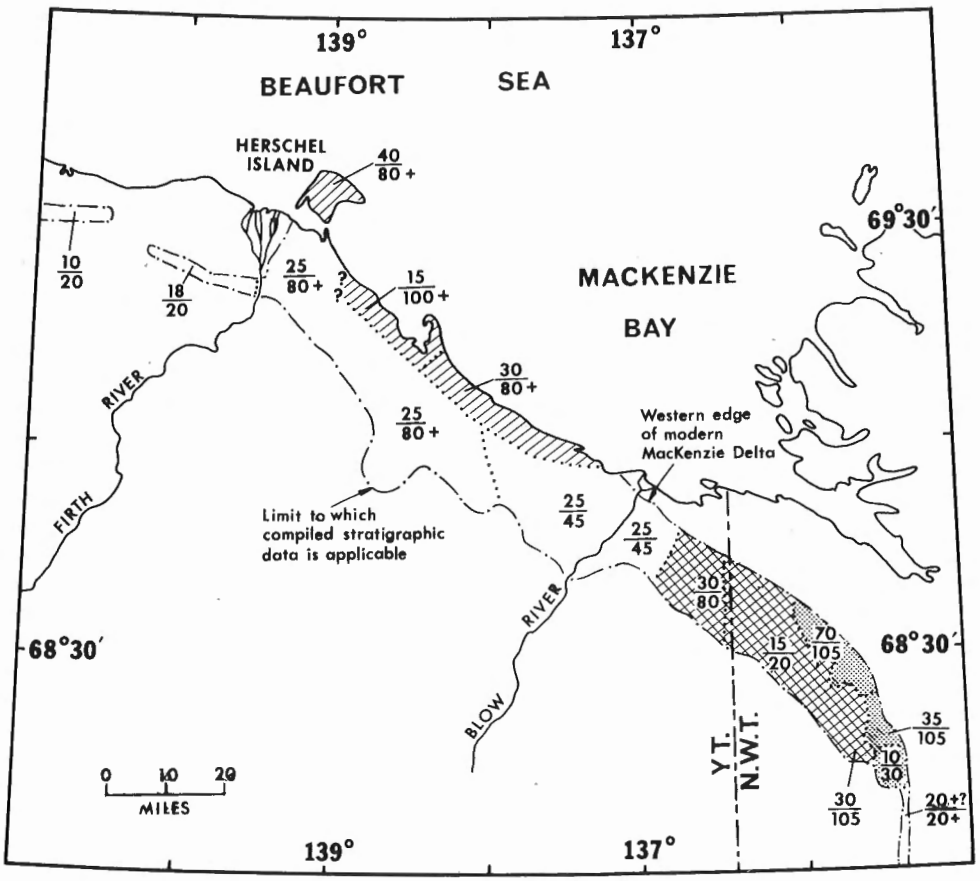

Figure 1. Ground-ice conditions of the Yukon coastal plain and adjacent area. Explanation: In the hachured areas, sediments containing excess ice are not only common near the surface, but are often found as unique stratigraphic units at depth. In the stippled areas, shothole logs only occasionally report sediments as having excess ice. The upper numeral gives the general maximum depth of icy sediments in feet where they have been noted, and the lower numeral gives the maximum depth in feet at which icy sediments have been noted. In the cross-hachured areas, figures are based on an extrapolation from a minimum number of drillhole logs.

in the thin veneer of fine-grained sediments and organic deposits where they cap bedrock, pediment surfaces, and glaciofluvial and fluvial deposits. Only bedrock, fluvial and glaciofluvial deposits lacking a cover of fine-grained sediments or organic deposits, modern beach deposits, and modern floodplain deposits are relatively free of excess ice.

The icy sediments and massive ice generally form the upper stratigraphic units in most drillholes, and the maximum depths to which excess ice in the sediments are commonly reported has been recorded on Figure 2. For example, in the area directly south of Herschel Island, icy sediments and

Figure 2. Ice wedges and lenses in ice-rich till and colluvium exposed along the Yukon coast west of Shingle Point. Exposure is about 35 feet high (photo by J.G. Fyles). GSC Photo 201695.

massive ice are commonly reported in drillhole logs from the surface to a depth of 25 feet; although some drillholes have bottomed in icy sediments at 80 feet, icy sediments below 25 feet are uncommon. Exceptions to this near-surface occurrence of icy sediments and massive ice occur on Herschel Island and the coastal strip to the southeast (Fig. 2) where icy sediments and massive ice have occasionally been reported below sediments lacking excess ice.

East of longitude 137°, icy sediments are not commonly reported in shot-hole logs. However, in areas where both shot holes and engineering test holes have been drilled, the engineering test-hole logs generally report the upper 20 feet of sediment to contain excess ice. Thus, the shot-hole logs from east of longitude 137° must be viewed with some skepticism in the evaluation of ground-ice conditions, and areas on Figure 2 from which sediments with excess ice are only occasionally reported may, in fact, have an abundance of near-surface sediments containing excess ice.

---

[1] Ripley, Klohn and Leonoff Alberta Ltd.: Evaluation of sub-surface conditions, Mackenzie Valley Pipeline (1970).

[2] Rampton, V.N.: Quaternary geology, Mackenzie Delta and Arctic coastal plain, District of Mackenzie; in Report of Activities, Part A, April to October, 1969; Geol. Surv. Can., Paper 70-1, Part A, pp. 181-182 (1970).

[3] Rampton, V.N.: Surficial geology, Herschel Island-Aklavik; Geol. Surv. Can., Open File Report 21 (1970).

42. PRELIMINARY INTERPRETATION OF SHALLOW SEISMIC REFLECTION PROFILES FROM THE WEST SIDE OF MACKENZIE BAY, BEAUFORT SEA

Project 700092

James M. Shearer

About 250 nautical miles of shallow reflection profiling using a Huntec 2A sparker unit were obtained during the month of August, 1970 in the Mackenzie Bay area of the Beaufort Sea from the C.H.S. Richardson (Fig. 1). A few short lines using a side scan sonar unit were also run.

Throughout most of the area traversed, except in depths of less than 20 to 30 feet, considerable thicknesses of recent (postglacial) muds were observed (Figs. 2, 3, 3a and 4). Wave action is apparently strong enough to prevent deposition of clay in the summertime and to erode what fine sediments were deposited during the winter at these shallow depths (<30 feet). In depths of less than 150 to 200 feet this mud unit has a very irregular surface, which is attributed to cumulative scouring by the bottoms of ice islands and pressure ridges (Figs. 2 to 4). Work using the side scan sonar (Fig. 5) demonstrated that these observed features were, in fact, continuous (usually quite linear) thus supporting the ice scouring hypothesis.

Underlying this blanket clay deposit were a number of features, the most notable being a buried trough or canyon (Figs. 3, 4) which appears to be consistent throughout the study area between 3 to 5 miles off the west coast of Mackenzie Bay. Ice-thrusted marine sediments form the topographic ridge between King and Kay Points[1]. Offshore in that area, a structureless unit lying under the recent muds is found to increase in thickness shoreward and eventually surfaces to become the seabottom (Figs. 3, 3a). This unit is designated as the offshore equivalent of the ice-thrust horizon found on shore. The similarity of this unit to the basal unit in the buried canyon (Fig. 3) implies a similarity in formation. In this respect, it is proposed that the canyon was formed by erosion from a continental glacier tongue moving seaward. Branches emanating from this tongue were probably sufficient in size to cause the deformation observed between King and Kay Points.

The relationship of this buried canyon to the Mackenzie Canyon observed on bathymetric charts is unknown. The present surface over the buried canyon is almost flat (slope 1/300) with the maximum slope existing along the edge of the Mackenzie Canyon being around 1/60. Both these slopes are a different order of magnitude from that slope of the buried canyon wall (slope 1/2 to 1/4).

A change in slope of the wall of this canyon (Figs. 3, 4) indicates the depth at which modification by fluvial and/or marine processes occurred. In this case, the erosion and truncation of the west bank is thought to be due to marine action alone, as the deposits contemporaneous with a given level of incision are found in the trough (canyon) at some depth below this level. They are best interpreted as bottom-set beds or submarine outwash deposits laid down in 50 to 100 feet of water with the corresponding delta front or glacier front some miles to the south. This change in slope of the canyon wall is designated hereafter as the "breakpoint" and is thought to be representative of the sea level at the time the Wisconsin ice first receded beyond this point.

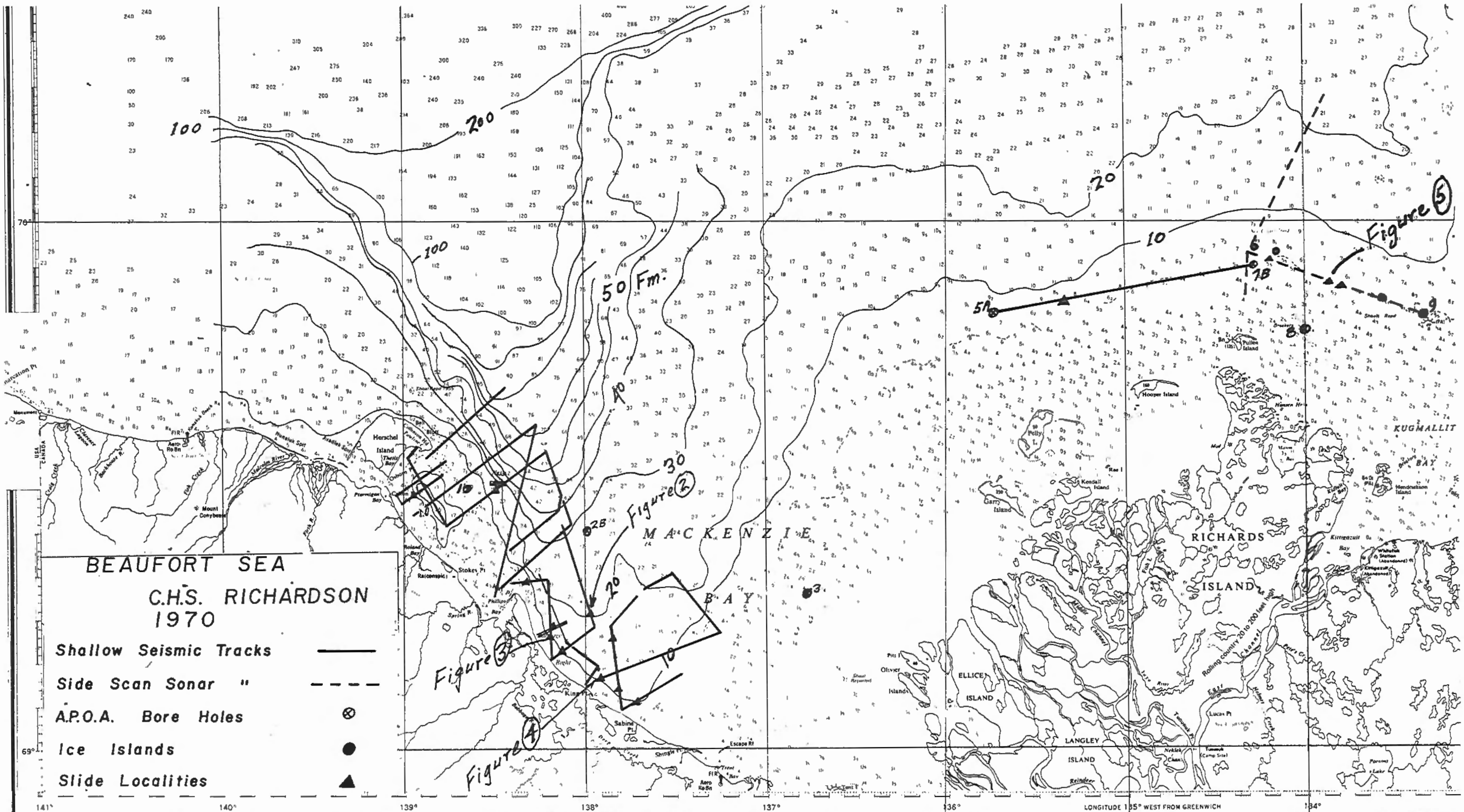

Figure 1. Track chart of C.H.S. Richardson superimposed onto rough bathymetry of Mackenzie Canyon (contour interval of 10 fathoms to 100 fathoms).

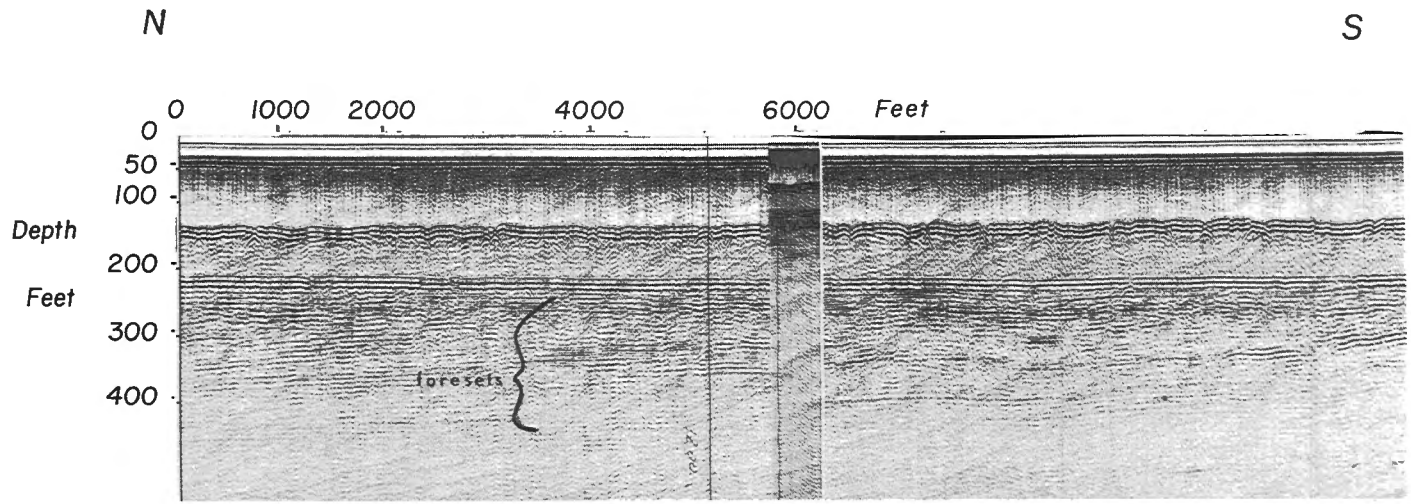

Figure 2. Sparker profile (north on the left hand side) indicating about 80 feet of the upper mud unit (post-glacial? in age) overlying a very well developed topset unit at about 210-215 feet (speed of sound in water) below the sea surface. These topset beds grade into large-scale forest beds which have a slope of about 1/100 in the northward directions.

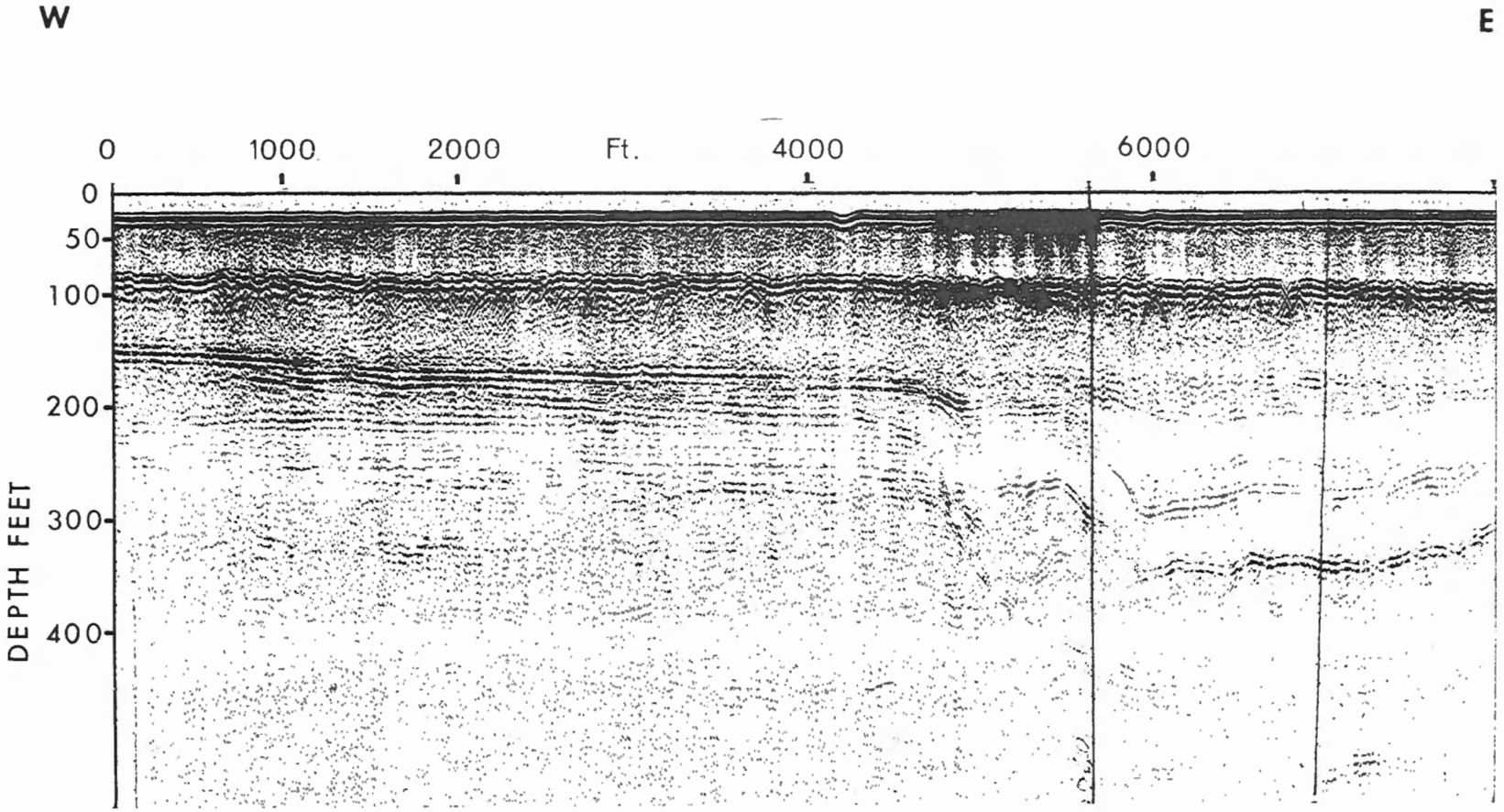

Figure 3. Sparker profile running over west side of buried canyon. Examination of this figure with a tracing of the same record (Fig. 3a) should serve to point out the various units referred to in the text. The "breakpoint" on this particular section is found around 220 feet below the present datum.

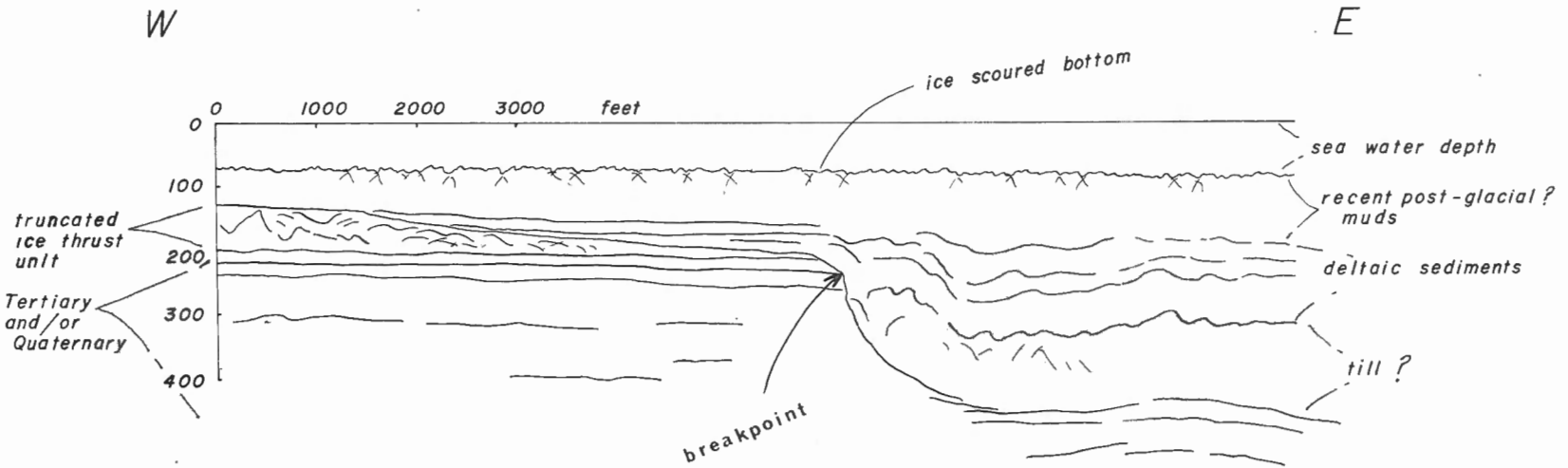

Tracing of Seismic Profiler Section across Buried Valley

Figure 3a. Tracing of original record shown in Figure 3 using same scale. Note irregular topography on surface of till(?) unit and conformable units overlying it.

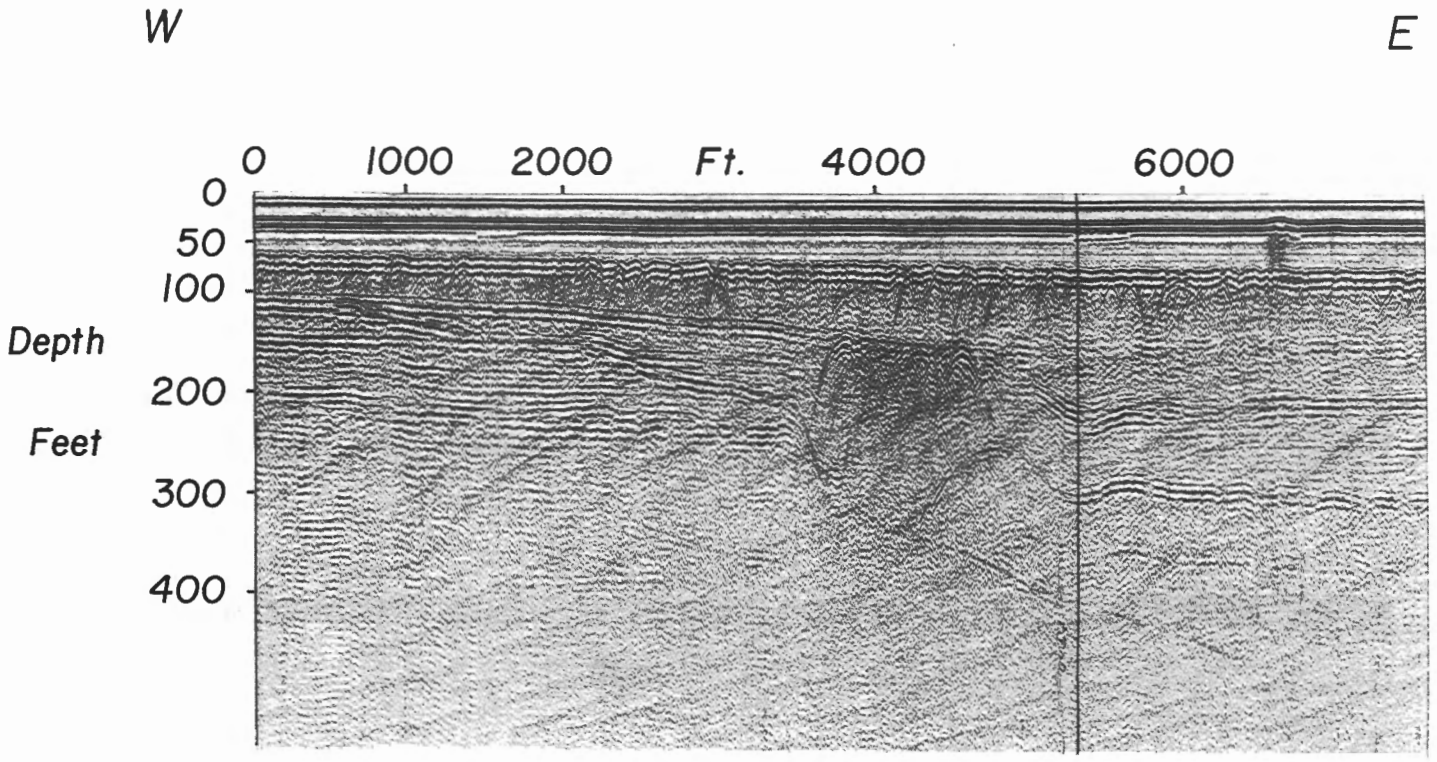

Figure 4. Another sparker profile over west bank of buried canyon. The "breakpoint" seems to occur at around 200 feet, with truncation of the various units having taken place in a manner similar to that observed in Figure 3. The origin of the very strong reflector located about 4,000 feet out and at a depth of 150 feet in unknown but may represent a ground ice occurrence or a boulder beach.

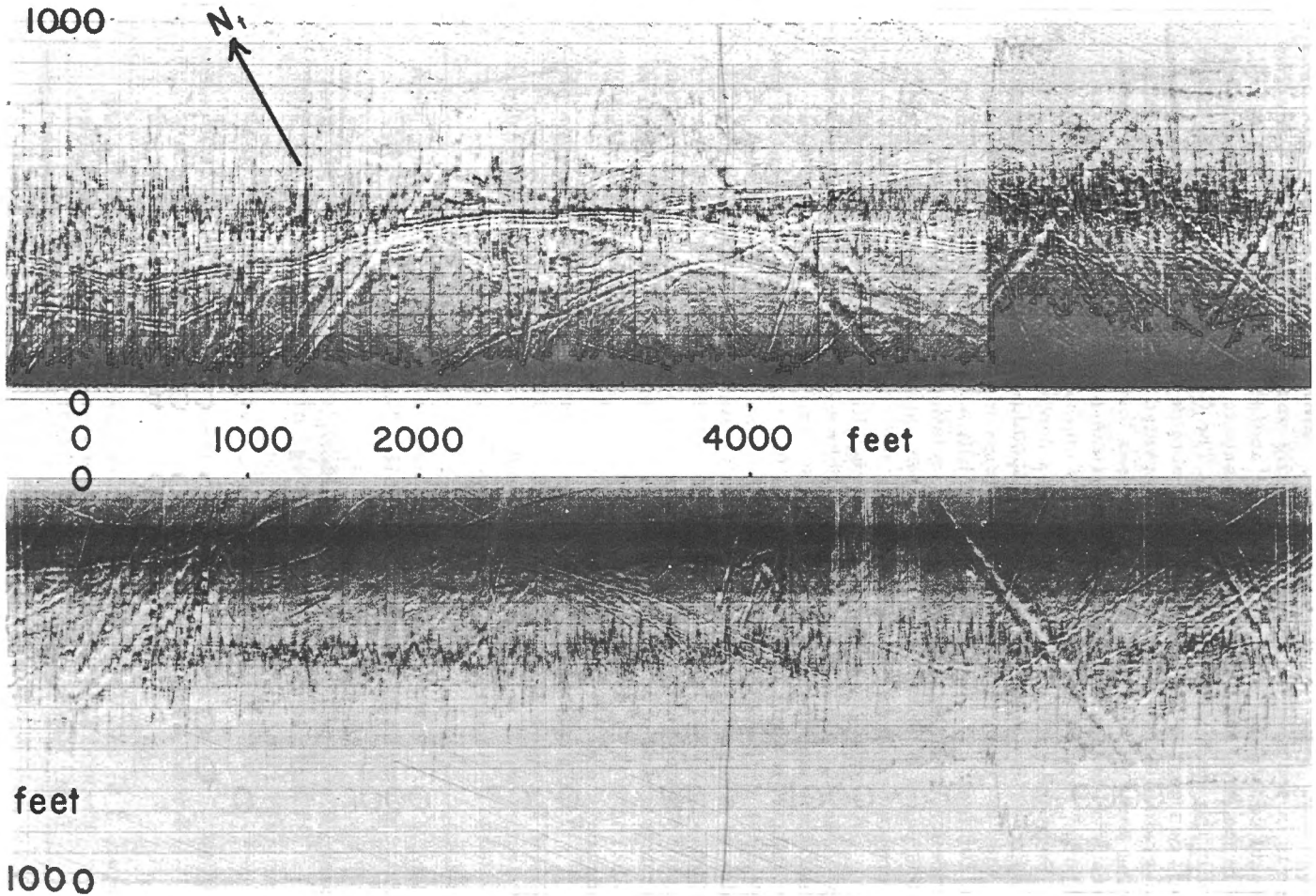

Figure 5. A side scan sonar (S.S.S.) profile in about 40 feet of water showing scour paths of icebergs. Some scours appear very flat on the bottom, whereas others appear to be quite jagged. The saw tooth nature of some scours is thought to be due to the movement of the S.S.S. fish undertow.

The world wide sea level datum was much lower than the present during the time when the large continental glaciers existed over the North American land mass[2, 3]. Creager and McManus[4] have some evidence of lower sea levels in postglacial times in the Bering and Chukchi Seas and, excluding significant crustal subsidence by tectonic and/or glacier ice loading mechanisms in the Mackenzie delta area, it is safe to conclude that lower sea levels existed in the study area at these times. The C.S.S. Hudson, working in the Beaufort Sea east of the canyon in 1970, obtained a number of well-sorted coarse-grained sands which may be interpreted as relict beach sands, thus providing some past evidence of a lower sea level regime. Picking a world-wide sea level transgression curve[2] the time of formation for any given "breakpoint" may be estimated. Directly offshore (ca. 10 naut. miles) from Stokes Point the "breakpoint" is found at a depth of about 270 feet, corresponding to a time on the curve around 16,000 years B.P. South of Stokes Point, the "breakpoint" is found at progressively shallower depths, being around 200 feet (ca. 14,000 years B.P.) just north of Sabine Point. From this evidence it can be proposed that deglaciation in this area occurred 16,000 to 14,000 years B.P. and that, in fact, retreat was quite slow (ca. 40 km/2,000 yrs. = ca. 20 m/yr.).

Another way of accounting for the offshore slope of the "breakpoints" is to propose (for practical purposes) synchroneity in their development with postglacial rebound causing a distortion of a once almost level shoreline. The warping observed (20 m/40 km = ca. 0.5 m/km) is not unreasonable and implies crustal displacements increasing to the south. The maximum possible value of crustal displacement at Stokes Point (which assumes deglaciation at the lowest eustatic level ca. -360 feet) is about 160 feet (360-200 feet). If deglaciation did not occur when the sea was at its lowest level, then the total crustal depression is somewhat less than 160 feet. It is not known which of these alternatives is the correct one, the most likely answer being that some combination of both mechanisms occurred.

Times of stability seem to have existed during the truncation process by the transgressing sea (Figs. 3 to 5). The uppermost reflector (bottom of recent muds) is quite persistent and is correlated to the topset deposits of a large postglacial Mackenzie River (Fig. 2).

---

[1] Mackay, J.R.: Glacier ice-thrust features of the Yukon coast; Can. Dept. Mines Tech. Surv., Geog. Bull., No. 13, pp. 5-21 (1959).

[2] Shepard, F.P. and Curray, J.R.: Carbon-14 determination of sea level changes in stable areas; in Prog. in Oceanog., vol. 4, pp. 283-291 (1967).

[3] Milliman, J.D. and Emery, K.O.: Sea levels during the past 35,000 years; Science, vol. 162, pp. 1121-1123 (1968).

[4] Creager, J.S. and McManus, D.A.: Geology of the floor of Bering and Chukchi Seas - American studies; in The Bering Land Bridge, D.M. Hopkins, ed., pp. 7-31 (1967).

AUTHOR INDEX